JASMIN LINDNER

ANÁLISE DO CATABOLISMO DA HEMOGLOBINA DE *PLASMODIUM FALCIPARUM*

Tese apresentada ao Programa de Pós-Graduação em Biologia da Relação Patógeno-Hospedeiro do Instituto de Ciências Biomédicas da Universidade de São Paulo, para obtenção do título de Doutor em Ciências.

São Paulo
2017

JASMIN LINDNER

ANALYSIS OF THE HAEMOGLOBIN CATABOLISM OF *PLASMODIUM FALCIPARUM*

Ph. D. Thesis presented to the Post-graduation program Biology of Host-Pathogen Interactions at the Institute of Biomedical Sciences of the University of São Paulo, in order to obtain the degree of Doctor in Sciences.

São Paulo
2017

JASMIN LINDNER

ANÁLISE DO CATABOLISMO DA HEMOGLOBINA DE *PLASMODIUM FALCIPARUM*

Tese apresentada ao Programa de Pós--Graduação em Biologia da Relação Patógeno-Hospedeiro do Instituto de Ciências Biomédicas da Universidade de São Paulo, para obtenção do título de Doutor em Ciências.

Área de concentração: Biologia da Relação Patógeno-Hospedeiro

Orientador: Carsten Wrenger
Co-Orientador: Christian Betzel

Versão original

São Paulo
2017

JASMIN LINDNER

ANALYSIS OF THE HAEMOGLOBIN CATABOLISM OF *PLASMODIUM FALCIPARUM*

Ph. D. Thesis presented to the Post-graduation program Biology of Host-Pathogen Interactions at the Institute of Biomedical Sciences of the University of São Paulo, in order to obtain the degree of Doctor in Sciences

Area of : Biology of Host-Pathogen Interactions

Supervisor: Carsten Wrenger
Co- Supervisor: Christian Betzel

Original Version

São Paulo
2017

CATALOGAÇÃO NA PUBLICAÇÃO (CIP)
Serviço de Biblioteca e informação Biomédica
do Instituto de Ciências Biomédicas da Universidade de São Paulo

Ficha Catalográfica elaborada pelo(a) autor(a)

Lindner, Jasmin
Análise do catabolismo da hemoglobina de Plasmodium falciparum / Jasmin Lindner; orientador Carsten Wrenger; coorientador Christian Betzel. -- São Paulo, 2017.
139 p.

Tese (Doutorado)) -- Universidade de São Paulo, Instituto de Ciências Biomédicas.

1. Plasmodium falciparum. 2. catabolismo de hemoglobina. 3. Protease. 4. Anemia falciforme. I. Wrenger, Carsten, orientador. II. Betzel, Christian, coorientador. III. Titulo.

UNIVERSIDADE DE SÃO PAULO
INSTITUTO DE CIÊNCIAS BIOMÉDICAS

Candidato(a): Jasmin Lindner

Titulo da Dissertação/Tese: Análise de catabolismo da hemoglobina de *Plasmodium falciparum*.

Orientador: Carsten Wrenger

A Comissão Julgadora dos trabalhos de Defesa da Dissertação de Mestrado/Tese de Doutorado, em sessão publica realizada a **...../...../.....**, considerou o(a) candidato(a):

( ) Aprovado(a) ( ) Reprovado(a)

Examinador(a): Assinatura: .....
Nome: .....
Instituição: .....

Examinador(a): Assinatura: .....
Nome: .....
Instituição: .....

Examinador(a): Assinatura: .....
Nome: .....
Instituição: .....

Presidente: Assinatura: .....
Nome: .....
Instituição: .....

UNIVERSIDADE DE SÃO PAULO
INSTITUTO DE CIÊNCIAS BIOMÉDICAS

Cidade Universitária "Armando de Salles Oliveira"
Av. Prof. Lineu Prestes, 2415 – CEP. 05508-000 São Paulo, SP – Brasil
Telefone :(55) (11) 3091-7733 - telefax : (55) (11) 3091-8405
e-mail: cep@icb.usp.br

Comissão de Ética em Pesquisa

CERTIFICADO DE ISENÇÃO

Certificamos que o Protocolo CEP-ICB Nº **570/12** referente ao projeto intitulado: "*Análise do catabolismo da hemoglobina na proliferação de plasmodium falciporum em eritrócitos geneticamente modificados*" sob a responsabilidade de **Jasmin Lindner,** foi analisado na presente data pela CEUA - COMISSÃO DE ÉTICA NO USO DE ANIMAIS e pela CEPSH- COMISSÃO DE ÉTICA EM PESQUISA COM SERES HUMANOS, tendo sido deliberado que o referido projeto não utilizará animais que estejam sob a égide da lei 11.794 de 8 de outubro de 2008, nem envolverá procedimentos regulados pela Resolução CONEP nº196 de 1996.

São Paulo, 12 de dezembro de 2012.

PROF. DR. WOTHAN TAVARES DE LIMA
Coordenador da CEUA - ICB/USP

PROF. DR. PAOLO M.A ZANOTTO
Coordenador da CEPsh - ICB/USP

Acknowledegments

At this point, I would like to thank Prof. Dr. Carsten Wrenger in particular for providing this interesting topic and thus for making this PhD thesis possible. I also thank for the support and inspiring advice that was especially helpful in times when nothing seemed to work.

My special thanks also go to Prof. Dr. Dr. Christian Betzel for the opportunity to perform crystallisation experiments in his laboratory at DESY, Hamburg, Germany. Furthermore, I would like to thank the entire lab group Betzel for the wonderful working atmosphere. In particular, I would like to thank Robin Schubert for the great cooperation in the APP project. Without you, the solution of the crystal structure would not have been possible. In addition, I would like to thank Rutineia Ferraz-Jansen for the great, untiring assistance.

I would also like to thank the entire lab group of Carsten Wrenger and Gerhard Wunderlich for their extremely pleasant and cheerful atmosphere. Your open way has made it easier for me to settle in with you and to feel good with you. Our Churrascos were a great diversion and gave me new power for the doctoral thesis.

In addition, I would like to thank Kamila A. Meissner not only for the motivating and professionally valuable discussions, but above all for the many activities outside the lab.

Lastly, I would like to thank my mother Martina Hintelmann and Torsten Hintelmann as well as my father Lothar Lindner, my brother Sascha Lindner and my friends for your interest in my work, the encouragement and the great support in all living situations.

Meus maiores agradecimentos vão para o meu marido e pai do meu filho, Douglas Jesus de Souza, porque você me faz feliz. Eu aprecio muito como você me encorajou, especialmente na fase final para que eu pudesse terminar meu doutorado. Eu também quero agradecer Jannik por ter entrado em nossas vidas e por ser esse bebe alegre, gentil e simpático que nos faz sorrir todo dia. Eu amo vocês, minha pequena família linda.

This work was supported by the São Paulo state funding agency FAPESP (Grants 2012/12790-3).

Para mim e minha família!

Resumo

LINDNER, J. **Análise do catabolismo da hemoglobina de Plasmodium falciparum.** 2017. 137 f. Tese (Doutorado em Parasitologia) - Instituto de Ciências Biomédicas, Universidade de São Paulo, São Paulo, 2017.

Células altamente proliferativas, como o parasita da malária *Plasmodium falciparum* exigem um nível acelerado de macromoléculas, tais como proteínas, para o fornecimento de energia para manutenção de processos intracelulares. Os aminoácidos necessários para a síntese das proteínas podem ser conseguidos por síntese *de novo*, importação a partir do plasma da célula hospedeira e pela digestão de hemoglobina. Durante a digestão da hemoglobina, o heme vai ser lançado, que precisa ser desintoxicado em hemozoína. Os seres humanos que abrigam doenças eritrocitárias relacionadas com a arquitetura de hemoglobina, como anemia falciforme, ganham uma vantagem protetora quando infectados com o patógeno da malária. O objetivo desta tese é obter ideias sobre o modo de ação do crescimento do parasita dentro de eritrócitos geneticamente diferentes, concentrando-se na via catabólica da hemoglobina plasmodial usando parasitas transgênicos. Todos os construtos clonados (12 das 13 enzimas originais) foram transfretados com sucesso para *P. falciparum* 3D7 e foram realizados ensaios de crescimento em eritrócitos geneticamente modificados. Surpreendentemente, a Dipeptidil amino peptidase 1 (DPAP1) mostrou um efeito negativo em ensaios de proliferação no sangue de células falciformes. Curiosamente, a DPAP1 foi co-localizada no vacúolo alimentar e no citosol assim como outras estruturas, presumivelmente vesículas assumindo que a DPAP1 poderia desempenhar um papel fora do catabolismo da hemoglobina. Por outro lado, a cisteína protease FP2 que participa nas duas primeiras etapas de degradação da hemoglobina, prolifera três vezes mais elevada no sangue de células falciformes do que o Mock, a célula de controle. Adicionalmente, estudos de inibidores indicam que FP2 é uma proteína essencial para o parasita sendo que a sua inibição bloqueia a hidrólise da hemoglobina e o desenvolvimento do parasita. Uma vez que os detalhes estruturais poderiam realçar o modo de ação destas proteínas e, consequentemente, poderiam ser exploradas para a descoberta de medicamentos, a cristalização de uma APP truncada e optimizada para códons foi realizada no DESY em Hamburgo, Alemanha que resultou uma estrutura cristalina difratando até 1,7 Å. Afim de analisar o perfil de atividade da amino peptidase cristalizada, foi estabelecido um ensaio de atividade em cooperação com o CEFAP e mostrou proteína ativa. O metabolismo de nutrientes do parasita abriga um alto potencial para o desenvolvimento de novos alvos de drogas. Portanto, é essencial uma compreensão da ocorrência da digestão da hemoglobina e da natureza protetora das variantes da hemoglobina.

Palavras-chave: *Plasmodium falciparum*. Hemoglobina. Protease. Anemia falciforme.

Abstract

LINDNER, J. **Analysis of the haemoglobin catabolism of *Plasmodium falciparum*.** 2017. 137 p. PhD (Parasitology) - Instituto de Ciências Biomédicas, Universidade de São Paulo, São Paulo, 2017.

Highly proliferating cells such as the malaria parasite *Plasmodium falciparum* necessitate an increased level of macromolecules, such as proteins, for the maintenance of their cellular structure and function. The required amino acids for the synthesis of the proteins can be achieved by *de novo* synthesis, import from host cell plasma and digestion of haemoglobin. During haemoglobin digestion heme is going to be released which needs to be detoxified into hemozoin. Humans who harbours erythrocytic diseases related to the haemoglobin architecture such as sickle cell disease gain a protective advantage during malaria infections. The aim of this thesis is to get insights into the mode of action of parasite growth within genetically different erythrocytes by focussing on the plasmodial haemoglobin catabolic pathway using transgenic parasites.
All cloned constructs (12 from original 13 enzymes) were successfully transfected into *P. falciparum* 3D7 and growth assays in genetically modified erythrocytes were carried out. Surprisingly, the Dipeptidyl aminopeptidase 1 (DPAP1) showed a negative effect in proliferation experiments in sickle cell blood. Interestingly, DPAP1 was co-localised to the food vacuole and the cytosol as well as other structures, presumably vesicles assuming that DPAP1 could play a role outside of the haemoglobin catabolism. On the other hand, the cysteine protease FP2 which participates in the first two steps of haemoglobin degradation, proliferated three times higher in sickle cell blood than the Mock control cell line. Additionally, inhibitor studies indicate that FP2 is an essential protein to the parasite given that its inhibition blocks haemoglobin hydrolysis and parasite development.
Since structural details could highlight the mode of action of these proteins and consequently could be exploited for drug discovery, crystallisation of a truncated and codon optimised APP was performed at the DESY in Hamburg, Germany and resulted in a solved crystal structure diffracting up to 1,7 Å. In order to analyse the activity profile of the crystallised aminopeptidase, an activity assay has been established in cooperation with the CEFAP and showed active protein. Parasite's nutrient metabolism shelters a high potential for the development of novel drug targets. Therefore, a clear understanding of the occurring haemoglobin digestion and the protective nature of haemoglobin variants is essential.

Keywords: *Plasmodium falciparum*. Haemoglobin. Protease. Sickle cell trait.

LIST OF FIGURES

LIST OF TABLES

LIST OF ABBREVIATIONS AND ACRONYMS

A_{260}	Absorption at a wavelength of 260 nm
A_{280}	Absorption at a wavelength of 280 nm
A_{600}	Absorption at a wavelength of 600 nm
AAP	Alanyl Aminopeptidase
AB	Antibody
AHT	Anhydrotetracycline
Amp	Ampicillin
APP	Aminopeptidase P
APS	Ammonium persulfate
ATP	Adenosine triphosphate
Avr	*Anabaena variabilis*
Bcl	*Bacillus caldolyticus*
BLAST	Basic Local Alignment Search Tool
bp	Base pairs
bsa	*Bacillus stearothermophilus*
BSA	Bovine Serum Albumin
BSD	Blasticidin
$CaCl_2$	Calcium chloride
CD	Circular dichroism
CDC	Centres for Disease Control and Prevention
cDNA	complementary DNA
CEFAP	Centro de Facilidades para a Pesquisa
cm	Centimeter
cm^2	Square centimeter
CO_2	Carbon dioxide

Da	Dalton
DESY	Deutsches Elektronen Synchrotron
dH_2O	deionised water
DLS	Dynamic light scattering
DNA	Deoxyribonucleic acid
dNTPs	Deoxynucleotide triphosphates
DPAP	Dipeptidylaminopeptidase
Dpn	*Diplococcus pneumoniae*
DTT	Dithiotreitol
ECL	Enhanced Chemiluminescence
E. coli	*Escherichia coli*
EcoR	*Escherichia coli*
EDTA	ethylenediaminetetraacetic acid
e.g.	For example
EMBL	European Molecular Biology Laboratory
et al.	lat. *and other*
Fig.	Figure
Fl	Falcilysin
FP	Falcipain
FPLC	Fast protein liquid chromatography
g	Gram
gDNA	genomic DNA
GFP	Green fluorescent protein
GST	glutathione-S-transferase
h	hour
hdHFR	Human Dihydrofolate reductase
H_2O	Water

HABA	Hydroxy-Azophenyl-Benzoic Acid
HCl	Hydrochloric acid
HDP	Heme Detoxification Protein
HEPES	Hydroxyethyl-piperazineethanesulfonic acid
Hind	*Haemophilus influenza*
HRP	Horseradish peroxidase
HT-PBS	*human tonicity-phosphate-buffered saline*
IgG	Immunoglobulin G
k	kilo
KCL	Potassium chloride
KH_2PO_4	Potassium hydrogen phosphate
Kpn	*Klebsiella pneumoniae*
l	Liter
LB	Luria Bertani
M	Molar
mA	Milliamperes
MBP	Maltose binding protein
mg	Milligram
$MgCl_2$	Magnesium chloride
min	Minute
ml	Milliliter
mM	Millimolar
$MnCl_2$	Manganese chloride
mRNA	messenger RNA
ms	Millisecond
MW	Molecular weight
N_2	Nitrogen

NaCl	Sodium chloride
NAG	N-aceytlglucosamine
NaH_2PO_4	Sodium dihydrogenphosphate
Na_2HPO_4	Disodium hydrogen phosphate
NAM	N-acetylmuraminic acid
NaOH	sodium hydroxide
ng	Nanogram
Ni-NTA	Nickel-Nitrilotriacetic acid
nm	Nanometer
O_2	Oxygen
ORFs	open reading frames
p	Pico
PAGE	Polyacrylamide gel electrophoresis
PBS	phosphate buffered saline
PCR	polymerase chain reaction
PDB	Protein Data Bank
PEG	Polyethylene glycol
Pf	*Plasmodium falciparum*
Pfu	*Pyrococcus furiosus*
PM	Plasmepsin
pH	Hydrogen ion concentration“
PMSF	Phenylmethylsulfonylfluoride
RNA	Ribonucleic acid
ROS	Reactive oxygen species
rpm	revolutions per minute
RPMI	Roswell Park Memorial Institute
RT	Reverse transcription

RT	Room temperature
SCT	Sickle Cell Trait
SDS	Sodium dodecyl sulfate
sec	Second
Tab.	Table
TAE	Tris-Acetate-EDTA
Taq	*Thermus aquaticus*
TE	Tris-EDTA
Temed	N, N, N', N'-tetramethylenediamine
TLS	Translation/Libration/Screw
Tris	tris(hydroxymethyl)aminomethane
TPP	Techno Plastic Products
UK	United Kingdom
USP	Universidade de São Paulo
UV	Ultraviolet
V	Volt
v/v	volume per volume; percentage by volume
w/v	weight per volume
WB	Western Blot
WHO	World Health Organization
WR	WR 99210
WT	wildtype
Xba	*Xanthomonas badrii*
Xho	*Xanthomonas holcicola*
Xma	*Xanthomonas malvacearum*

LIST OF SYMBOLS

∞	Infinity
≈	Almost equal to
° C	Degree Celsius
α	Alpha
Å	Angstrom
β	Beta
ε	Open E
γ	Gamma
λ	Lambda
µg	Microgram
µl	Microliter
µM	Micromolar
®	Registered sign
™	Trade mark sign

TABLE OF CONTENTS

1. INTRODUCTION

1.1 Malaria

1.1.1 Short history of Malaria

Malaria is one of the oldest and most devastating parasitic diseases in humans which afflicted human being already 3000 years before Christ in advanced civilizations such as Egypt, India and China. Nevertheless, there have also been several malaria epidemics in Southern and Central Europe in the middle Ages. The cause of the as the "intermittent fever" or "marsh fever" known disease was suspected in the bad air (Old Italian "mal 'aria"). This expression arose from the idea that the pathogens are transmitted in swamps through the air. Therefore, the draining of swamps was an important step in the fight against malaria (WESTHEIDE; RIEGER, 1996). Only in 1880 the French doctor Charles Louis Alphonse Laveran discovered in the blood of deceased malaria patients the malaria parasite Plasmodium (CALMETTE, 1922). However, the association to carriers could only be formed 17 years later by the British physician Ronald Ross (LUCIUS; LOOS-FRANK, 2008).

The origin of *malaria* in South America is controversial. On the one hand, a recent introduction is suspected by the European colonization and the transatlantic slave trade (CONWAY et al., 2000; CONWAY, 2003; NEAFSEY et al., 2008). On the other hand, other archaeological and genetic studies suggested a much older origin (CALDAS DE CASTRO; SINGER, 2004; JOY et al., 2003; TAYLOR et al., 2013). Brazilian malaria was first reported as “tertian and quartan fevers” affecting the Tupinambá Indians in 1587 (COURA et al., 2006; DEANE 1986).

1.1.2 Distribution

Globally, an estimated 3,2 billion people in 95 countries and territories are living in malaria endemic areas (Figure 1). This devastating parasitic disease is widespread in Africa, Asia and South America, but also occurs with much lower frequency in the Middle East and in some areas of Europe.

There were approximately 214 million cases (uncertainty range 149–303 million) of malaria worldwide and approximately 438 000 malaria deaths (range 236 000–635 000), where children in the African region aged under 5 years accounted two thirds of all death (WORLD HEALTH ORGANISATION, 2015).

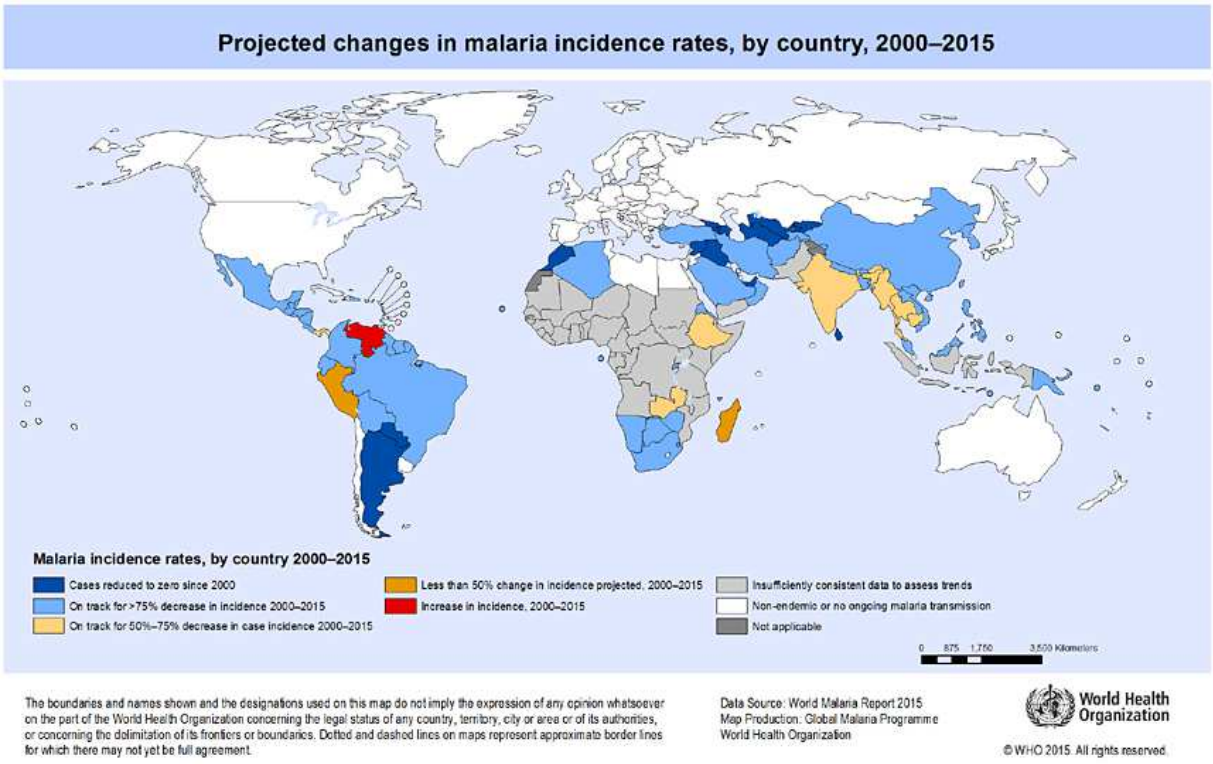

Figure 1 - Global occurrence of Malaria according to WHO (2015).
Tropical and subtropical distribution, including much of the sub-Saharan Africa, South-East Asia, South- and Central Americas.

1.1.3 Types of malaria

Since the disease progress can vary a lot, it may be distinguished between the falciparum malaria, the tertian malaria and quartan malaria. Tertian malaria is caused by the two parasites *P. ovale* or *P. vivax*. This disease leads to fever attacks that recur classically in a rhythm of 48 hours. Due to the regularity of these bouts of fever and low parasitaemia (up to 2%), this form of malaria can be treated well. However, both types form dormant stages in the liver (so called hypnozoites) as opposed to the following ones. Thereby, even after month- or yearlong asymptomatic intervals new malaria relapses may be triggered. Infection with *P. malariae* causes quartan malaria which is characterized by a 72-hour fever rhythm. The mortality for this form of the disease with a low parasitaemia of up to 1% is very low. Indeed, current research indicates that so far as *P. malariae* infections diagnosed, fatal malaria cases were often caused by *P. knowlesi* (COX-SINGH et al., 2008). The falciparum malaria is considered the most dangerous of the known types of malaria, caused by *P. falciparum*. Due to the occurrence of irregular bouts of fever and with a parasitaemia of up to 20% the infection takes a rapid and severe course. The only type of human-pathogenic *Plasmodium* inducing the formation of small structures lying in the erythrocyte

membrane (knobs) is *P. falciparum*. They are composed of proteins that mediate cytoadherence. Thereby, infected erythrocytes can easily adhere to endothelia of capillaries and other erythrocytes (rosetting) impairing or preventing the blood flow. The resulting circulatory disorders can cause serious damage to the brain and other organs (MEHLHORN; PIEKARSKI, 2002). The described cerebral form of malaria is difficult to treat and often leads to death (CENTER FOR DISEASE CONTROL AND PREVENTION, 2005; KAYSER et al., 1997), which is also one of the causes of high mortality among infection with falciparum malaria. Malaria is presently undergoing resurgence and the fight against *P. falciparum* - the most virulent species accounting for over 90% of deaths - has become a significant problem (GREENWOOD et al., 2008).

1.1.4 Comprehensive life cycle of Plasmodium falciparum

The life cycle of the various *Plasmodium* species is very similar in many respects. An obligate host alternation between the final host, the female Anopheles mosquito, and the intermediate host, the human in the case of *P. falciparum,* is essential for proliferation. Two asexual proliferation steps (schizogonies) in the intermediate host held specifically in the liver and in the erythrocytes, are realized, whereas the sexual reproduction (Sporogony) takes place in the mosquito.

During a blood meal by a female Anopheles mosquito approximately 8-15 sporozoites enter the bloodstream or lymph of the human host quickly invading hepatocytes. During the next 6 days, the liver stage parasites differentiate and undergo asexual multiplication resulting in about 30000 merozoites that burst from the hepatocyte (exoerythrocytic schizogony) (GREENWOOD et al., 2008). After their release from the merosomes (merozoites-filled vesicles) individual merozoites infect erythrocytes and undergo an additional round of multiplication producing 12-16 merozoites within a schizont (erythrocytic schizogony) (STURM et al., 2006). The length of this erythrocytic stage of the parasite lifecycle depends on the parasite species: irregular cycle for *P. falciparum*, 48 hours for *P. vivax* and *P. ovale*, and 72 hours for *P. malariae*. Whereas the exoerythrocytic multiplication only occurs once, the subsequent erythrocytic schizogony is a permanently repeating process (LUCIUS; LOOS-FRANK, 2008). Upon penetration of the merozoite in the erythrocyte that is enclosed by the host membrane. Within the resulting parasitophorous vacuole (PV) the parasite evolves from the ring

stage over the young and old trophozoites to mature schizonts. During lysis of the erythrocytes proteins and other metabolites of the parasite are released. These antigens are recognized by the immune system causing the clinical manifestations of malaria: fever and chills. The released merozoites go on to invade further erythrocytes. Not all merozoites divide into schizonts, some differentiate into sexual forms, male and female gametocytes (exflagellation). These gametocytes are taken up by the female Anopheles mosquito during another blood meal. Within the mosquito midgut, the male gametocyte undergoes a rapid nuclear division producing eight flagellated microgametes that fertilize the female macrogamete. The resulting zygote become motile and elongated, so called ookinete, and traverses the mosquito gut wall and encysts on the exterior of the gut wall as an oocyst. Sporogony is taking place in the oocyst and subsequently, the oocyst ruptures releasing hundreds of sporozoites into the mosquito body cavity where they eventually migrate to the mosquito salivary glands and the life cycle can start again (LUCIUS; LOOS-FRANK, 2008; MEHLHORN; PIEKARSKI, 2002).

Figure 2 - Comprehensive lifecycle *of Plasmodium falciparum* (according to DELVES et al., 2012). Obligate host alternation. Asexual reproduction (exoerythrocytic and erythrocytic schizogony) in the intermediate host, the human, and sexual reproduction (Sporogony) within the final host, the Anopheles mosquito

1.1.5 Haemoglobin digestion

For proliferation, the malaria parasite requires amino acids for the synthesis of its proteins. There are three sources of amino acids: *de novo* synthesis, import from host cell plasma, and digestion of haemoglobin. Haemoglobin is an extremely abundant protein in the erythrocyte cytoplasm and serves as the major source of amino acids for the parasite. Malaria parasites degrade 65 - 75% of host haemoglobin (SKINNER-ADAMS et al., 2009). During the initial stage of erythrocyte infection, known as the ring stage, haemoglobin is taken up by pinocytosis resulting in double membrane vesicles where the digestion of haemoglobin takes place during the early trophozoite stage.

Lysosomal vesicles transfer haemoglobin to acidic digestive vacuoles in an actin-dependent process that is regulated by Rab5 and PfPI3K proteins (ELLIOTT et al., 2008; VAID et al., 2010) which subsequently fuse with the food vacuole. The inner membrane (originally the PVM) is lysed and the haemoglobin is released into the food vacuole (SLOMIANNY, 1990; YAYON et al., 1984). The food vacuole is an acidic compartment (pH 5,0 - 5.4) that contains acidic protease and phosphatase activities for the digestion of proteins, in particular haemoglobin, and dephosphorylation of nutrients (GLUZMAN et al., 1994, MÜLLER et al., 2010). During haemoglobin digestion heme is going to be released. Free heme is toxic due to its ability to form reactive oxygen species (ROS) and thereby destabilizes the food vacuole membrane as well as other membranes which results in the death of the parasite. Heme can be detoxified within the parasite by polymerisation. Currently, three mechanisms by which heme could be detoxified have been identified. One suggestion how heme detoxification could take place is that H_2O_2 oxidizes the porphyrin ring which leads to its opening and subsequent breakdown. Another possibility is that some of the heme translocates across the food vacuole membrane into the host cytoplasm where it is oxidized by reduced glutathione. Currently, a new protein, HDP (heme detoxification protein) was identified. JANI et al (2008) investigated that HDP binds heme with a high affinity and converts it rapidly to hemozoin, also known as the malaria pigment. HDP then delivers the produced hemozoin dimers to the lipid nanospheres and it is proposed that interaction between HDP and lipids form the hemozoin crystals. Furthermore, HDP is also expressed at mosquito and liver stages suggesting that the protein has more than one function.

Several distinct protease activities, representing three of the four major classes of proteases, have been identified in the food vacuole (multiple plasmepsins, falcipains and falcilysins). Haemoglobin is sequentially digested by aspartic proteases, cysteine proteases, metalloproteases, and aminopeptidases by a semi-ordered process involving the sequential action of different proteases (GOLDBERG et al., 2005). Several plasmepsin genes have been identified in the genome of *P. falciparum* and four of these appear to function in the food vacuole (BANERJEE et al., 2002). Plasmepsin-1 and Plasmepsin-2 are the best characterised and initiate the degradative process by cleaving non-denatured haemoglobin between phenylalanine and leucine residues. Cleavage at this site presumably causes the globin subunits to dissociate and partially unfold exposing additional protease sites within the globin polypeptide

chains. The other plasmepsins and falcipains are then able to further degrade these large globin fragments. It has been suggested that falcipain-2 (SHENAI et al., 2000), and possibly falcipain-3 (SIJWALI et al., 2001), are capable of digesting either native haemoglobin. The proposed pathway of haemoglobin digestion involves an initial cleavage by plasmepsin-1 (and possibly falcipain-2) followed by the combined actions of several plasmepsins and falcipains (Figure 3). The peptide fragments produced by these digestions (up to 20 amino acids) are then digested into smaller peptides by falcilysin leading to the formation of 6-8 amino acids in length. Initially no food vacuole associated exopeptidase activity could be identified within the food vacuole (KOLAKOVICH et al., 1997). However, two further amino peptidases (*Pf*APP and *Pf*AAP) were identified within the food vacuole (DALAL; KLEMBA, 2007), which are able to convert peptides into amino acids. In addition, a dipeptidyl aminopeptidase (*Pf*DPAP1) activity was found in the food vacuole (KLEMBA et al., 2004). Moreover, a neutral aminopeptidase activity has been identified in cytoplasm of several *Plasmodium* species (CURLEY et al., 1994; FLORENT et al., 1998). This implies that the digestion of the small peptides also takes place in the parasite cytoplasm, and therefore must be transported across the membrane of the food vacuole into the parasite's cytoplasm. *Pf*mdr-1, a member of the ATP-binding cassette (ABC) transporter superfamily, has been localized in the food vacuole membrane. Some ABC transporters function to translocate polypeptides across membranes as it has also been suggested for complementation assays for *Pf*mdr-1 (VOLKMAN et al., 1995) (Figure 3).

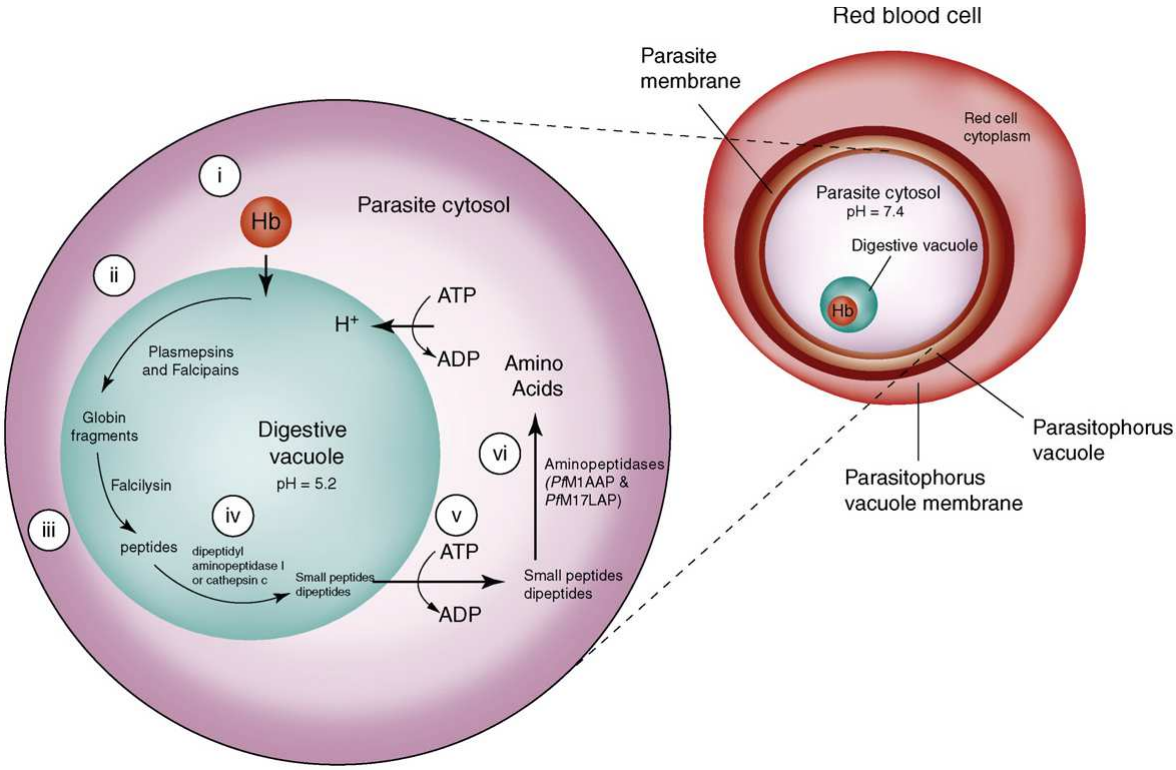

Figure 3 - Suggested haemoglobin catabolism pathway in *P. falciparum* (SKINNER-ADAMS et al., 2009). Haemoglobin is taken up by pinocytosis and transported to the food vacuole by vesicles where digestion of haemoglobin is carried out by diverse aspartic, cysteine, metalloproteases as well as dipeptidyl- and aminopeptidases. Cytosolic aminopeptidase activity implies the presence of a transporter located within the food vacuole membrane mediating the transport of dipeptides across the food vacuole membrane.

The critical importance of haemoglobin digestion is illustrated by the fact that inhibition of the aspartic and cysteine as well as some aminopeptidases prevents parasite development (DALAL; KLEMBA, 2007; DEU et al., 2010; FRANCIS; SULLIVAN; GOLDBERG, 1997; JIN et al., 2014; PANDEY et al., 2006; SKINNER-ADAMS et al., 2009). These unique enzymes within the haemoglobin degradation may represent new drug targets.

1.1.6 Treatment of malaria

There is no efficient vaccine available at this moment, but several studies are ongoing in this regard. RTS,S/AS01 is the most advanced vaccine candidate (phase 3 of clinical trials) against the deadliest form of malaria, *P. falciparum* (WHO, 2016). It targets the pre-erythrocytic stage of *P. falciparum* inducing humoral and cellular immune responses to the circumsporozoite protein (CSP) present on the surface of sporozoites and liver stage schizonts. There was detected a protection against clinical episodes of

malaria in the range of 30% - 60%. In a large African phase 3 trial, this vaccine had an efficacy against clinical malaria of 55,8% (50% – 60%) in children aged 5 – 17 months and 31,3% (23,6% – 38,3%) in infants aged 6 – 12 weeks over the first year after vaccination. Furthermore, protection against severe malaria was noted, but protection wanes over the time in both age categories (OLOTU et al., 2016; RTS,S CLINICAL TRIALS PARTNERSHIPS, 2012; RTS,S CLINICAL TRIALS PARTNERSHIPS, 2015). Recently, a combination of the vaccine candidate RTS,S/AS01 with Chimpanzee Adenovirus 63 and modified Vaccinia Ankara vectored vaccines expressing ME-TRAP (ChAD63/MVA/ME-TRAP) yield in a vaccine efficacy of 78,7% (75 - 82,4%). Whereas, the individual vaccine candidates lose their efficacy over the time, vaccine candidates remain immunogenic when the regimens are combined (85,4% (83,3 - 87,5%) after six months) (RAMPLING et al., 2016).

Treatment and Prophylaxis of malaria is based on a small number of drugs. The most important drugs currently in use are focused either on the food vacuole - a special organelle for the digestion of host haemoglobin - of ring-stage and trophozoites of blood-stage parasites or on enzymes in the trophozoite folic acid biosynthesis pathway (WILSON et al., 2013). Only a few drugs, including artemisinin, Artemisinin-based Combination Therapies (ATCs), methylene blue, primaquine and thiostrepton target the sexual stages of *Plasmodium falciparum* life cycle (BEAUDOIN; AIKAWA, 1968; DELVES et al., 2012; DELVES et al., 2013; KISZEWESKI 2011). Primarily, the antimalarial drugs can be divided into eight main classes namely the endoperoxides, 4-aminoquinolines, 8-aminoquinolines, antifolates, sulphonamides, antibiotics, amino alcohols and others (Figure 4). Currently, most potent antimalarials against asexual blood stages are the natural, semi-synthetic and synthetic endoperoxides: artemisinin, DHA, artesunate, OZ277 and OZ439 (DONDORP et al., 2010; WHITE 1997; WILSON et al., 2013). These antimalarials likely act by alkylating heme and other vital biomolecules of the parasite (KLONIS et al., 2011; O'NEILL et al., 2010), such as *Pf*TCTP (BHISUTTHIBHAN et al., 1998; CALDERON-PEREZ et al., 2014), and degrading phospholipids in parasite membranes (KUMURA et al., 2009). Furthermore, 4-aminoquinolines are also highly active against asexual blood-stages, while 8-aminoquinolines are not. The latter class of antimalarials is known to be active on the hypnozoite liver form of *P. vivax*. Additionally, amodiaquine inhibits haemoglobin digestion and exflagellation/gametocyte maturation. Besides asexual blood stages atovaquone targets efficiently the electron transport chain in liver and vector (DELVES

et al., 2012). In addition to known antimalarials, trichostatin A which acts by inhibiting the histone deacetylase (HDAC) by modifying gene expression (ANDREWS; TRAN; FAIRLIE, 2012) and cycloheximide, an antibiotic inhibiting the protein translation, are promising compounds for treatment of malaria (GEARY; JENSEN, 1983).

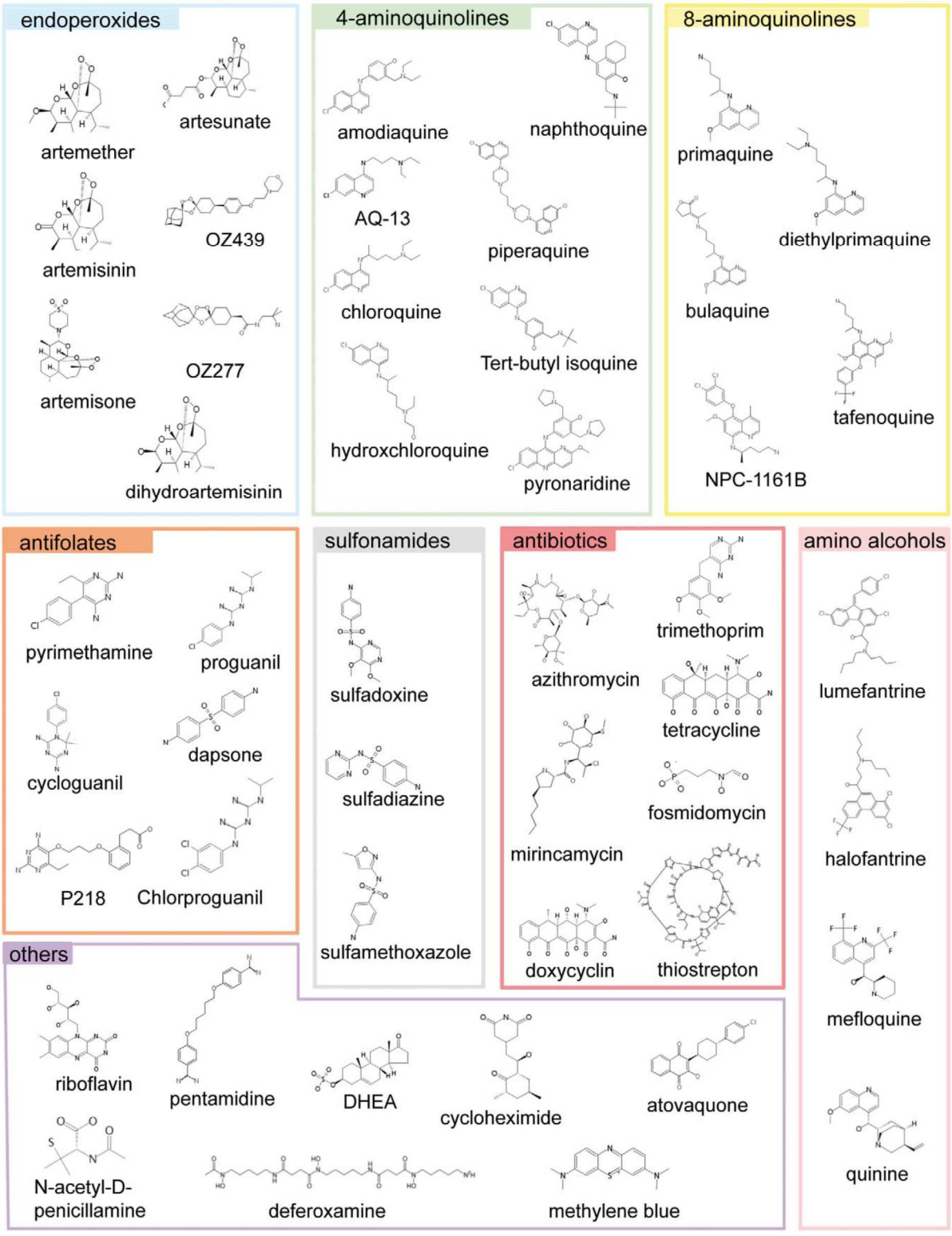

Figure 4 - The main classes of antimalarial drugs (DELVES et al., 2012).
Treatment and prophylaxis of malaria is solely based on a small number of drugs. Best available treatment, particularly against *P. falciparum*, are Artemisinin-based Combination Therapies (ACTs).

Due to the high mutational rate of the parasite and its resulting rapid adaptation to environmental changes, drug resistance is increasing. In the mid-1990s, where resistance to all available antimalarial drugs had developed (Figure 5), the artemisinin-based combination therapies (ACTs) were introduced. Artemisinin resistant *P. falciparum* is firmly established in eastern Myanmar, western Cambodia and Thailand and southern Vietnam and is emerging in southern Laos and north-eastern Cambodia. The resistance is triggered by a single nucleotide polymorphism (SNP) in the kelch protein gene on chromosome 13 (*kelch13*) after position 440 and is characterised by a slow parasite clearance (Parasite clearance half-life > 5 hours) which reflects the reduced susceptibility of ring-stage parasites. So far, ACTs are still efficacious in areas where standard three-day treatments with artemisinin are failing (ASHLEY et al., 2014).

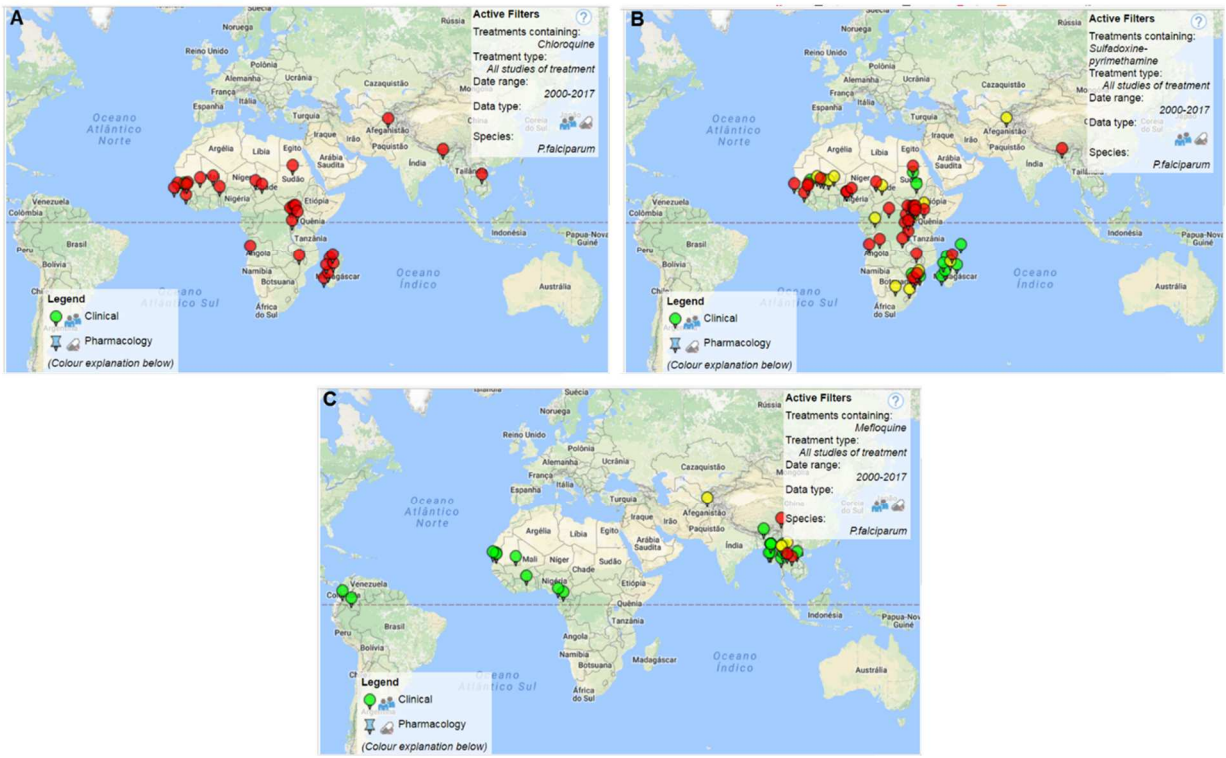

Figure 5 - Overview of occurring drug resistance. Antimalarial drug resistance surveillance obtained from WWARN Molecular Surveyor: **A** exhibiting the chloroquine drug resistance with incidence of *Plasmodium falciparum* chloroquine resistance transporter K76T mutation, **B** presenting the frequency of *Pf*dhfr gene with 51I mutation in association with resistance to sulfadoxine-pyrimethamine drug, **C** Mefloquine resistance in *Plasmodium falciparum* has been related to increased copy numbers of multidrug-resistant gene 1 (*Pf*mdr1).

However, not only the parasite has developed resistance, but also the human in the sense of natural protection. Epidemiological studies revealed that there is a high

correlation between abnormalities of erythrocytes and *falciparum* endemic countries (PIEL et al., 2010). Figure 6 and 7 show clearly a co-localisation of malaria occurrence and haemoglobin-inherited disorders (Haldane´s malaria hypothesis), such as the sickle cell trait.

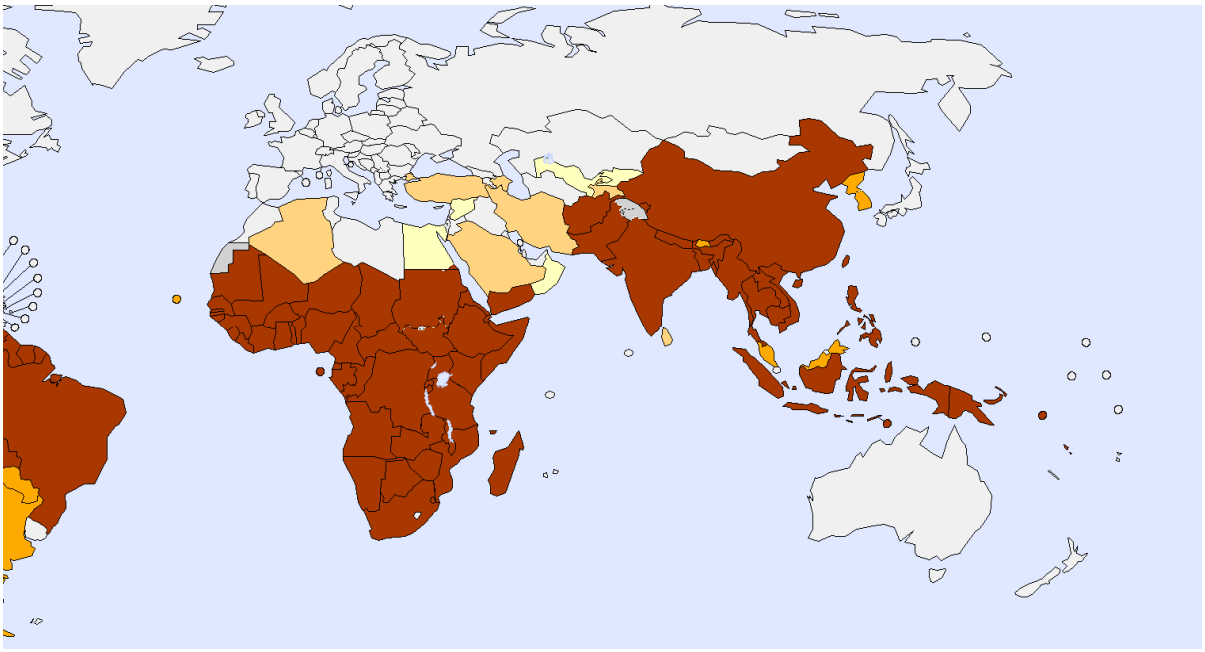

Figure 6 - Occurrence of malaria (WHO, 2014). Malaria occurrence in tropical and subtropical regions with focus on Africa and South-East Asia.

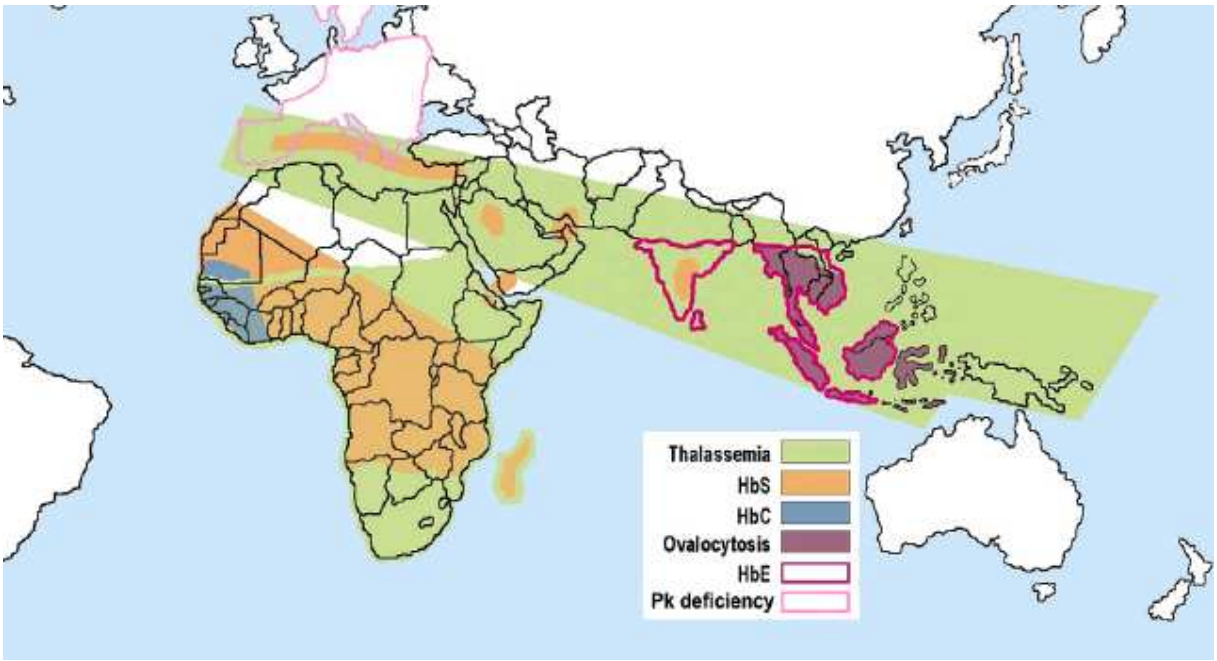

Figure 7 - Occurrence of haemoglobin-inherited disorders (LÓPEZ et al., 2010). Haemoglobin-inherited disorders, such as sickle cell disease are localised to tropical and subtropical regions including much of Africa and South-East Asia.

1.2 Human haemoglobin

To date, well over 200 haemoglobin variants have been described. Human haemoglobin is a globular metalloprotein transporting oxygen from the lungs to the tissues and facilitating the return transport of carbon dioxide (MARENGO-ROWE, 2006). It consists of four polypeptide subunits, known as 2α-globin chains and 2 β-globin chains, similar in length but differing in amino acid sequence. They are held together by ionic bonds, hydrogen bonds, hydrophobic interactions, and van der Waals forces, as well as four non-protein heme pigments, one in each of the subunits (WAZIR, 2015). These heme groups contain positively-charged iron (Fe^{2+}) ions which can reversibly bind to oxygen molecules and transport them to various areas of the body (Figure 8). The binding or release of oxygen is attendant on conformational changes within the entire haemoglobin which alter its affinity for oxygen. Besides the oxygen haemoglobin can also bind other molecules such as carbon monoxide, carbon dioxide and nitric oxide. The binding affinity for carbon monoxide is two hundred and fifty times greater than its affinity for oxygen. To bind oxygen successfully iron must be in the ferrous (Fe^{2+}) oxidation state. Oxidation to the ferric (Fe^{3+}) state without oxygen converts haemoglobin into methaemoglobin, which cannot bind oxygen (THOM et al., 2013).

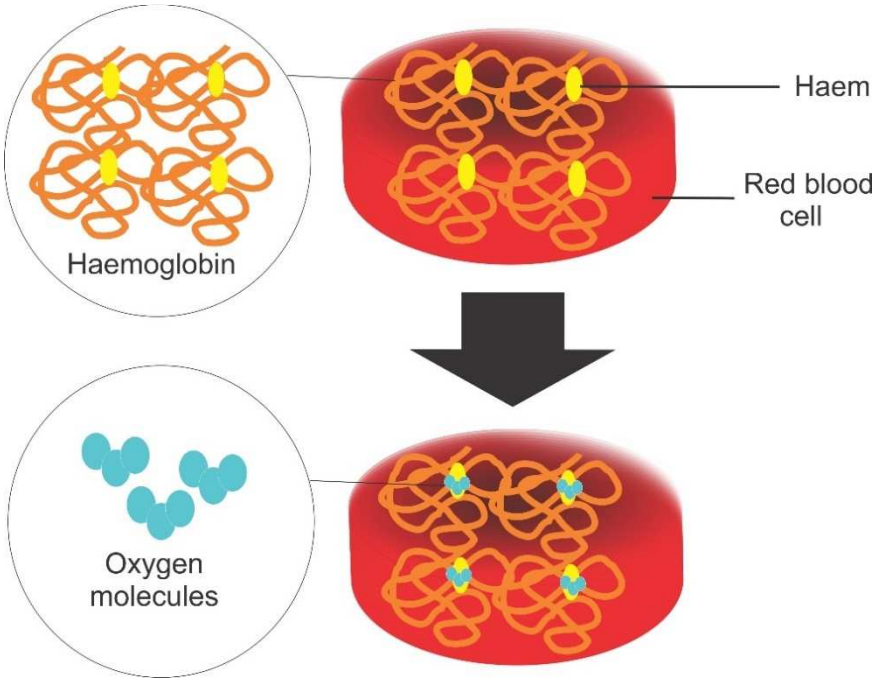

Figure 8 – Model of human haemoglobin modified according to U.S. National Library of Medicine (NIH). The binding or release of oxygen is attendant on conformational changes within the entire haemoglobin which alter its affinity for oxygen. To bind oxygen successfully iron must be in the ferrous (Fe^{2+}) oxidation state.

The alpha chain of all human haemoglobins, embryonic and adult, is the same. The normal adult haemoglobin HbA ($\alpha_2\beta_2$) is the most common with a normal amount over 97%. HbA_2 is a normal variant of HbA and consists of 2 α and 2 δ chains. It exists in small amounts in all adult humans (1,5 - 3,5% of all haemoglobin molecules). Albeit its biological importance is not yet known, it may be increased in people with the sickle-cell disease. In the first trimester of intrauterine life, zeta, epsilon, alpha, and gamma chains attain significant levels and in various combinations form Hb Gower I ($\zeta_2\varepsilon_2$), Hb Gower II ($\alpha_2\varepsilon_2$), Hb Portland ($\zeta_2\gamma_2$), and foetal haemoglobin (HbF) ($\alpha_2\gamma_2$) (SCHROEDER et al., 1968). Fetal haemoglobin (HbF) persists in the new-born roughly until 6 months and can bind oxygen with a higher affinity than adult HbA. In adults HbF is restricted to a small portion (5 - 8%) of red blood cells, termed F-cells (BOYER et al., 1975; MARENGO-ROWE, 1971). The level of HbF can be elevated in persons with sickle-cell disease and beta-thalassemia (SERJEANT, 2013).

1.3 Sickle Cell Disease

Sickle cells were first described in the peripheral blood of an anaemic patient from the West Indies by the Chicago physician Robert Herrick in 1910 (HERRICK, 1910). Haemoglobin S ("the sickle cell haemoglobin") is a structurally variant form of normal haemoglobin (HbA) that result from a single base pair mutation in the gene for the beta-globin chain of adult haemoglobin where glutamic acid at position 6 of the beta chain of HbA is changed to valine (Figure 9) (BUNN, 1997; RAPHAEL, 2005; ROSENTHAL, 2011).

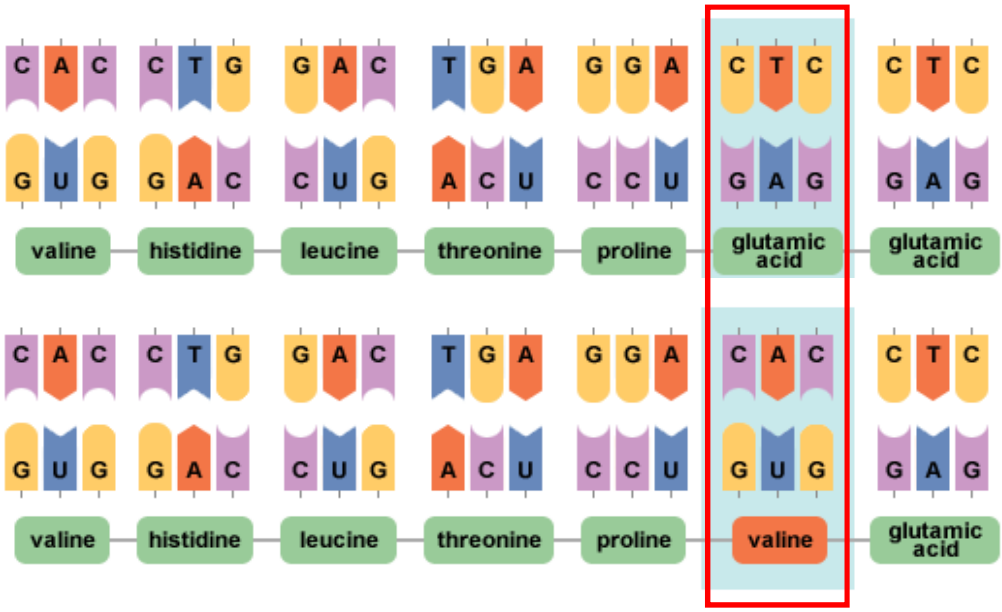

Figure 9 - The sickle cell mutation (www.bbc.vo.uk). Sickle cell disease is caused by only a point mutation within the beta-globin chain of adult HbA where glutamic acid at position 6 is substituted by a valine.

This substitution yields the electrophoretically distinct haemoglobin described by Linus Pauling in 1949 (PAULING et al., 1949). In sufficient concentration, these insoluble polymers give rise to the classical sickle morphology with polymerized HbS strands stretching and distorting the cell shape (Figure 10). This process causes severe damage to the erythrocyte membrane. Sickle red blood cells may adhere to endothelial cells or other normal erythrocytes resulting in aggregates and microvascular obstruction. (NAGEL; PLATT, 2001).

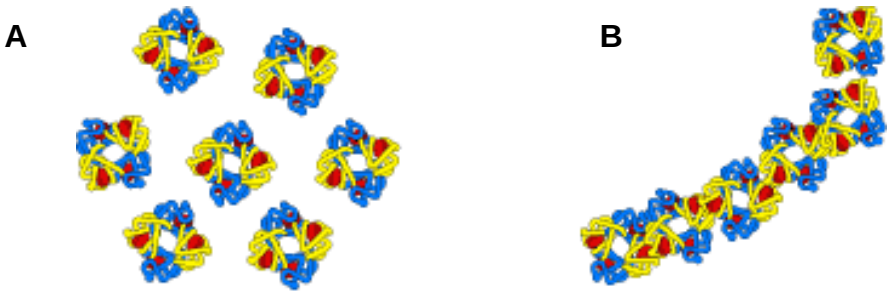

Figure 10 A - normal haemoglobin (HbA) **B -** polymerised haemoglobin (HbS) (sicklecellanemia2051.wordpress.com)

The sickle cell disease is characterised by the process of microthrombosis and microembolization which may result in stroke. Sickle cell anaemia exhibits polymorphic clinical complications, such as painful crises, priapism, dactylitis, pulmonary emboli, and osteonecrosis and ultimately damages every organ system including the retinae, spleen, liver, and kidneys (FARID, 2013; HEBBEL; MOHANDAS, 2001). Currently, the drug hydroxyurea is used as remedy which reduces significantly the clinical severity of SCD, for example by increasing the HbF levels. However, there are serious adverse effects, such as mutagenesis and carcinogenesis. Alternatively, blood transfusions and stem-cell based transplantations are used, though the costs are very high (FARID, 2013; STEINBERG et al., 2003; VERMYLEN; CORNU, 1997).

The occurrence of sickle cell disease has been analysed for more than 50 years (ALLISON, 1954; BEET, 1946) and the respective mode of action has been studied as well. However, a precise mechanism has not been identified yet and all hypothesis relating to a protective role against malaria fall into three main categories. Early work suggested that both erythrocytes containing HbS are less supportive for *P. falciparum* growth under low oxygen tensions as well as a reduced parasite invasion event into HbS carrying erythrocytes under low oxygen levels (FRIEDMAN, 1978; PASVOL et al.,

1978). Further it has been observed that HbS cells deposit oxidised, denatured haemoglobin at the inner site of the erythrocytic membrane (BROWNE et al., 1998), which occurs to a higher extent in HbS- than in HbA-red blood cells (RBC) and is even forced by release of non-haem iron that also binds to the RBC membrane (HEBBEL, 2003; SHENG et al., 1998). Due to these denaturing, pro-oxidative habitat the intracellular proliferation of the malaria parasite might be attenuated (BECKER et al., 2004). Secondly, a higher phagocytosis of parasite-infected sickled erythrocytes by host immune cells is suggested due to different shape facilitating the recognizing by immune cells (ABU_ZEID et al., 1991; LOPEZ et al., 2010). Recently, data have been accumulated which suggest that HbS might be involved in pathophysiological consequences of *P. falciparum* by reducing the quantity of proteins encoded by the *var*-gene family on the surface of the erythrocyte, such as *Pf*EMP1, which leads to a higher level of sequestration (CHOLERA et al., 2008; FAIRHURST et al., 2005). Indeed, in a very recent study by CYRKLAFF et al. (2011) it has been implicated that HbS carrying erythrocytes influence the actin cytoskeleton and the Maurer's cleft formation and thereby impair the vesicle transport towards the erythrocytic surface (Figure 11). More recently, it has been suggested that HbS is mediating a higher tolerance of the host as shown by a non-reduction of the parasite quantity or virulence (FERREIRA et al., 2011; HAQUE; ENGWERDA, 2011).

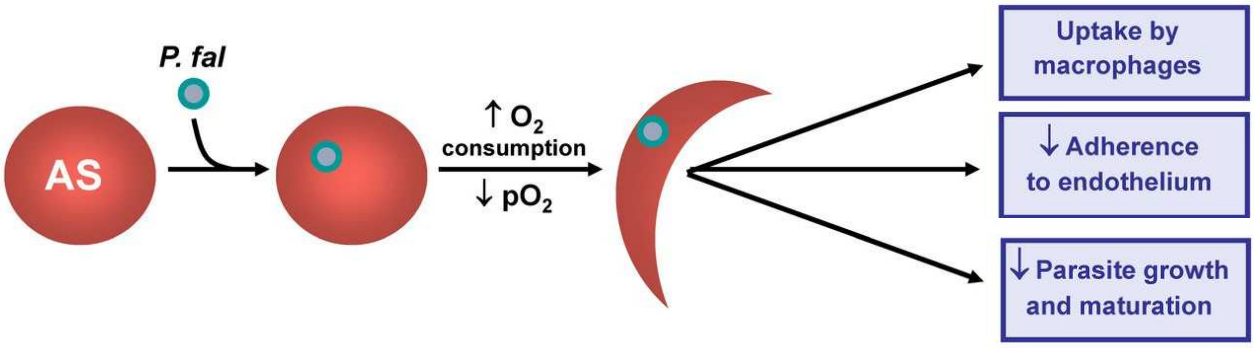

Figure 11 - Hypothesis for malaria protection (Modified according to BUNN, 2013).
Plasmodium falciparum infected erythrocytes suffer higher stress levels resulting in the different, sickle shape of the erythrocyte. First, an increased phagocytosis of infected sickled RBCs by macrophages was suggested to protect against malaria. Secondly, the protective role of sickle cell trait against malaria could be mediated by a decreased cytoadherence triggered by a reduced expression of the surface protein *Pf*EMP1. A third hypothesis proposed a diminished parasite growth and maturation in sickle cell RBCs.

Although these experiments were of some controversial nature as already outlined by ROSENTHAL (2011) the focus was on how the parasite is or not proliferating in an elevated oxidative environment. Human who are sickle cell carriers – either

homozygote or heterozygote – have higher levels of free, non-protein bound heme in the blood circulation (MÜLLER-EBERHARD et al., 1968), which is potentially toxic, due to its oxidative nature. It has been suggested that increased levels of human heme oxygenase 1 (HO-1) might detoxify free heme to CO, biliverdin and iron that binds subsequently to the protein ferritin H chain in HbS blood and thereby renders complicated (cerebral) malaria (FERREIRA et al., 2011). However, it remains questionable whether the protective nature of the increased level of free heme in HbS carriers is related to a higher tolerance to an increased level oxidative stressor mediated by HO-1 or by a higher susceptibility of the parasite by a decreased parasitaemia (ALLISON et al., 1954) within a pro-oxidative environment.

2. OBJECTIVES

The few existing antimalarials lose their efficacy due to the worldwide spreading of parasite's drug resistance. Therefore, the aim of this research project is to assess novel targets to interfere with. However, an intensive knowledge and understanding of the parasite's habit is required to interfere with the proliferation of the deadly pathogen. Over the past decades, it has been verified that genetically modified erythrocytes such as sickle cell trait reveal natural protection against malaria proliferation. This doctoral application is intended to analyse the mode of action of parasite growth within mutated human erythrocytes by focussing on the plasmodial haemoglobin catabolic pathway using transgenic parasites.

Key-Objectives:

(I) Amplification of open reading frames known to be involved in the plasmodial haemoglobin catabolism via PCR and cloning into the transfection vector pARL1a+

(II) Transfection of all cloned open reading frames into *P. falciparum*

(III) Verification of the respective protein expression via Western-blot analysis and protein trafficking by generation of GFP-chimeras

(IV) Growth analysis of transgenic parasites in wild type and genetically different erythrocytes

(V) Recombinant expression in *E. coli* for structural approaches – carried out in collaboration with Prof. Betzel at DESY, UHH, Germany.

3. MATERIAL AND METHODS

3.1 Instrumentation and Chemicals

3.1.1 Instrumentation

Agarose gel

Electrophoresis unit	Owl EasyCast B-Series Horizontal Gel Systems (Bio-Rad, USA)
Power Supply	Power PAC Basic (Bio-Rad, USA)

Balances	Practum 2102-15 (Sartorius, Germany) Practum 224-15 (Sartorius, Germany)
Beamlines	P14, EMBL, PETRA III, DESY (Hamburg, Germany)
CD-Spectrometer	J-815 (Jasco, UK)
Cytometer	Guava EasyCyte Mini (Guava Technologies, USA)
Centrifuges	Centrifuge 5804R (Eppendorf, Germany) Centrifuge 5415R (Eppendorf, Germany) Centrifuge 5424 (Eppendorf, Germany) Centrifuge 5415C (Eppendorf, Germany) Centrifuge 5810R (Eppendorf, Germany) Centrifuge 5418 (Eppendorf, Germany) Beckman Coulter™, Induction Drive Centrifuge J2-21M (Beckman, USA) PerfectSpin Mini (Peqlab, Germany) Mikro 22R (Hettich Centrifuges, UK) Megafuge 1.0 R (Heraeus, UK)
Clean bench	Biosafe B2 (Veco, Brasil)
Crystal imaging	CrystalScore (Diversified Scientific Inc., USA) Microscope SZX12 (Olympus, Japan)
Crystallisation robot	Honeybee 961 (Genomic Solutions, USA)

Crystal plate incubator	RUMED 3001 (Rubarth, Germany)
DLS instrumentation	Spectrolight300 (XtalConcepts, Germany) Spectrolight600 (XtalConcepts, Germany)
Electroporator	Gene Pulser Xcell™ Electroporation Systems #1652660 (Bio-Rad, Germany)
FPLC	ÄKTA Purifier P-901 (GE Healthcare, UK) ÄKTA Prime (GE Healthcare, UK)
Freezer	
-20 °C	Freezer vertical defrost 203L (FE26) (Electrolux, Brazil)
-80 °C	Thermo Forma 8600 (Thermo Fisher Scientific, Germany)
Incubator	IR AUTO FLOW Co_2 Water-Jacked Incubator (NUAIRE, USA)
Micropipette	Micropipette ResearchPlus (Eppendorf, Germany)
Microscope	Nikon Eclipse E200 MVR (Nikon, Tokyo) Primo Star (Zeiss, Germany) Imager M2 (Zeiss, Germany)
Laser source	HXP120C (Zeiss, Germany)
Microscope source	Eplax Vp232-2 Power Supply (Zeiss, Germany)
Microwave	Microwave Easy Clean 23L, LG MS2355R(A) (LG, Brazil)
Multichannel pipette	Multichannel pipette ResearchPlus (Eppendorf, Germany)
PCR machines	Mastercycler nexus (Eppendorf, Germany) Mastercycler nexus gradient (Eppendorf, Germany) Mastercycler Personal (Eppendorf, Germany)

pH Meter	S220 SevenCompact™ pH/Ion Benchtop Meter (Mettler-Toledo, USA)
Real-Time PCR	Mastercycler Epgradient S (Eppendorf, Germany)
Rocker	Rocker 3D digital (IKA,
Scanner	Cannon Brother
SDS PAGE	
Power Supply	Power PAC Basic (Bio-Rad, USA)
Electrophoresis unit	Mini-PROTEAN® Tetra Vertical Electrophoresis Cell (Bio-Rad, USA)
Sonifier	BRANSON Digital Sonifier 102C (Boston Industries Inc., USA)
SONICC	SONICC (Formulatrix, Germany)
Spectrophotometer	GeneQuant 1300 (GE Healthcare, UK) Nanodrop 2000c (Thermo Fisher Scientific, Germany) UVICON 933 (BIO-TEK Kontron Instruments, US)
Stirrer	C-MAG HS7 / MS7 (IKA, Germany)
Thermoblock	Thermomixer comfort (Eppendorf, Germany) Digital Thermoblock, HX-1 und HX-2 (Peqlab, Germany)
Tube Rotator	Roller 6 digital (IKA, Germany)
Ultrasonic bath	Elmasonic P60H (Elma, Germany)
UV-light source	CrystalLIGHT 100 (Nabitec, Germany)

UV Transilluminator	Image Quant 300 (GE Healthcare,UK)
Vortex	Vortex mixer Vixar VM3000 (Axygen/Corning, Brasil)
	Vortex-Genie-2 (Scientific Industries, USA)
	Vortex 3 (IKA, Germany)
Water bath	Microprocessor Controlled 280 Series water bath PRECISION
	PolyScience 5L-M (PolyScience, USA)
Western Blot	Trans-BLOT SD semi-dry transfer cell (Bio-Rad, USA)
	Power PAC HC (Bio-Rad, USA)

3.1.2 Utilised Chemicals

The chemicals used are, unless indicated otherwise, from the Company Sigma (Darmstadt, Germany), Hi-media (Mumbai, India), Carl Roth (Karlsruhe, Germany).

3.1.3 Bacterial strains and plasmids

3.1.3.1 Bacterial strains

The following competent bacterial strains of the species *E. coli* were used:

E. coli DH5α	Stratagene, USA
E. coli XL10 Gold	Stratagene, USA
E. coli BLR (DE3)	Stratagene, USA
E. coli pGro7/BL21	Stratagene, USA

The following *Plasmodium falciparum* strain was used:

3D7	Wellcome Trust, Dundee

3.1.3.2 Plasmids

pASK-IBA3	IBA, Germany
pARL1a-hDHFR	
pARL1a-BSD	

The map of the vector used is shown in the appendix.

3.1.4 Enzymes

Fermentas

RNase A	10 mg/ml

New England Biolabs

Bsa I	10000 U/ml
Hind III	10000 U/ml
Xba I	10000 U/ml
Dpn I	10000 U/ml
T4-DNA-Ligase	5000 U/ml

Sigma-Aldrich

Proteinase K	> 800 U/ml

3.1.5 Nutrient media and agar plates

The following nutrient media were used for the cultivation and selection of suitable *E. coli* bacteria:

LB medium (per liter): 10 g NaCl
10 g of Bacto-Tryptone BBL
5 g of Bacto Yeast extract

L agar: 15 g of Agar-Agar on 1 liter of LB medium

All prepared media were autoclaved for 20 min at 120 °C (2.1 bar) immediately after their preparation. In the case of selective media for the selection of the above mentioned bacterial strains and vectors, the corresponding antibiotics were added to the cooled media. Ampicillin at a final concentration of 100 µg/ml was used. Ampicillin inhibits D-alanine trans-peptidase in the synthesis of murein sacculus. Chloramphenicol was used with a final concentration of 34 µg/ml and inhibits protein synthesis by blocking peptidyl transferase.

The following medium was used for *Plasmodium falciparum* cell culture:

RPMI 1640 medium (1 L) 15,9 g RPMI 1640
1 g of sodium bicarbonate
2 g of D - (+) - glucose
5 g Albumax II
27.2 mg of hypoxanthine
pH 7,4

All the prepared media were sterile filtered immediately after their preparation under a sterile clean bench.

3.1.6 Overnight culture

To selectively amplify individual bacterial colonies, they were transferred from the selection plate to a 3 - 4 ml medium using a sterile toothpick or pipette tip. In order to ensure that only the desired clones grow, the liquid medium was previously mixed with either the antibiotic ampicillin in a ratio of 1:1000 or with both chloramphenicol (1:1000) and ampicillin. The cells were subsequently grown overnight in an incubator at 37 °C under shaking conditions.

3.1.7 Glycerin stocks

Glycerin stocks are used to store a clone for longer periods. 1 ml of the incubated overnight culture was mixed with 800 µl of 30% glycerol and frozen at -80 °C.

3.1.8 Buffers, solutions and consumables

Agarose-Gelelectrophoresis

TAE-buffer (50x)	2 M Tris, 0,05 M EDTA, 1 M acetic acid, pH 8,5
Loading dye (5x)	0,25% bromophenol blue, 0,25% xylene cyanol, 1 mM EDTA, 50% glycerol
DNA Marker	GeneRuler 1 kb DNA Ladder (Thermo Scientific, Germany), GeneRuler 1 kb plus DNA Ladder (Thermo Scientific, Germany)
Ethidium bromide	stock 10 mg/ml (Sigma, Germany)

Enzymes

AvrII	#R0174S (New England BioLabs, USA)
BclI	#R0160S (New England BioLabs, USA)
BsaI	#R0535S (New England BioLabs, USA)
EcoRI	#R0101S (New England BioLabs, USA)
HindIII	#R0104S (New England BioLabs, USA)
KpnI	# R0142S (New England BioLabs, USA)
XbaI	#R0145S (New England BioLabs, USA)
XhoI	#R0146S (New England BioLabs, USA)
XmaI	#R0180S (New England BioLabs, USA)
T4-DNA-ligase	#M0202S (New England BioLabs, USA)

Preparation of Competent *E. coli* cells

Solution 1	80 mM $CaCl_2$
Solution 2	80 mM $CaCl_2$, 20% (v/v) glycerol

Isolation of gDNA

gDNA lysis buffer	50 mM Tris/HCl pH 8,0, 2% SDS, 20 mM EDTA
Proteinase K	stock solution 10 mg/ml
Salt solution	NaCl, saturated in dH_2O

Precipitation of gDNA

Salt solution	3 M sodium acetate, pH 4,8

Protein expression

Anhydrotetracycline	stock solution 2 mg/ml in 50% ethanol (IBA)

Protein purification via Strep-Tag

PMSF	stock solution 0,1 M PMSF in isopropanol
Buffer E (Elution buffer)	100 mM Tris/HCl, 150 mM NaCl, 1 mM EDTA, 2,5 mM desthiobiotin, pH 8,0 (adjustment with HCl)
Buffer R (Regeneration buffer)	100 mM Tris HCl, 150 mM NaCl, 1 mM HABA, pH 8,0 (adjustment with HCl)
Buffer W (Wash buffer)	100 mM Tris, 150 mM NaCl, pH 8,0

Protein purification via His-Tag

His-lysis buffer	Buffer W with 10 mM imidazole (imidazole addition after autoclaving)
His-washing buffer	Buffer W with 20 mM imidazole (imidazole addition after autoclaving)
His-elution buffer	Buffer W with 50-100 mM imidazole (imidazole addition after autoclaving)

Ni-NTA agarose regeneration

SDS buffer	2% (w/v) in dH_2O
EDTA buffer	100 mM, pH 8,0 in dH_2O
NiSO4 buffer	100 mM in dH_2O
Regeneration buffer	6 M guanidine chloride, 0,1 M acetic acid

SDS-PAGE

Ammoniumpersulfate	10% (w/v) in dH_2O
TEMED	~99% (Sigma Aldrich, Germany)
Separation gel buffer	1,5 M Tris/HCl, pH 8,9
Stacking gel buffer	0,5 M Tris/HCl, pH 6,8
Electrophoresis buffer	0,1% SDS (w/v), 192 mM glycine, 25 mM Tris
6 x SDS sample buffer	2% SDS (w/v), 50 mM Tris, pH 6,8, 10% (w/v) glycine, 0,02% (w/v) bromphenol blue, 0,05% (v/v) β-mercaptoethanol

Staining solution	staining solution A and B in the ratio 1:1
Staining solution A:	0,2% (w/v) Coomassie Brilliant Blue R-250 in 96% ethanol
Staining solution B:	20% (v/v) of glacial acetic acid in dH_2O
Destaining solution	20% (v/v) ethanol, 10% (v/v) glacial acetic acid in dH_2O
SDS-PAGE Marker	Pierce™ Unstained Protein MW Marker #26610 (Thermo Fisher Scientific, Germany) Spectra™ Multicolor Broad Range Protein Ladder #26634 (Thermo Fisher Scientific, Germany)

<u>Western-Blot</u>

Nitrocellulose membrane	Nitrocellulose Membrane, 0,2 µm #1620112 (Bio-Rad, USA)
Ponceau S	0,2% (w/v) Ponceau S in 5% (v/v) acetic acid
Transfer buffer	25 mM Tris, 192 mM glycine, 20% (v/v) methanol
Stripping solution	50 mM Tris/HCl, 50 mM NaCl, pH 2,5
PBS	10 mM Na_2HPO_4, 1,8 mM KH_2PO_4, 2,6 mM KCl, 136,9 mM NaCl, pH 7,4
Blocking solution	3% BSA, 1x PBS
PBS-Tween 20 0,03%	0,03% Tween 20, 1x PBS
PBS-Tween 20 0,3%	0,3% Tween 20, 1x PBS

<u>Antibodies and WB detection</u>

1st antibodies	StrepMAB-Classic, purified, lyophilized, IgG1, # 2 1507-001 (IBA, Germany) Anti-GFP, monoclonal (Dianova, Germany) Anti-Myc-tag, monoclonal (Dianova, Germany)
2nd antibody	Goat anti-mouse IgG-HRP (Jackson Immunoresearch Laboratories, UK)
ECL (enhanced chemiluminescence) detection	Amersham ECL Western Blotting Detection Reagents (Thermo Fisher Scientific, Germany)

Activity assay

Buffer	50 mM Tris/HCl, 1 mM $MnCl_2$, pH 7,5

Plasmodium falciparum culture and lysis

1 x HT-PBS	16 mM Na_2HPO_4, 4 mM NaH_2PO_4, 126,6 mM NaCl, pH 7,2
Sorbitol	5% (w/v) D-sorbitol in HT-PBS
Saponin	0,2% (w/v) saponin in HT-PBS
Giemsa staining solution	Giemsa's azure-eosin-methylene blue solution

Crystallization screens

AmSO4-Suite	Qiagen, Germany
JCSG-plus (MD1-40)	Molecular Dimensions, UK
Morpheus (MD1-47)	Molecular Dimensions, UK
PACT premier (MD1-36)	Molecular Dimensions, UK
Stura Footprint (MD1-20)	Molecular Dimensions, UK

3.1.9 Bioinformatics tools and software

Adobe Photoshop	Version CS5.1, Adobe Systems Inc, 2010
NCBI-BLAST	www.ncbi.nlm.nih.gov/BLAST
PlasmoDB	www.plasmodb.org
ExPASy	www.expasy.org
Generunner	Hasting Software Inc., 2004
Corel DRAW X5, 2011	
Corel PHOTO-PAINT X5, 2010	
GraphPad Prism 6	
XtalPred Server	www.ffas.burnham.org/XtalPred-cgi/xtal.pl
TMHMM Server	www.cbs.dtu.dk/services/TMHMM/

3.2 General molecular biology methods

3.2.1 Polymerase-chain reaction (PCR)

PCR is a common method for selectively amplifying a defined section from a complex DNA mixture. Either the thermostable Taq DNA-polymerase was used within the PCR

Supermix (Invitrogen) or the *Pfu* polymerase (Promega), which has the ability of 3'-proof reading. One cycle of PCR consists of denaturation of DNA (94 - 98 °C), the annealing of primers (50 - 60 °C) and the DNA synthesis (elongation, at 72 °C). The annealing temperature is dependent on the length and GC ratio of the open reading frame (ORF) to be amplified. Thus, guanine and cytosine have three hydrogen bonds and therefore have a higher melting temperature than adenine and thymine, which have only two hydrogen bonds. After about 30 repetitions of this cycle, the PCR is terminated and the desired DNA sequence is amplified exponentially. The reaction mixture was prepared on ice according to the following scheme (Table 1).

Table 1 - Pipetting scheme for a 50 µl PCR mixture.

Components	Volumes
Template (129 µg/ml)	1 µl
Forward Primer (30 µM)	1 µl
Reverse Primer (30 µM)	1 µl
PCR-Supermix (Invitrogen)	47 µl

The PCR was carried out according to the following program (Table 2):

Table 2 - PCR-Cycling Program

Reaction step	Temperature	Duration
Primary denaturation	94 °C	3-5 min
Denaturation	94 °C	30 sec
Annealing	45 - 48 °C	45 sec
Elongation	68 °C	1 - 2 min/1kb
Final Elongation	68°C	1 - 2 min/1kb
Hold	4°C	∞

30 Cycles

The amplified PCR product was detected by applying 5 µl to a 1% agarose gel staining the DNA with the intercalating fluorescent dye ethidium bromide (see 3.2.4).

3.2.2 Reverse-Transcription-PCR (RT-PCR)

The method of reverse-transcriptase-PCR (RT-PCR) was commonly used to selectively amplify transcribed genes from RNA. The first step involves the rewriting of RNA into cDNA by the RNA-dependent DNA polymerase, the reverse transcriptase, an enzyme derived from retroviruses. When using an oligo (dT) primer, all transcripts with a poly-A tail are unspecifically rewritten. The oligo (dT) is attached to the poly-A tail of the messenger RNA (mRNA). In this thesis, the SuperScriptIII One Step RT-PCR system with Platinum® Taq DNA polymerase (Invitrogen) was used according to the manufacturer's instructions.

3.2.3 DpnI digestion

DpnI digestion is performed for the digestion of parental plasmid DNA, which serves as template in a PCR. The plasmid DNA of various *E. coli* strains is methylated while the PCR products are not methylated. DpnI endonuclease specifically cleaves methylated DNA, the recognition sequence is shown in Figure 12.

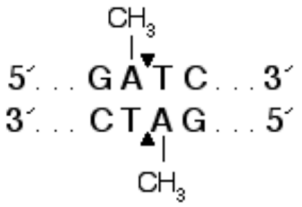

Figure 12 - Recognition sequence (New England Biolabs).

Each PCR reaction was digested with 1 µl DpnI (New England Biolabs) overnight at 37 °C.

3.2.4 Electrophoretic separation of nucleic acids

In gel electrophoresis, charged molecules (DNA, RNA, proteins) migrate through the pores of a gel matrix (e.g. agarose) in an electric field and are separated in molecular mass. The pore size depends on the concentration of the agarose gel. The higher the agarose concentration in the gel, the more "fine-meshed" is the gel. Accordingly, small molecules migrate faster and farther than large molecules. Due to the negatively charged phosphate groups of the sugar-phosphate backbone of nucleic acids, they

always migrate in the electric field from the cathode to the anode. In order to make a statement about the individual molecular mass of the fragment, a molecular mass marker is applied. The nucleic acids separated in the gel are visualized by the intercalating dye ethidium bromide. The molecule is incorporated between the bases of RNA and DNA molecules. After the nucleic acid-dye-complexes have been excited with UV light at a wavelength of 312 nm, the orange-red light can be documented using the geldocumentation system (Image Quant 300, GE Healthcare, UK).

To separate DNA fragments with a molecular weight between 0,5 and 7 kb, a 1% agarose gel is used:

0,4 g of agarose were boiled in 40 ml of 1 x TAE, cooled down to about 60 °C and the gel was poured after the addition of 2,5 µl of ethidium bromide (10 mg/ml). Prior to loading the gel, DNA samples were supplemented with sample loading buffer to increase the density. One tenth of the volume of PCR products or cloning digestion, as well as the entire batch of analytical digestion, was applied. In addition, 3,5 µl of a DNA marker (GeneRuler™ 1kb DNA Ladder, Thermo Scientific, Germany) was applied, by which the size of the DNA fragments could be estimated (Figures 13A and 13B). Electrophoresis was performed at a constant voltage between 100 and 120 V.

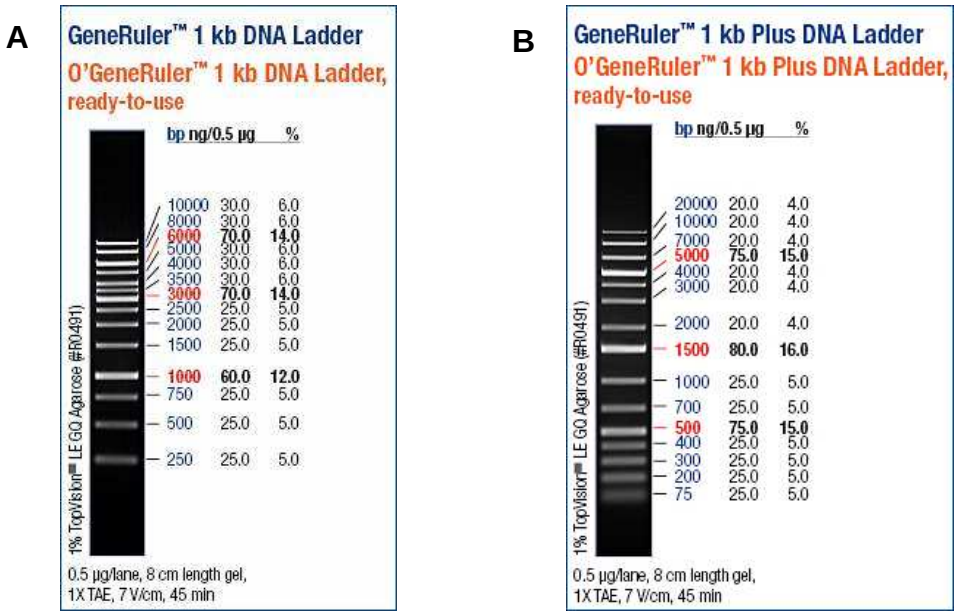

Figure 13 A - GeneRuler™ 1kb DNA Ladder, Thermo Scientific, Germany
B - GeneRuler™ 1kb Plus DNA Ladder, Thermo Scientific, Germany

3.2.5 Purification of DNA via affinity columns

Purification of PCR products and digested vectors was performed via a DNA affinity column. Thereby, DNA binds to a silica matrix and can then be eluted with dH_2O. Thus, DNA is relieved from salts, enzymes and free nucleotides. In this thesis, the peqGOLD Microspin CyclePure Kit (Peqlab, Germany) was used according to the manufacturer's instructions. The elution was carried out in a volume of 30 - 50 µl of warm dH_2O.

3.2.6 Determination of the concentration of nucleic acids by nanodrop

The determination of the concentration of isolated total RNA and DNA was carried out by means of nanodrop (Thermo Scientific, USA) with 1,0 µl sample each. The measurement is based on the absorption maximum of the nucleic acids at 260 nm and allows a statement about the quantitative success of the purification. Aromatic rings of the bases are responsible for absorption. An RNA absorbance value of 1 corresponds to a concentration of 40 ng/µl. On the other hand, an absorbance value of 1 of a DNA solution corresponds to a concentration of 50 ng/µl, meanwhile DNA has a lower absorption due to its double strands. Since the proteins have an absorption maximum of 280 nm, the ratio of the absorbance at 260 nm to the absorbance at 280 nm is determined in order to be able to determine the purity of the nucleic acid solution. A pure nucleic acid solution has an A260/A280 value between 1,8 and 2,1. A smaller value indicates a contamination with proteins or phenol.

3.2.7 Restriction enzyme digestion

Restriction enzyme digestion was used to prepare DNA fragments and the respective vector for latter ligation into the plasmid. Both were digested with appropriate restriction enzymes (see chapter 4.1.1 - 4.1.13) according to manufacturer’s protocol for 2 h at 37 °C. The PCR product and vector were purified (see chapter 3.2.5) separately and eluted in 30 µl dH_2O.

3.2.8 Ligation

Within the ligation reaction, the terminal 5'-phosphate groups and 3'-hydroxyl groups of the sugar-phosphate backbone of DNA molecules are linked to one another by means of the ATP-dependent T4 DNA forming phosphodiester bonds. Either the vector

pASK-IBA3 (IBA, Germany) or pARL1a-hDHFR or pARL1a-BSD were used for ligation. The batch was prepared on ice as shown in the following scheme (Table 3).

Table 3 - Pipetting scheme for ligation reaction

Components	Volumes
Vector	2 µl
PCR product	10 µl
10 x T4-DNA-Ligase-buffer	2 µl
T4-DNA-Ligase	1 µl
dH_2O	5 µl
Total volume	20 µl

Ligation was performed for two hours at room temperature or overnight at 14 °C (SAMBROOK et al., 1989).

3.2.9 Preparation of chemically competent E. coli cells by means of $CaCl_2$

A single *E. coli* colony was inoculated into 10 ml of LB medium and incubated overnight at 37 °C under shaking conditions. The pre-culture was cultured at a ratio of 1:100 in 200 ml of LB medium and incubated at 37 °C by a spin of 150 rpm until an A600 of 0,5-0,7 was reached. The bacterial culture was then cooled in ice water for 15 min. All further steps were carried out on ice (solutions and rotors cooled). The culture was pelletized for 15 min at 3000 x g under cooling conditions. Subsequently, the supernatant was completely removed and the pellet resuspended in 50 ml of 80 mM $CaCl_2$. After an incubation of at least 40 min on ice, the suspension was again centrifuged (15 min, 3000 x g, 4 °C). The supernatant was removed and discarded, the pellet was dissolved in 5 ml of 80 mM $CaCl_2$ supplemented with 20% (v/v) glycerol, and the cells were then aliquoted (approximately 200 µl) in pre-cooled 1,5 ml Eppendorf vials. The aliquots were immediately shock-frozen at -80 °C.

3.2.10 Transformation

During transformation DNA, such as plasmids, can be transformed into the host cells. Within the scope of this thesis, a heat shock transformation was performed with 200 µl of the competent *E. coli* cells (*E. coli* XL10 Gold, DH5α, BLR DE3 and BL21-pGro7, respectively). After adding of 10 µl of the ligation mixture or 0,5 - 2,0 µl of plasmid DNA, the reaction vessel was incubated for 30 minutes on ice. During this time, the DNA molecules bind to lipopolysaccharides (LPS) which is facilitated by the treatment of the competent cells with $CaCl_2$. The plasmids can be subsequently integrated into the bacterial cell by means of a 60 second heat shock at 42 °C, which caused a short-term permeability of the membrane. After two-minute incubation on ice, 1 ml of LB medium was added to the cells for growth and formation of antibiotic resistance. The culture was incubated for 45 - 60 min in a thermoblock at 37 °C under shaking conditions (400 rpm) and was then centrifuged for one minute at 13000 x g in the Eppendorf table centrifuge. The supernatant was discarded and the bacterial pellet was resuspended in the reflux. Finally, the suspension was plated on an LB agar plate with appropriate selective antibiotic (e.g. ampicillin or chloramphenicol) and incubated overnight at 37 °C (SAMBROOK et al., 1989).

3.2.11 Plasmid isolation

A common method for isolation of plasmids is the alkaline lysis developed in 1979 by Birnboim and Doly. The bacterial cells were first resuspended by addition of an RNase-containing re-suspension buffer. The subsequent lysis buffer contains SDS, which breaks up the bacterial cells and NaOH, which denatures the bacterial genomic DNA and the recombinant plasmids by the alkaline pH. Finally, a neutralisation buffer was added to the lysate. By the sudden neutralisation of the pH value, the nucleic acids re-nature, whereby the large genomic DNA precipitates with the cell debris and can be separated from the plasmids remaining in solution by simple centrifugation. The solute plasmids were reversibly bound to a silica membrane and thus separated from other soluble cell components. Last impurities could be removed by several washing steps. The plasmid DNA was eluted from the column by 50 µl of warm, nuclease-free water. The samples were stored at -20 °C until further use. The preparation was carried out using the PeqGOLD Plasmid Miniprep Kit (Peqlab, Germany) according to the manufacturer's instructions. The resulting DNA was used directly for restriction

analyses, transformations or sequencing carried out by the Human Genome and stem cell Center (USP, Brazil).

3.2.12 Analytic digestion

An analytic digestion considers whether the plasmids contain the desired fragment. Plasmids are digested by restriction endonucleases, which are isolated from bacteria. In bacteria, restriction enzymes protect their own DNA from foreign DNA, such as viruses. These restriction enzymes have the property of recognizing a defined base sequence of DNA and, within this base sequence, cutting the DNA sequence specifically. Only type II restriction enzymes were used in this study. This type of restriction enzymes intersects the DNA within or in immediate adjacency of its recognition sequence, which is mostly palindromic. They do not require ATP and have no methyltransferase activity. The name of the restriction enzymes derived from bacteria from which they were isolated. In the present thesis, the enzymes AvrII from *Anabaena variabilis,* BclI from *Bacillus caldolyticus,* BsaI from *Bacillus stearothermophilus*, EcoRI from *Escherichia coli*, HindIII from *Haemophilus influenza*, KpnI from *Klebsiella pneumoniae*, XbaI from *Xanthomonas badrii,* XhoI from *Xanthomonas holcicola* and XmaI from *Xanthomonas malvacearum* (all New England Biolabs) were used. Isolated plasmids were digested with relevant restriction endonucleases, typically XbaI and HindIII (pASK-IBA3 cloning) or KpnI or rather XmaI and XhoI (all New England Biolabs, USA). Due to the small amounts, e.g. of enzyme, which had to be pipetted, a master mix was established. After mixing the components by pipetting several times, the batch was incubated for 2 hours at 37 °C in the heating block. The approximate size of the integrated fragment was then determined by means of electrophoretic separation in an agarose gel (see 3.2.4).

3.2.13 Sequencing

In order to examine the DNA sequence of the cloned construct regarding mutations DNA sequencing was performed. The sequencing reaction was carried out according to the principle of dideoxy chain termination synthesis (SANGER et al., 1977). Similarly to PCR, a DNA strand is synthesized starting from only one primer, however this strand is randomly interrupted by the incorporation of fragmentation nucleotides. These so-called terminators are 2'-3'-dideoxy nucleotides. They are labelled with four different

fluorescent dyes and allow optical detection of the differently sized chain termination fragments. A sequencing approach resides:

5 µl of plasmid DNA (1µg)
2,5 µl sequencing primer (5 µM).

Sequencing of the prepared samples was carried out by the Human Genome and stem cell Center (USP, Brazil). The sequences were analysed by means of GeneRunner version 6.2.07.

3.3 Methods of protein biochemistry

3.3.1 Recombinant expression

Prior to expression, the desired DNA construct was first transformed into an expressible bacterial strain, such as *E. coli* BLR-DE3. A 10 ml pre-culture was inoculated in form of a single colony in LB-Amp medium (10 µg/ml) overnight at 37 °C under shaking conditions. On the following day, the expression culture was inoculated under the same conditions in a ratio of 1:100 and cultured to an A600 of 0,5 - 0,7. After reaching the optical density, the culture was induced with anhydrotetracycline (AHT, 2 mg/ml) at a ratio of 1:10000. Induction was performed overnight at 20 °C under shaking conditions. The next morning, the culture was centrifuged for 15 min at 7000 x g under cooling conditions (4 °C) and the pellet was stored at -20 °C until further use.

3.3.2 Disruption of bacterial cell

The frozen bacterial pellet was thawed in a beaker with cold tap water for about 20 minutes and re-suspended in the respective protein buffer. Subsequently, a spatula tip lysozyme was added. Lysozyme is an enzyme which hydrolyses β-1,4-glycosidic bonds between N-acetylmuraminic acid (NAM) and N-aceytlglucosamine residues (NAG) in peptidoglycans. The cell walls of bacteria consist of just these peptidoglycans and are thus degraded. After incubation for 20 min on ice, the protease inhibitor PMSF (phenylmethylsulfonyl fluoride, 0,1 M) was added at a ratio of 1:1000. The breakdown of the bacterial cell was achieved by sonification in a Branson sonifier at 35 kHz for 6 x 30 seconds. The obtained bacterial lysate was pelletised for one hour at 16500 x g and 4 °C (Beckman Coulter ™, Induction Drive Centrifuge J2-21M).

3.3.3 Protein purification via Strep-tag

2 ml Strep-Tactin-Sepharose (50% suspension) was added to an empty column and the matrix was equilibrated with a column volume of cold buffer W. The supernatant of the centrifuged bacterial lysate was added to the column and the flow through was discarded. A spatula tip of the pellet fraction re-suspended in 100 µl of buffer W as well as 100 µl of the supernatant and 100 µl of the flow through of the affinity chromatography were supplemented with 25 µl of 6 x SDS sample buffer, boiled for 10 min and then stored at -20 °C until separation in a SDS-PAGE. The sepharose was then washed twice with 1 column volume of buffer W each. Elution was carried out by adding buffer E (containing Desthiobiotin) to the matrix and the eluate was collected. For regeneration of the sepharose, a volume buffer R as well as two column volumes of buffer W, were added successively to the matrix and the flow was discarded.

3.3.4 Protein quantification

3.3.4.1 Bradford assay

The protein concentration of purified proteins was determined according to Bradford (BRADFORD 1976). The colorimetric detection is based on the specific binding of the trimethylmethane dye Coomassie Brilliantblue G250 to proteins. The dye binds preferentially to arginine residues via specific hydrophobic and electrostatic interactions, as well as to a lesser extent to some other basic and aromatic amino acid residues (COMPTON; JONES, 1985). Furthermore, this dye is present in two forms with different absorption maxima. In an acidic solution, the protonic, cationic form with an absorption maximum of 470 nm (red) is predominant. The formation of the dye-protein complex displaces the equilibrium towards the anionic form of the dye which has an absorption maximum of 595 nm (blue) (COMPTON; JONES, 1985). The extinction coefficient of the dye-protein complex is much higher than that of the free dye. Therefore, the increase in absorbance at 595 nm can be photometrically measured by the formation of the complex with high sensitivity against free Bradford reagent (ECKERT; KARTENBECK, 1997). The most commonly used bovine serum albumin (BSA) was chosen as standard. For protein quantification, 2 µl of protein solution were mixed with 1 ml of Bradford reagent in a cuvette and absorption at 595 nm (A595) was measured in a GeneQuant 1300 (GE Healthcare, UK).

3.3.4.2 Protein quantification with the Nanodrop 2000c

A much more precise determination of the protein concentration was carried out via the nanodrop 2000c (Thermo Fisher Scientific, Germany). Prior to measurement 2 µl protein buffer were applied on the sensor to blank measurement. Subsequently, the procedure was repeated by applying 2 µl of protein solution. Measurements were carried out in duplicates. To determine the exact protein concentration values for molar extinction coefficient (ε) and molecular weight were applied to Lambert-Beer-Law:

$$A_{280} = \varepsilon * b * c$$

A_{280}= absorption at 280 nm
ε= molar extinction coefficient [M-1 cm-1]
b= path length [cm]
c= protein concentration [mg/ml]

3.3.5 SDS-polyacrylamide gelelectrophoresis (SDS- PAGE)

The basic principle of all electrophoretic separation techniques for proteins is the migration of charged molecules in an electric field. The separation of the molecules occurs not only via charges, but also by size and shape of proteins. Adding SDS (sodium dodecyl sulfate), the secondary and tertiary structures of proteins are dissolved and, on the other hand, charges of the proteins are effectively covered so that the migration in the electric field occurs only because of the negative charge of the SDS. Thus, the proper charge of the examined proteins does not interfere in separating process via polyacrylamide gel electrophoresis (PAGE). The separation takes place exclusively on the basis of their molecular mass. Since large proteins suffer a greater friction force in the narrow-pored gel matrix and have a decreasing mobility (LAEMMLI, 1970). By co-electrophoresis of calibration proteins of known size, the molecular weight of the separated proteins can be estimated. The utilized protein ladders are demonstrated in figure 14. The PAGE was performed in a vertical, discontinuous system (BioRAD Laboratories GmbH, Germany).

In the following, only 10 - 12% separating gels were used with 5% stacking gels (Table 4), which were incubated with a maximum current of 35 mA. Samples previously

supplemented with 6 x SDS sample buffer were boiled and centrifuged for 5 min at 14000 x g (Eppendorf centrifuge 5424) to remove any residues (SAMBROOK et al., 1989). The gel was loaded with 5 µl of sample from the pellet, 10 µl of supernatant and flow through fraction, as well as with 20 µl of elution fraction (0,5 µg for Coomassie blue staining and 2 µg of purified protein or rather 10 µg protein from cell lysate or tissue homogenate for Western Blot analysis) and 7 µl of marker.

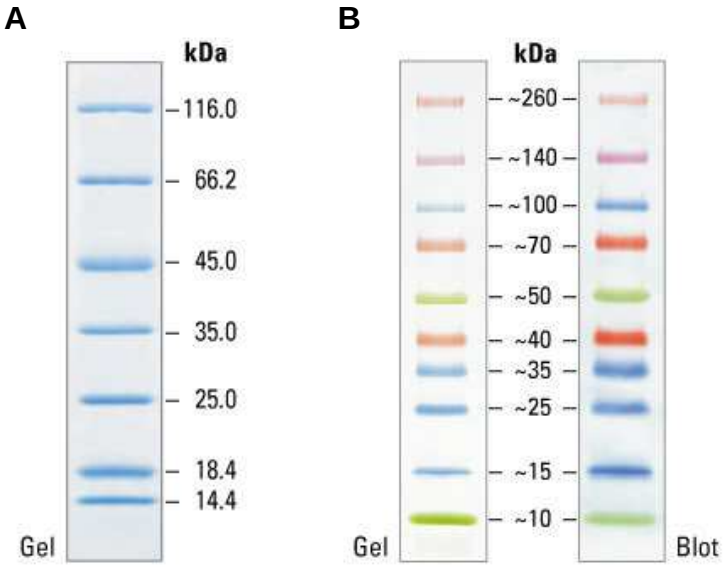

Figure 14 A - Pierce™ Unstained Protein MW Marker (Thermo Fisher Scientific, Germany), **B -** Spectra™ Multicolor Broad Range Protein Ladder (Thermo Fisher Scientific, Germany).

Table 4 - Scheme for the preparation of two polyacrylamide gels.

Component	10% Separating gel	5% Stacking gel
1,5 M Tris-HCl, pH 8,0	3 ml	----
0,5 M Tris-HCl, pH 6,8	----	1 ml
30% Acrylamide	4,6 ml	720 µl
10% SDS	120 µl	40 µl
dH_2O	6 ml	2,49 ml
10% APS	120 µl	40 µl
TEMED	10 µl	5 µl
Total volume	13,85 ml	4,295 ml

3.3.6 Coomassie staining of SDS-Gels

Coomassie Brilliant Blue R-250 is conventionally used for staining of polyacrylamide gels. The triphenylmethane dye is attached to basic side chains of amino acids and can therefore colour proteins unspecifically.

The SDS gels were either stained for one hour or overnight in Coomassie R-250 staining solution and then maintained in destaining solution until the protein bands became clearly visible.

The documentation of the destained gel was carried out by scanning. However, if an electrophoretic transfer is to be carried out, Coomassie staining is omitted and the separating gel is blotted immediately after ending of electrophoresis.

3.3.7 Electrophoretic transfer of proteins (Western Blot)

Immediately after completion of the SDS-PAGE, the in size separated proteins are transferred to a nitrocellulose membrane (SAMBROOK et al., 1989). In electrophoretic transfer, the proteins are transferred to the membrane from the gel by applying a voltage. In this thesis, the semi-dry blot was used which compared to the wet blot, facilitate a faster transfer and requires less transfer buffer. Due to the methanol content in the transfer buffer, the binding of the proteins to SDS can be loosened by means of wetting the membrane. This results in an increased binding of the proteins to the nitrocellulose membrane. For the transfer, the separating gel and the blotting papers from BioRad were incubated for a few minutes in transfer buffer and then placed on top of each other (Figure 15). Electrophoretic transfer was performed for 30 min at a constant voltage of 10 V per gel.

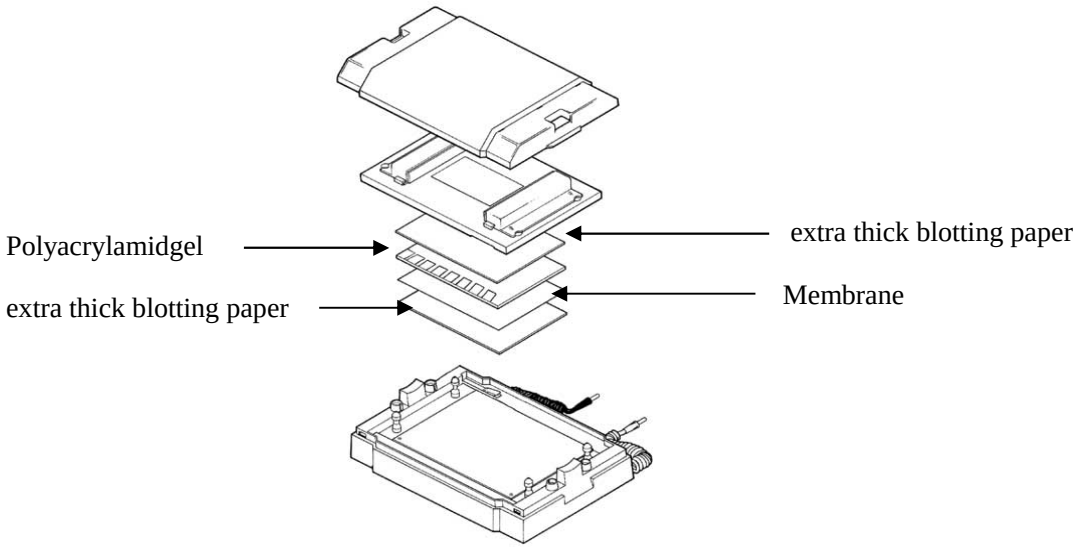

Figure 15 - Model of the semi-dry Western Blot system (Bio-Rad).

Subsequently, the proteins on the membrane can be stained by means of the red dye Ponceau S (Sigma-Aldrich, Germany) and the efficiency of the transfer can be verified. Afterwards, the immunological detection was continued directly.

3.3.8 Immunological detection

Before starting the detection reaction, blots must be saturated in order to saturate free protein binding sites of the membrane and to prevent nonspecific binding of the detection reagents. Blocking was carried out by incubation overnight in 3% bovine serum albumin (BSA) diluted in 1 x PBS at 4 °C. Subsequently, the blocking solution was poured off and the first antibody diluted 1:1000 in the freshly prepared blocking solution (1% BSA, 0,03% Tween 20 in 1 x PBS) was applied. The incubation was carried out for one and a half hour at room temperature on the rocker. Thereafter, the first antibody solution was decanted and after three washing steps with the wash buffer (0,3% Tween 20 in 1 x PBS) for 10 minutes each, the second antibody (second AB Goat anti-mouse lgG, HRP-conjugated, Jackson Immunoresearch Laboratories, UK) was added to the membrane at a dilution of 1:10000 (1% BSA, 0.03% Tween 20 in 1 x PBS). The incubation took place at room temperature for one hour using a tube rotator. This was followed by three ten-minute washing steps with the wash buffer (0,3% Tween 20 in 1 x PBS) before the detection reaction could be started.

The detection reaction is based on the enzyme horseradish peroxidase (HRP), which is coupled to the second antibody. The enzyme catalyses a chemical reaction of substrates contained in the detection solution. The resulting colour change makes the bound second antibody and thus the protein to be detected visible. Detection was done by chemiluminescence according to the instructions of the Enhanced Chemiluminescence (ECL) Plus Western Blot Detection System (Pierce). After incubation for 5 min in the dark, the blot was exposed to x-ray film (retina) and developed.

3.3.9 Stripping of the Nitrocellulose membrane

To remove bound antibodies from a nitrocellulose membrane, the membrane was incubated for 5 min in 50 mM Tris-HCl, 50 mM NaCl, pH 2,5. This step was repeated and the reaction was then stopped by addition of 1N NaOH at the ratio 1:250. After a short washing step in 1 x PBS, the membrane was again blocked with 3% BSA (w/v) in PBS and could then be incubated again with antibodies.

3.3.10 Fast protein liquid chromatography (FPLC)

For further purification of proteins under non-reducing conditions 2 mg of protein was applied to a HiLoad 16/600 Superdex 200 pg (GE-Healthcare) gelfiltration column. Prior to protein application, the FPLC was rinsed with water and protein buffer in order to equilibrate the column. The run was initiated by the software and the UV unit emitting light of 280 nm was switched on. All fractions were collected and peak fractions were pooled and analysed by SDS-PAGE and DLS. Protein size was determined by means of the respective equilibration curve according to the manufacturer's instructions.

3.3.11 Dynamic Light Scattering (DLS)

DLS was performed in order to verify dispersity as well as the hydrodynamic radius (R_H) of proteins in solution. Sample preparation by means of centrifugation at 16000 x g for at least 30 min was ever carried out before each measurement. Both, the SpectroSize 300 as well as the SpectroSize 600 function with a red laser (λ = 690 nm). Whereas the SpectroSize 300 necessitates a quantity of 10 µl, the SpectroSize 600 consume less sample (1-2 µl) and permits to observe the development of dispersity

over a long period. Sample temperature was always monitored and stabilised by both devices.

3.3.12 Circular dichroism (CD)

Besides determination of general secondary structure elements in proteins thermal stability and folding properties are examined by means of CD spectroscopy. The device operated in this thesis was the J-815 CD-Spectrometer (Jasco, Germany). *Pf*APP was dialysed against a buffer containing 10 mM Tris, pH 8,0 and subsequently diluted to a final protein concentration of 2 µM. 100 µL of this sample were filled into a 1 mm quartz glass cuvette (Hellma-Analystics, Germany) scanning the near UV wavelength 190-260 nm. Given that the absorption exceeded 3 at a wavelength below 195 nm, the spectra were cut at this wavelength. Standard curves according to YANG et al. (1986) served as a basis for determining secondary structure elements. Typically, α-helixes exhibit characteristic minima at 208 and 220 nm respectively and a maximum at 192 nm (Figure 16, black curve), whereas a minimum at 215 nm and a maximum at 195 nm indicates a high β-sheet content (Figure 16, grey curve). On the other hand, turn structures show a single minimum at 200 nm in the CD Spectra and random coil structures possess a minimum between 190 and 200 nm and a maximum at 220 nm (Figure 16, random). All these values are not absolute values, but signposts for CD spectra analyses.

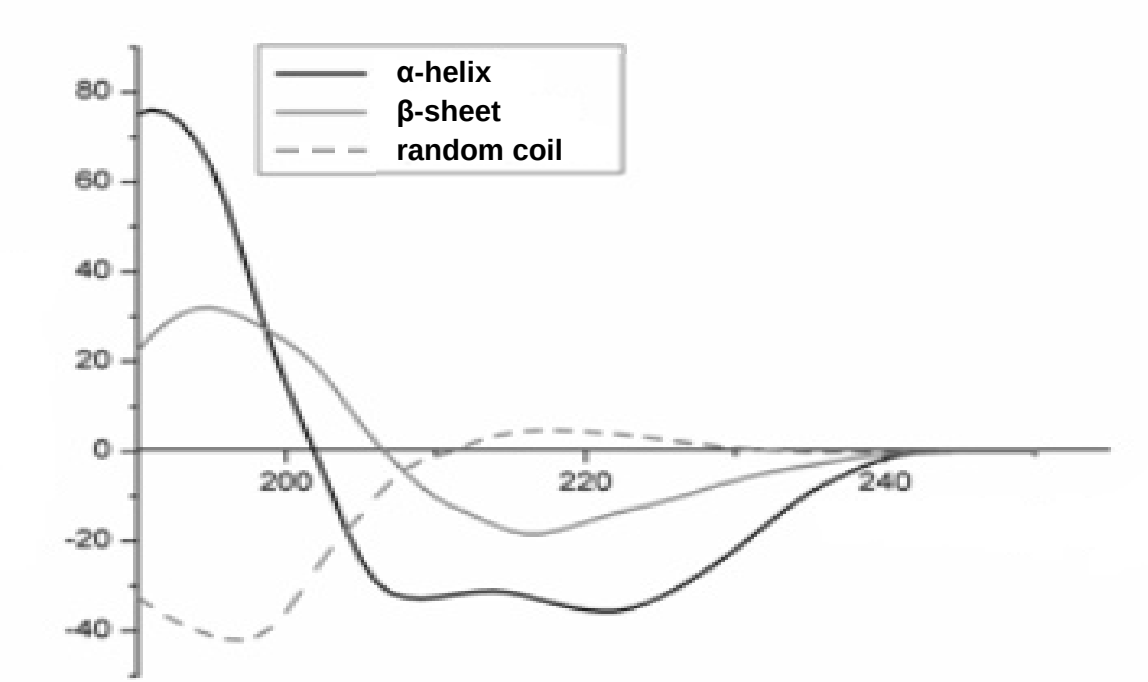

Figure 16 - Standard curves for CD measurements modified according to TREUEL et al., 2010. Typically, α-helixes exhibit characteristic minima at 208 and 220 nm respectively and a maximum at 192 nm (black line), whereas a minimum at 215 nm and a maximum at 195 nm indicates a high β-sheet content (grey line). On the other hand, turn structures show a single minimum at 200 nm in the CD Spectra and random coil structures possess a minimum between 190 and 200 nm and a maximum at 220 nm (dashed line).

3.3.13 Activity assay

The protein to be examined was purified via His-tag affinity chromatography and further purified in terms of FPLC. The reaction was prepared in Tris-HCl buffer, pH 7,7 supplemented with 1 mM $MnCl_2$. Each peptide was added with a final concentration of 5 µg (different vials), reaction was initiated by adding 250 ng APP respectively and carried out at 37 °C. After two hours, the reaction was stopped by adding 10 % acetic acid and samples were centrifuged for 5 min at 16000 x g. Supernatant was transferred to a new vial and 100 µl 0,1% formic acid was added. Subsequently, the amount of uncleaved peptide was identified by mass spectrometry. Mass spectrometry data collection and analysis was performed in cooperation with the CEFAP at USP. A penta-peptide, which has a glycine in P1 ' position instead of the proline (Tyr-Pro-Trp-Thr-Gln → Tyr-Gly-Trp-Thr-Gln), was used as control to verify the substrate specificity of the enzyme.

3.4 Crystallisation and data collection

3.4.1 Sample preparation for protein crystallisation

In the first step, APP was purified via Ni-NTA affinity chromatography utilizing the C-terminal His6-tag and subsequently applied to a Hi Load 16/60 Superdex 200 size exclusion chromatography (GE Healthcare, UK) to separate the catalytically active APP dimer from larger oligomers and aggregates. After protein purification, samples were stepwise concentrated to a range of 7 to 11 mg/mL by means of an Amicon centrifugal filter concentrator (Merck Millipore, Germany). DLS was performed to monitor the dispersity of the protein in solution (3.3.11). After centrifugation of 30 min at 16100 x g, crystallisation trials were performed as vapor diffusion method in a sitting drop. The crystallisation process was carried out according to BEGUM et al., 2011; DREBES et al., 2011; WRENGER et al., 2011.

The commercial crystallization screens PACT premier (MD1-36), JCSGplus (MD1-40), Morpheus (MD1-47), Stura FootPrint (MD1-20) (all Molecular Dimensions, Suffolk, UK) and AmSO4 (Quiagen) were tested and pipetted by a Honeybee 961 pipetting robot (Genomic Solutions, Huntingdon, UK) into 96-well SWISSCI MRC2 plates (Hampton Research, USA). The reservoir was filled with 45 µl of precipitant solution and 400 nl protein were mixed with 400 nl precipitant on the sitting shelf. The plates were sealed, stored at 16 °C and regularly monitored to identify crystal formation using a microscope.

3.4.2 Data collection

Crystals were cryo-protected by adding 25% glycerol as all measurements were performed at -173 °C and their diffraction pattern was subsequently examined by using the EMBL P14 beamline at the synchrotron source PETRA III in Hamburg, Germany. The exposure time of each diffraction pattern was 40 milliseconds and the crystal was rotated by 180° in 0,05° increments. Data collection, evaluation, phasing and refinement was conducted by Robin Schubert and processing of the data set was performed by the programs XDS (KABSCH, 2010) and SCALA (EVANS, 2006). Further structure refinement was obtained by molecular replacement using the software MOLREP (VAGIN; TEPLYAKOV, 2010) implemented in the CCP4 suite (WINN et al., 2011) revealing a sequence identity of 35% between *Pf*APP and human

cytosolic X-prolyl aminopeptidase (PDB: 3CTZ). Figures were drawn by using the program PYMOL (DeLano Scientific, San Carlos, USA).

3.5 Cell biological methods

3.5.1 Cultivation of Plasmodium falciparum

The cultivation of *P. falciparum* was carried out in RPMI-HEPES medium with a haematocrit value of 4%. Blood erythrocyte concentrates of the blood group 0+ (InCor or ProSangue) were used and the parasites were cultivated to a maximum parasitaemia of 20%. The culture was maintained in TPP bottles (150 cm^2) under an oxygen-poor atmosphere (90% N_2, 5% O_2, 5% CO_2) at 37 °C (TRAGER; JENSEN, 1976; JENSEN; TRAGER, 1977). The culture was diluted regularly every two days in the ratio 1:10 or 1:5, depending on the amount of parasitaemia.

3.5.2 Determination of parasitaemia

Parasitaemia was determined by means of a blood smear. For this purpose, an air-dried blood smear was fixed for 5 sec in methanol, incubated for 5 sec in an erythrocyte staining solution and then stained again in a Giemsa solution for 5 sec. After rinsing under tap water, the slides were air-dried and examined by microscopy at a magnification of 100 times under immersion oil. To determine the parasitaemia, the percentage of the infected erythrocytes was determined by counting 1000 cells. Alternatively, samples were stained for 15 min by applying the intercalating dye Ethidium bromide and after 3 times washing with PBS applied to a cytometer.

3.5.3 Isolation of parasites by saponin lysis

For the isolation of the parasites, the culture was mixed with 1% warm saponin at a final concentration of 0,05% and then centrifuged immediately after careful mixing for 10 min at 4 °C and 1500 x g. The supernatant was discarded and the pellet re-suspended in 1 ml of HT-PBS buffer and centrifuged at 10000 x g and 4 °C for one minute. This step was repeated for a maximum of four times.

3.5.4 Isolation of total RNA from Plasmodium falciparum (KYES et al., 2000)

For the extraction of total RNA, a cell culture containing predominantly trophozoites was centrifuged and the parasites were isolated by means of saponin lysis. The cell pellet was re-suspended in 1 ml of Trizol and stored until further processing at -80 °C. The frozen trizol lysate was thawed for 5 min at 37 °C to isolate the RNA and 0,2 ml chloroform was added. By repeated inversion, the suspension was mixed well and then centrifuged for 30 min at 4 °C and 13000 x g. 0,5 ml of ice-cold (-20 °C) isopropanol were then added to the aqueous phase. Thus, RNA was precipitated by incubation on ice for at least 2 hours or alternatively overnight at –20 °C and subsequently pelleted (30 min, 13000 x g, 4 °C). The pellet was air-dried and taken up in 30 µl dH_2O. The concentration of the RNA was determined by means of nanodrop and the sample was stored at -80 °C until use.

3.5.5 Isolation of genomic DNA from Plasmodium falciparum

To obtain genomic DNA (gDNA) from *P. falciparum*, the parasites isolated via saponin lysis were resuspended in 500 µl of lysis buffer. Lysed cells were treated with 10 µl of proteinase K (10 mg/ml) and incubated overnight at 37 °C. The cell debris were precipitated by adding of 170 µl of saturated NaCl solution and incubation on ice for 10 min and pelletised by centrifugation for 30 min at 5000 x g and 4 °C. The supernatant was transferred into a new 2,0 ml Eppendorf vessel and 2 µl of RNase A were added to remove RNA and incubated for 15 min at 37 °C. This was followed by a phenol/chloroform extraction with one volume of phenol/chloroform/isoamyl alcohol (25:24:1) centrifuging for 1 minute at 13000 x g. The aqueous phase was treated with 1 volume of chloroform to remove the remaining phenol. After renewed centrifugation for 1 min at 13000 x g and 4 °C, 2,5 volumes of ice-cold 100% ethanol was added and DNA was precipitated at -20 °C overnight. The DNA was pelletised for 30 min at 4 °C and 13000 x g, the pellet was then washed with 500 µl of 70% ethanol, again centrifuged (10 min, 13,000 x g, 4 °C) and dried. The dried pellet was re-suspended in 30 µl of DNase-free water and the concentration of the isolated nucleic acid was determined by means of nanodrop.

3.5.6 Stabilates of Plasmodium falciparum

In order to prepare stabilates, the culture was centrifuged for 10 min at 1500 x g. The supernatant was removed to 1 ml and 1 ml of 60% glycerol was added. The suspension was mixed by repeated inverting and immediately frozen in liquid nitrogen (≈ -195 until -210 °C).

3.5.7 Transfection of all cloned open reading frames into P. falciparum

A single colony of the respective plasmid was inoculated in 400 ml medium containing ampicillin and incubated overnight at 37 °C under shaking conditions. The plasmid DNA was purified via Maxipreparation Kit (#12165, Qiagen, USA) allowing a preparation of up to 500 µg plasmid DNA. Purification was performed according to manufacturer's instructions and purified plasmid DNA was aliquoted in vials, each vial containing 120 ng DNA. Subsequently, the DNA was centrifuged for 1 hour at 16000 x g under cooling conditions and washed once with 70% Ethanol. The pellet was dried until it gets transparent under a clean bench and in the meantime, the parasites were prepared. Synchronisations were performed by treating parasitized erythrocytes with 5% sorbitol for 10-15 min (WALLIKER; BEALE, 1993). For electroporation, red blood cells (usually containing 10% parasitized forms) were pelleted and resuspended in 800 µl of incomplete Cytomix (120 mM KCl, 0,15 mM CaCl, 2 mM EGTA, 5 mM $MgCl_2$, 10 mM K_2HPO_4/KH_2PO_4, 25 mM Hepes, pH 7,6) (VAN DEN HOFF et al., 1992) containing plasmid DNA previously re-suspended in pre-warmed 50 µl TAE buffer.

The red blood cells were electroporated using the Gene Pulser Xcell™ Electroporation Systems (Bio-Rad, Germany) at 0,31 kV and 900 mF. Time constants were 10-16 ms. Electroporated samples were immediately mixed with 10 ml of culture medium, placed into 25-cm^2 canted-neck culture flasks (TPP), and cultivated with daily medium replacement. Parasites were grown for 24 h without drug selection before the medium was supplemented with WR 99210 (5nm) or BSD (1 µg/µl) respectively (MÜLLER et al., 2010).

3.5.8 Growth analysis of transgenic parasites in wild type and genetically different erythrocytes

P. falciparum 3D7-strain will be maintained in continuous culture according to TRAGER and JENSEN as modified (DAS GUPTA et al., 2005). To establish the

influence of the transgenic parasites during proliferation in genetically different erythrocytes deriving from sickle cell patients (InCor-USP, approved by the ethical committee of USP) a proliferation assay was applied. Synchronisations were performed by treating parasitized erythrocytes with 5% sorbitol for 10-15 min (WALLIKER; BEALE, 1993). Parasitaemia was determined by means of counting 1000 cells. Subsequently, parasites were diluted to 1% parasitaemia and cultured in 6-well plates in 2% haematocrit and 3 ml RPMI medium. Parasite cultures reaching a parasitaemia of 8 - 10% will be diluted and cumulative parasitaemia will be calculated by extrapolation from observed parasitaemia and the corresponding dilution factors that will be employed at each sub-culturing step. Every second day 1 µl samples were re-suspended in 500 µl PBS buffer and stained with 0,5 µl of the intercalating dye Ethidium bromide (10 mg/ml). The mixture was incubated for 15 min in the dark and then washed three times with PBS prior to measurement by the Guava EasyCyte Mini cytometer (Guava Technologies, USA). To determine the impact of genetically modified parasites on growth, the transgenic parasites were normalised against parasites carrying the mock plasmid as already previously generated (KNÖCKEL et al., 2012; MÜLLER et al., 2009) and the resulting growth curves were analysed by Microsoft Excel and GraphPad Prism 6.0 (GraphPad Software, USA).

3.5.9 Fluorescence-microscopy

Transgenic parasites were cultured according to TRAGER and JENSEN (1976) and subsequently applied to fluorescence microscopy in order to visualise GFP fluorescence of the respective plasmodial proteins and the counterstaining HOECHST (Invitrogen) *in vivo* according to MÜLLER et al. (2010).

4. RESULTS

4.1 Cloning

4.1.1 Plasmepsin I (PMI)

In order to analyse the gene structure of the aspartic protease plasmepsin I (PMI), sequence investigations were performed within the *P. falciparum* genome database, which showed that this open frame (ORF) contains no introns. Therefore, the amplification of this construct was performed by polymerase chain reaction (PCR) using freshly isolated genomic DNA from *P. falciparum* and gene specific primers encoding for a C-terminal Strep tag. The reaction mixture was prepared exactly according to the respective scheme in 3.2.1 (Table 1) and the PCR product was exponentially amplified by means of the PCR program in 3.2.1 (Table 2). The PCR product of *Pf*PM1 with a molecular mass of 1359 bp was detected by agarose gel electrophoresis (Fig. 17A). After purification, both the vector and the fragment were digested with *KpnI* and *AvrII* and subsequently ligated. After the transformation into *E. coli* XL10-Gold, plasmid DNA was isolated and test digested by *KpnI* and *XhoI.* The analytical digestion was separated in an 1% agarose gel which showed two bands, one about 6653 bp (vector without GFP) and the other about 2079 bp (insert + GFP) (Fig. 17B). The sequencing of this and all further constructs was performed according to the sequencing-method of Sanger and revealed that there are no mutations, so that this construct can be used for the transfection experiments. The determined sequences are shown in the appendix for all cloned constructs. Figure 17C is a schematic illustration of the obtained vector pARL1a-hDHFR *Pf*PMI with the calculated molecular masses (vector 8608 bp and insert (1359 bp).

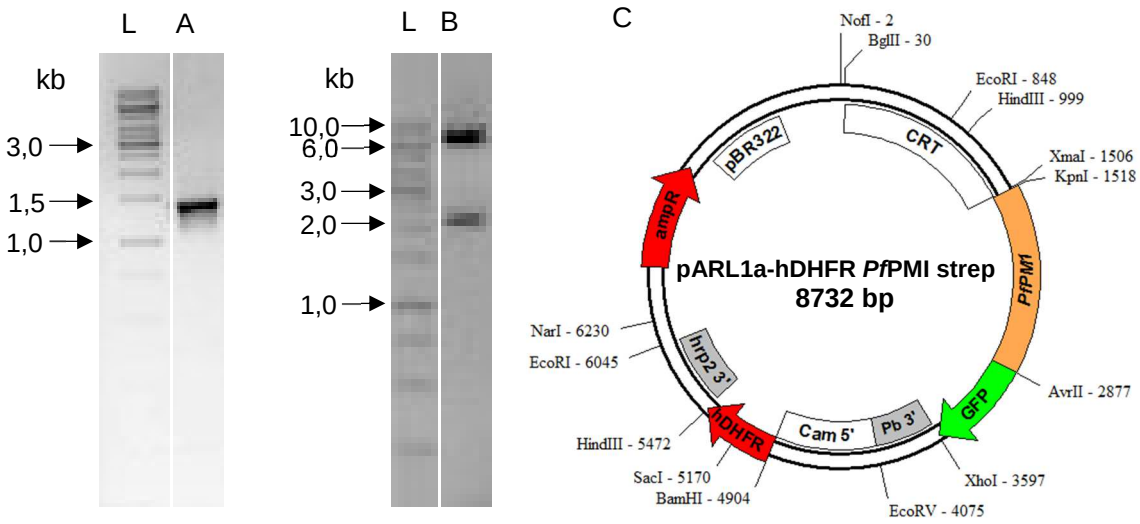

Figure 17 - Results of the cloning of *Pf*PMI into the pARL1a-hDFHR vector. **L -** GeneRulerTM 1 kb DNA Ladder (Fermentas), **A -** 1/10 volume of the PCR product in 6 x DNA loading Dye, **B -** analytical digestion of a plasmid preparation with the enzymes *KpnI* and *XhoI*. **C -** vector map of the resulting pARL1a-hDHFR vector with *Pf*PMI.

4.1.2 Plasmepsin II (PMII)

Via intensive BLAST searches in the genome database of *P. falciparum* it was possible to determine by means of sequence comparisons that the ORF of the aspartate protease Plasmepsin II (PMII) contains no introns. Therefore, the amplification of the ORF of PM2 was obtained by PCR using freshly isolated gDNA from *P. falciparum* and gene specific primers encoding for a C-terminal Myc tag. The reaction mixture was prepared exactly according to the pipetting scheme in 3.2.1 (Table 1) and the PCR product was exponentially amplified by means of the PCR program in 3.2.1 (Table 2). One tenth of the PCR product was subsequently separated in size in a 1% agarose gel (Fig. 18A). There was detected a band with a molecular mass of about 1400 bp. The ORF of the 1362 bp large construct was successfully amplified. Subsequent purification via an affinity column frees the DNA from salts, enzymes and free nucleotides. After digestion with the restriction enzymes *KpnI* and *AvrII*, the vector and the PCR product are purified another time and can subsequently be ligated to each other. The succeeding transformation into *E. coli* XL10-Gold was followed by the isolation and test digestion of plasmid DNA. By digesting with *KpnI* and *XhoI* the insert and the GFP were cut out. The vector band (6799 bp) and the band of the insert and GFP (2082 bp) were detected in the agarose gel (Fig. 18B). The sequencing of this

construct revealed that there are no mutations, so that this construct can be used for the transfection experiments.

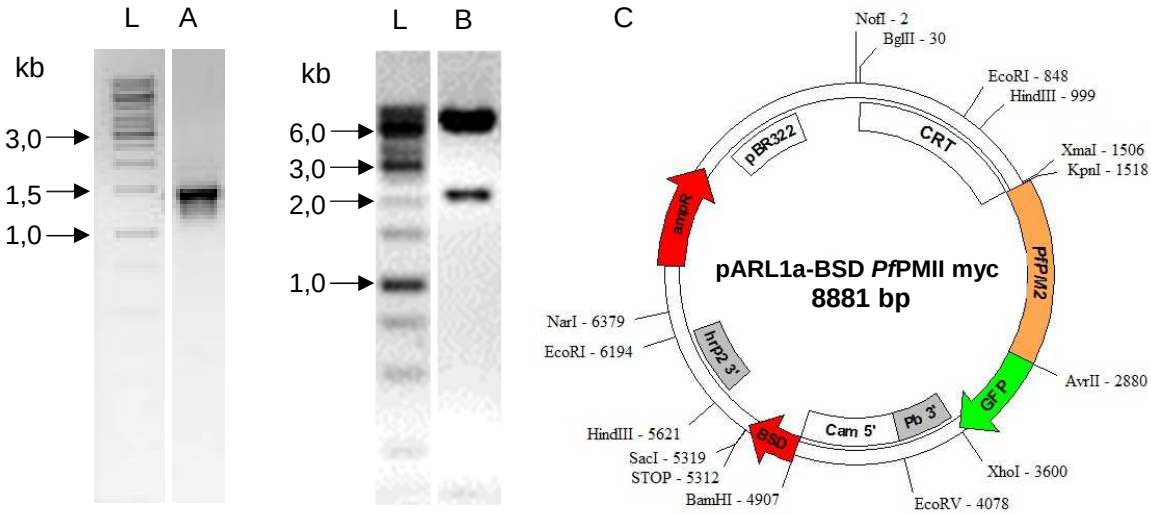

Figure 18 - Results of the cloning of *Pf*PMII into the pARL1a-BSD vector. **L -** GeneRuler™ 1 kb DNA Ladder (Fermentas), **A -** 1/10 volume of the PCR product in 6 x DNA loading Dye, **B -** analytical digestion of a plasmid preparation with the enzymes *KpnI* and *XhoI*. **C -** vector map of the resulting pARL1a-BSD vector with *Pf*PMII.

4.1.3 Plasmepsin III (PMIII) / histo-aspartic protease (HAP)

Such as with the previous construct, no introns were shown in this case by means of sequence analyzes in the plasmodial genome database, so that the amplification of the ORF was carried out by PCR with freshly isolated *Plasmodium falciparum* gDNA and gene specific primers encoding for a C-terminal Strep tag. The reaction mixture was prepared and the program was run as described above (3.2.1). The resulting PCR product was detected in a 1% agarose gel. In Figure 19A, a strong, defined band with an expected molecular weight of about 1356 bp was detected. After purification, the PCR product and the vector were cleaved by the restriction enzymes *XmaI* and *AvrII*. Subsequently, both the digested vector and the digested PCR product were purified again. The fragment and vector were ligated and afterwards transformed into *E. coli* XL10-Gold. The isolation of the plasmids was carried out according to the principle of alkaline lysis using the PeqGOLD plasmid miniprep kit (Peqlab, Erlangen). A subsequent analytical digestion with the enzymes *XmaI* and *XhoI* should prove that the desired insert was actually cloned into the pARL1a-hDHFR vector. Its separation in a 1% agarose gel revealed a band of a molecular mass of about 6641 bp (vector

without GFP) and a signal at a molecular mass of about 2076 bp (insert +GFP) (Fig. 19B). The sequencing of this construct revealed that there are no mutations, so that this construct can be used for the transfection experiments.

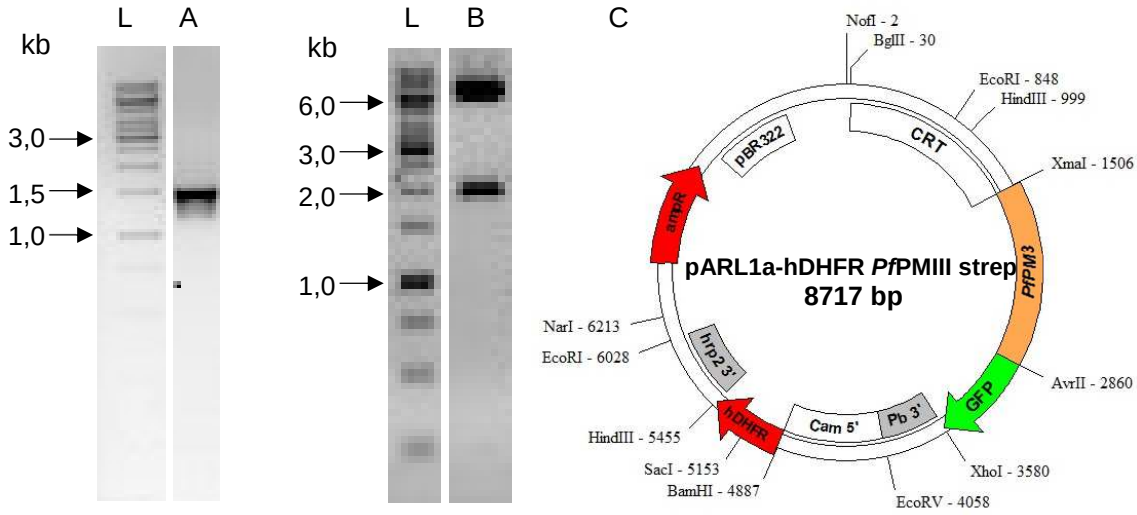

Figure 19 - Results of the cloning of *Pf*PMIII into the pARL1a-hDFHR vector. **L -** GeneRulerTM 1 kb DNA Ladder (Fermentas), **A -** 1/10 volume of the PCR product in 6 x DNA loading Dye, **B -** analytical digestion of a plasmid preparation with the enzymes *XmaI* and *XhoI*. **C -** vector map of the resulting pARL1a-hDHFR vector with *Pf*PMIII.

4.1.4 Plasmepsin IV (PMIV)

BLAST analyses disclosed that this construct contains no introns. Therefore, the amplification of this construct was performed by PCR using freshly isolated gDNA from *P. falciparum* and gene specific primers encoding for a C-terminal Strep tag. The reaction mixture was prepared exactly according to the pipetting scheme in 3.2.1 (Table 1) and the PCR product was exponentially amplified by means of the PCR program in 3.2.1 (Table 2). One tenth of the PCR product was subsequently separated in size in a 1% agarose gel (Fig. 20A). A band at the height of about 1300 bp was detected. The ORF of the 1350 bp large aspartic protease could thus be successfully amplified. After purification both the vector and the fragment were digested with *KpnI* and *XhoI* - as PMIV has an internal *AvrII* restriction site - and subsequently ligated by T4-DNA-Ligase. After the transformation into *E. coli* XL10-Gold, plasmid DNA was isolated and test digested by *KpnI* and *XhoI.* The analytical digestion was separated in an 1% agarose gel which exhibited two bands, one about 6799 bp (vector without GFP) and the other about 1350 bp (insert only) (Fig. 20B). The sequencing of this construct

revealed that there are no mutations, so that this construct can be used for the transfection experiments.

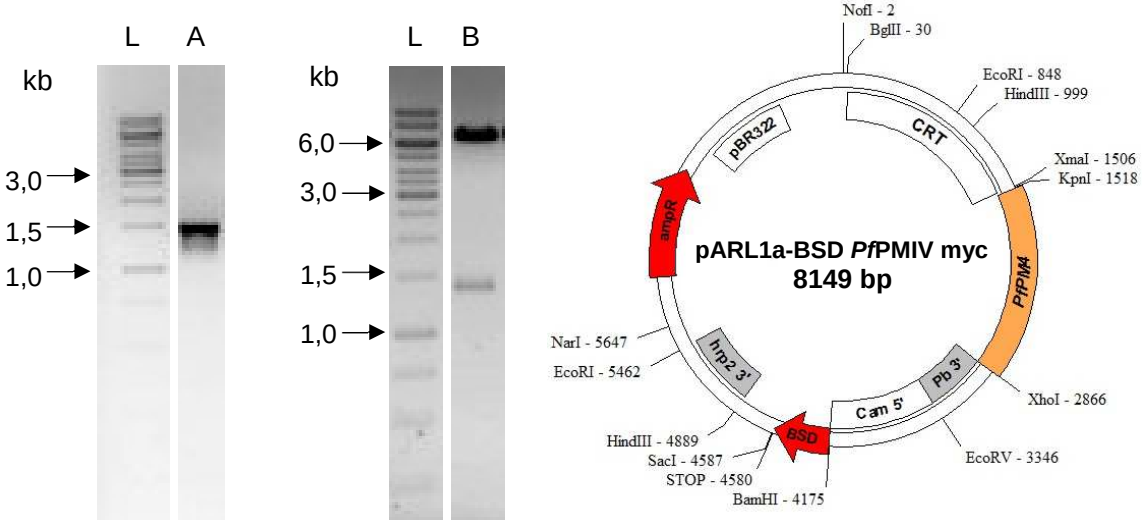

Figure 20 - Results of the cloning of *Pf*PMIV into the pARL1a-BSD vector. **L -** GeneRulerTM 1 kb DNA Ladder (Fermentas), **A -** 1/10 volume of the *PCR* product in 6 x DNA loading Dye, **B -** analytical digestion of a plasmid preparation with the enzymes *KpnI* and *XhoI*. **C -** vector map of the resulting pARL1a-BSD vector with *Pf*PMIV.

4.1.5 Falcipain 2 (FP2)

Via intensive investigations in the genome database of *P. falciparum* it was possible to determine by means of sequence comparisons that the ORF of the cysteine protease Falcipain 2 (FP2) contains no introns. Therefore, the amplification of the ORF of FP2 was obtained by PCR using freshly isolated gDNA from *P. falciparum* and gene specific primers encoding for a C-terminal Strep tag. The reaction mixture was prepared and the program was run as described above (3.2.1). The PCR product for *Pf*FP2 with a molecular mass of 1455 bp was detected by agarose gel electrophoresis (Fig. 21A). In preparation for successful ligation, both the pARL1a-hDHFR vector and the fragment were digested with *KpnI* and *AvrII*. The succeeding transformation into *E. coli* XL10-Gold was followed by the isolation and test digestion of plasmid DNA. By digesting with *KpnI* and *XhoI* the insert and the GFP were cut out. The vector band (6653 bp) and the band of the insert and GFP (2175 bp) were detected in the agarose gel (Fig. 21B). The sequencing of this construct revealed that there are no mutations, so that this construct can be used for the transfection experiments.

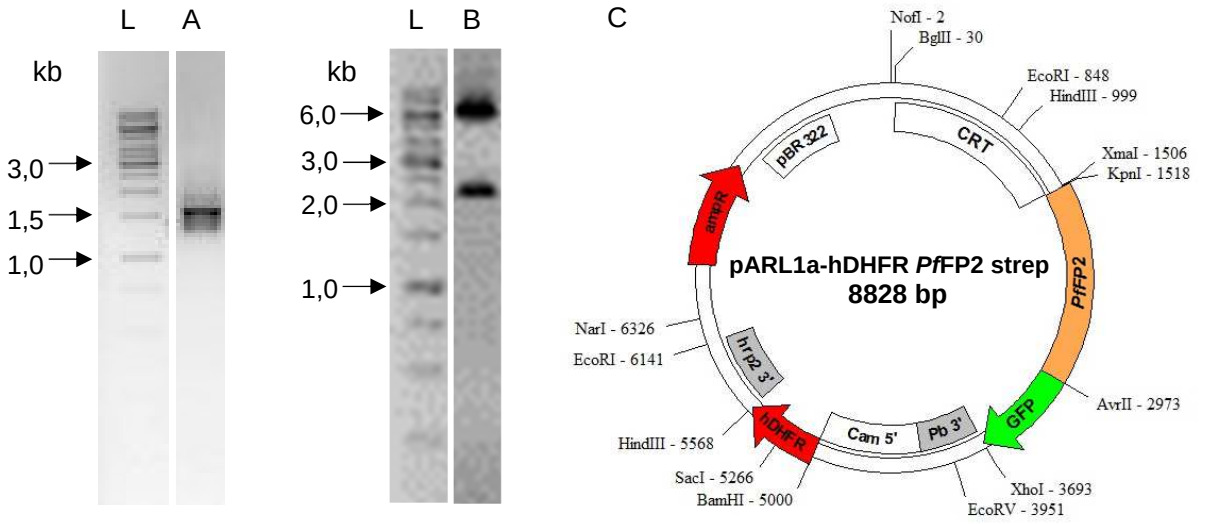

Figure 21 - Results of the cloning of *Pf*FP2 into the pARL1a-hDFHR vector. **L -** GeneRulerTM 1 kb DNA Ladder (Fermentas), **A -** 1/10 volume of the PCR product in 6 x DNA loading Dye, **B -** analytical digestion of a plasmid preparation with the enzymes *KpnI* and *XhoI*. **C -** vector map of the resulting pARL1a-hDHFR vector with *Pf*FP2.

4.1.6 Falcipain 3 (FP3)

Such as with the previous construct, no introns were shown in this case by means of sequence analyses in the plasmodial genome database, so that the amplification of the ORF was carried out by PCR with freshly isolated *Plasmodium falciparum* gDNA and gene specific primers encoding for a C-terminal Myc tag. The reaction mixture was prepared and the program was run as described above (3.2.1). The resulting PCR product was detected in a 1% agarose gel. In Figure 22A, a strong, defined band with an expected molecular weight of about 1479 bp was detected. Subsequent purification via an affinity column frees the DNA from salts, enzymes and free nucleotides. After digestion with the restriction enzymes *KpnI* and *AvrII*, the vector and the PCR product are purified another time and can subsequently be ligated to each other. After the transformation into *E. coli* XL10-Gold, plasmid DNA was isolated and test digested by *KpnI* and *XhoI.* The analytical digestion was separated in size in a 1% agarose gel and revealed a band of about 6799 bp (vector without GFP) and a band of about 2199 bp (insert +GFP) (Fig. 22B). The sequencing of this construct revealed that there are no mutations, so that this construct can be used for the transfection experiments.

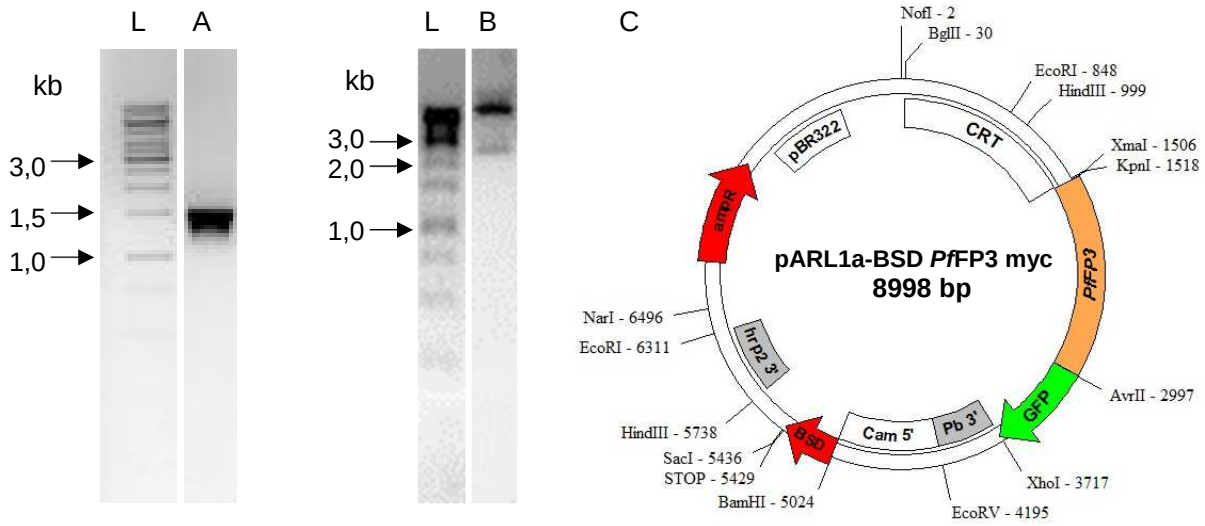

Figure 22 - Results of the cloning of *Pf*FP3 into the pARL1a-BSD vector. **L -** GeneRulerTM 1 kb DNA Ladder (Fermentas), **A -** 1/10 volume of the PCR product in 6 x DNA loading Dye, **B -** analytical digestion of a plasmid preparation with the enzymes *KpnI* and *XhoI*. **C -** vector map of the resulting pARL1a-BSD vector with *Pf*FP3.

4.1.7 Falcipain 2b (FP2b)

The amplification of the cysteine protease falcipain 2b (FP2b) occurred by PCR using freshly isolated gDNA from *P. falciparum* and gene specific primers encoding for a C-terminal Strep tag. The reaction mixture was prepared exactly according to the pipetting scheme in 3.2.1 (Table 1) and the PCR product was exponentially amplified by means of the PCR program in 3.2.1 (Table 2). One tenth of the PCR product was subsequently separated in size in a 1% agarose gel (Fig. 23A). A band at the height of about 1500 bp was detected. The ORF of the 1449 bp large aspartic protease could thus be successfully amplified. After purification both the vector and the fragment were digested with *KpnI* and *AvrII* and subsequently ligated by T4-DNA-Ligase. The ligation approach was transformed into the cloning strain *E. coli* XL-10 and the plasmid subsequently isolated using the plasmid miniprep kit (Peqlab, Erlangen) according to the manufacturer's instructions. A subsequent analytical digestion with the enzymes *KpnI* and *XhoI* should prove that the desired insert was actually cloned into the pARL1a-hDHFR vector. Its separation in a 1% agarose gel revealed a band of about 6653 bp (vector without GFP) and a band of about 2169 bp (insert +GFP) (Fig. 23B). The sequencing of this construct revealed that there are no mutations, so that this construct can be used for the transfection experiments.

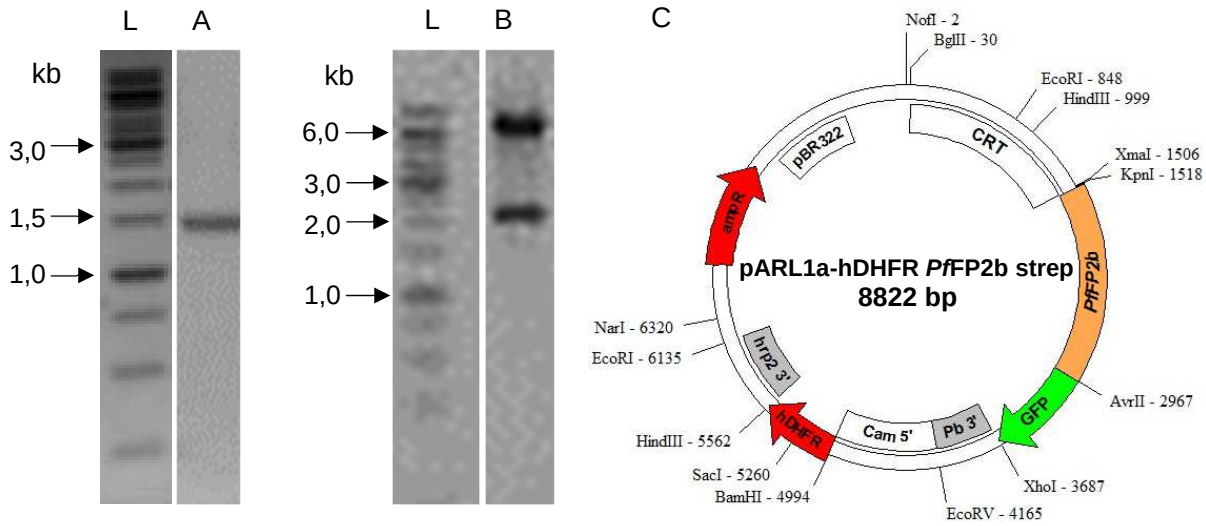

Figure 23 - Results of the cloning of *Pf*FP2b into the pARL1a-hDFHR vector. **L -** GeneRulerTM 1 kb DNA Ladder (Fermentas), **A -** 1/10 volume of the PCR product in 6 x DNA loading Dye, **B -** analytical digestion of a plasmid preparation with the enzymes *KpnI* and *XhoI*. **C -** vector map of the resulting pARL1a-hDHFR vector with *Pf*FP2b.

4.1.8 Falcilysin (Fl)

Sequence analyses in the *P. falciparum* genome database showed that this construct contains no introns. For this reason, the amplification of the ORF of the metalloprotease falcilysin (Fl) was performed on the basis of freshly isolated gDNA from *P. falciparum* and gene specific primers encoding for a C-terminal Strep tag. Thereby, the high-fidelity PCR supermix (Invitrogen, Karlsruhe) was used for the amplification and the quality of the resulting PCR product was checked in a 1% agarose gel. A band of about 3500 bp could be detected which corresponds to the expected molecular mass of 3582 bp (Fig. 24A). After purification via an affinity column, the vector and the resulting PCR product were cleaved with *XmaI* and *AvrII* and the ligation reaction was started. Subsequently, the ligation approach was transformed into competent *E. coli* XL10-Gold competent cells and the plasmid was then isolated for test digestion. By digesting with *XmaI* and *XhoI* the insert and the GFP were cut out. Unfortunately, the cloning of the entire Falcilysin fragment into the pARL1a-hDHFR vector was not successful. Therefore, an in-part cloning, dividing this construct into a 2438 bp (Falcilysin 1) and 1216 bp (Falcilysin 2) fragment, was aimed (Fig. 26). Both fragments could be amplified by PCR using high-fidelity PCR supermix (Fig. 25A, 25B) and the gene specific primers. After purification both the vector and the PCR product of Fl 1 were digested with *XmaI* and *AvrII* and subsequently ligated by T4-DNA-Ligase. The succeeding transformation into *E. coli* XL10-Gold was followed by the isolation

and test digestion of plasmid DNA. By digesting with *XmaI* and *XhoI* the respective insert and the GFP were cut out. The analytical digestions were separated in size in a 1% agarose gel and revealed a band of about 6653 bp (vector without GFP) and a band of about 3158 bp (insert + GFP) (Fig. 25C). The sequencing of this construct revealed that there are no mutations, so that this construct can be used for the second part-cloning. Therefore, the plasmid with the first part of Falcilysin (Fl 1) and the PCR product of the second part (Fl 2) were digested with *BclI* and *AvrII* and ligated via T4-DNA-Ligase. After the transformation into *E. coli* XL10-Gold, plasmid DNA was isolated and test digested by *XmaI* and *XhoI.* The analytical digestion was separated in size in a 1% agarose gel and revealed a band of about 6653 bp (vector without GFP) and a band between 3000 and 3500 bp which is supposed to be the Fl 1 fragment with the GFP (Fig. 25D). In the end, the Falcilysin could not be cloned in the pARL1a-hDHFR vector.

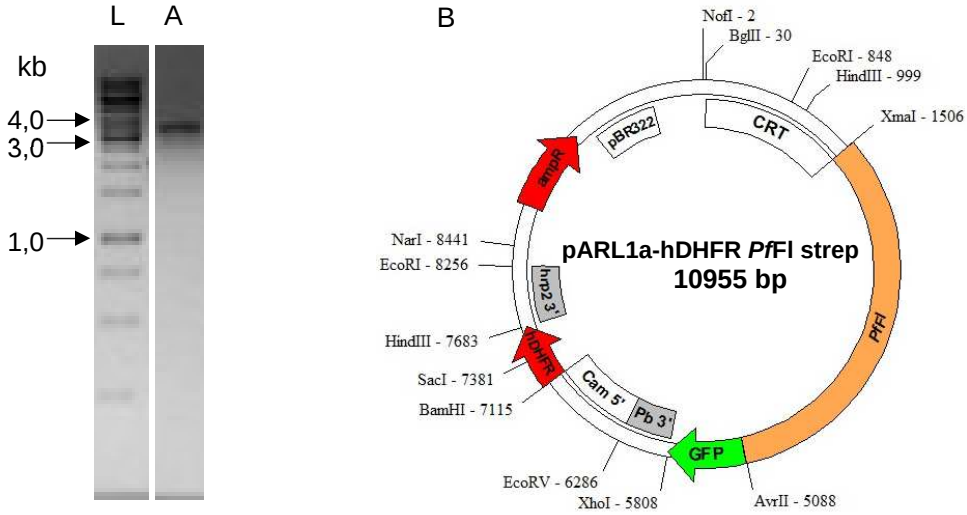

Figure 24 - Results of the cloning of *Pf*Fl into the pARL1a-hDFHR vector. **L -** GeneRulerTM 1 kb DNA Ladder (Fermentas), **A -** 1/10 volume of the PCR product in 6 x DNA loading Dye, **B -** vector map of the resulting pARL1a-hDHFR vector with *Pf*Fl.

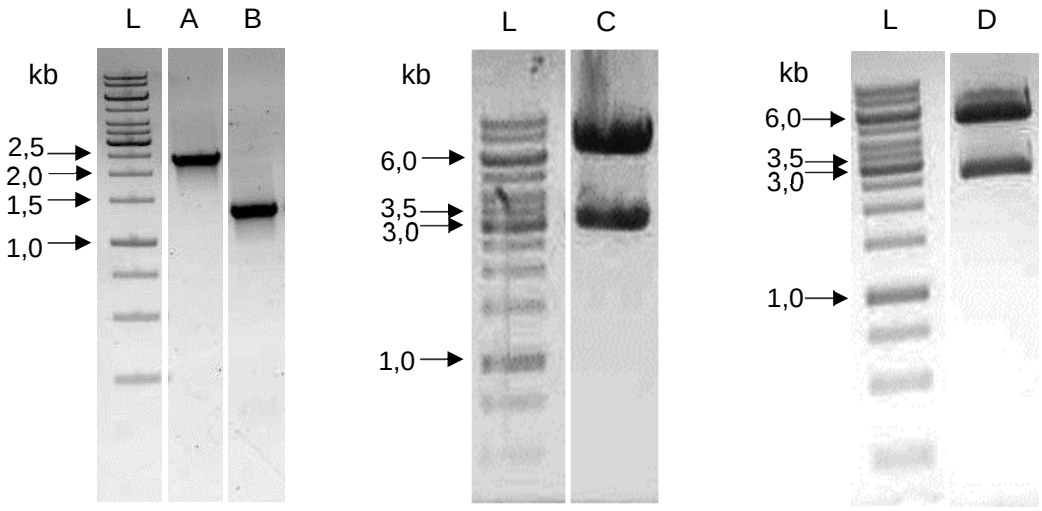

Figure 25 - Results of the in-part cloning of *Pf*Fl into the pARL1a-hDFHR vector. **L -** GeneRulerTM 1 kb DNA Ladder (Fermentas), **A -** 1/10 volume of the PCR product of *Pf*Fl 1 in 6 x DNA loading Dye, **B -** 1/10 volume of the PCR product of *Pf*Fl 2 in 6x DNA loading Dye, **C -** analytical digestion of a plasmid preparation of *Pf*Fl 1 with the enzymes *XmaI* and *XhoI*. **D -** analytical digestion of a plasmid preparation with the enzymes *KpnI* and *XhoI*.

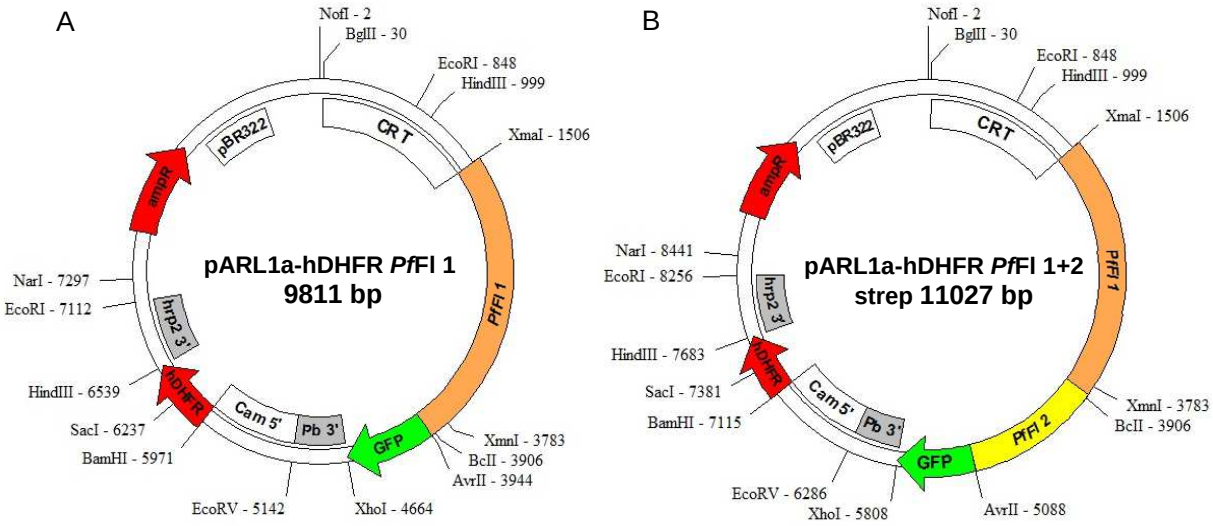

Figure 26 A - vector map of the resulting pARL1a-hDHFR vector with *Pf*Fl 1, **B -** vector map of the resulting pARL1a-hDHFR vector with *Pf*Fl 1 and *Pf*Fl 2.

4.1.9 Alanyl aminopeptidase (AAP)

BLAST analyses disclosed that this construct contains no introns. Therefore, the amplification of this construct was performed by PCR using freshly isolated gDNA from *P. falciparum* and gene specific primers. As the alanyl aminopeptidase (AAP) should be cloned in both the pARL1a-hDHFR and pARL1a-BSD vector two different set ups of primer were designed, one encoding for a C-terminal Strep tag and another encoding for a C-terminal Myc tag. The reaction mixture was prepared and the program was run as described above (3.2.1). The PCR product for *Pf*AAP with a molecular mass of 3258 bp was detected by agarose gel electrophoresis (Fig. 27A). In preparation for successful ligation, both the pARL1a-hDHFR vector and the pARL1a-BSD vector as well as the fragment were digested with *KpnI* and *AvrII*. The succeeding transformation into *E. coli* XL10-Gold was followed by the isolation and test digestion of plasmid DNA. A subsequent analytical digestion with the enzymes *KpnI* and *XhoI* should prove that the desired insert was actually cloned into both the pARL1a-hDHFR vector as well as the pARL1a-BSD vector. The expected bands with a molecular mass of 6653 bp (pARL1a-hDHFR vector without GFP), 3978 bp (insert + GFP) and 6799 bp (pARL1a-BSD vector without GFP) could be detected in a 1% agarose gel (Fig. 27B, 27C). The sequencing of these constructs revealed that there are no mutations, so that these constructs can be used for the transfection experiments.

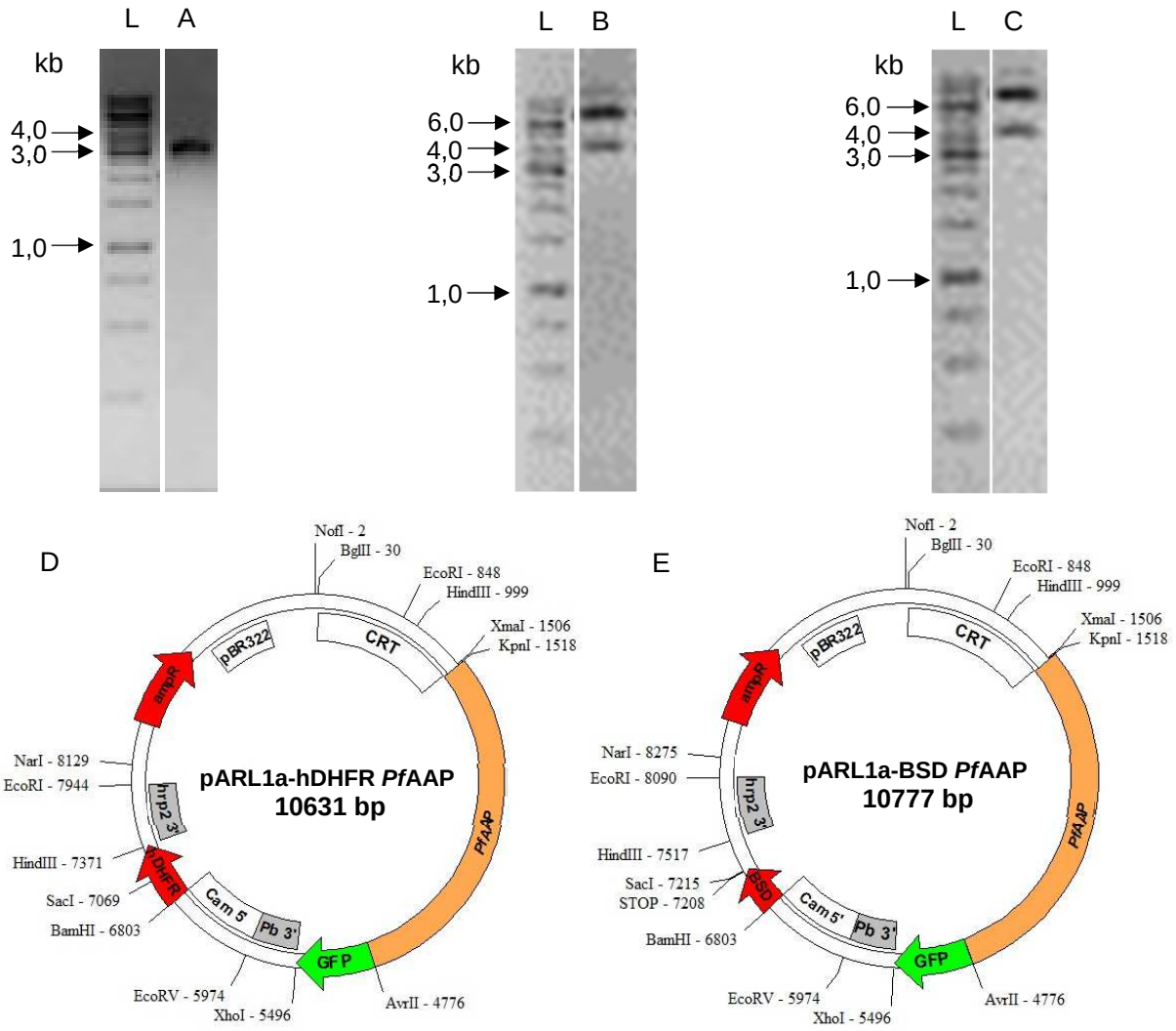

Figure 27 - Results of the cloning of *Pf*AAP into the pARL1a-hDFHR vector and pARL1a-BSD vector. **L-** GeneRulerTM 1 kb DNA Ladder (Fermentas), **A -** 1/10 volume of the PCR product of *Pf*AAP in 6 x DNA loading Dye, **B -** analytical digestion of the plasmid pARL1a-hDHFR-*Pf*AAP with the enzymes Kpn*I* and *XhoI*. **C -** analytical digestion of the plasmid pARL1a-BSD-*Pf*AAP with the enzymes Kpn*I* and *XhoI*. **D -** vector map of the resulting pARL1a-hDHFR vector with *Pf*AAP, **E -** vector map of the resulting pARL1a-BSD vector with *Pf*AAP.

4.1.10 Dipeptidyl aminopeptidase 1

Such as with the previous construct, no introns were shown in this case by means of sequence analyses in the plasmodial genome database, so that the amplification of the ORF was carried out by PCR with freshly isolated *Plasmodium falciparum* gDNA and gene specific primers. As well as the AAP, the dipeptidyl aminopeptidase (DPAP1) should be cloned in both the pARL1a-hDHFR and pARL1a-BSD vector. Therefore, two different set ups of primer were designed, one encoding for a C-terminal Strep tag and another encoding for a C-terminal Myc tag. The reaction mixture was prepared exactly

according to the pipetting scheme in 3.2.1 (Table 1) and the PCR product was exponentially amplified by means of the PCR program in 3.2.1 (Table 2). One tenth of the PCR product was subsequently separated in size in a 1% agarose gel. A band at the height of about 2000 bp was detected (Fig. 28A). The ORF of the 2103 bp large DPAP1 could thus be successfully amplified. After purification both the pARL1a-hDHFR vector and the pARL1a-BSD vector as well as the fragment were digested with *KpnI* and *AvrII* and subsequently ligated by T4-DNA-Ligase. After the transformation into *E. coli* XL10-Gold, plasmid DNA was isolated and test digested by *KpnI* and *XhoI.* The analytical digestion was separated in size in a 1% agarose gel and revealed a band of about 6799 bp (pARL1a-BSD vector without GFP), a band of about 6653 bp (pARL1a-hDHFR vector without GFP) and a band of about 2823 bp (insert + GFP) (Fig. 28B, 28C). The sequencing of these constructs revealed that there are no mutations, so that these constructs can be used for the transfection experiments.

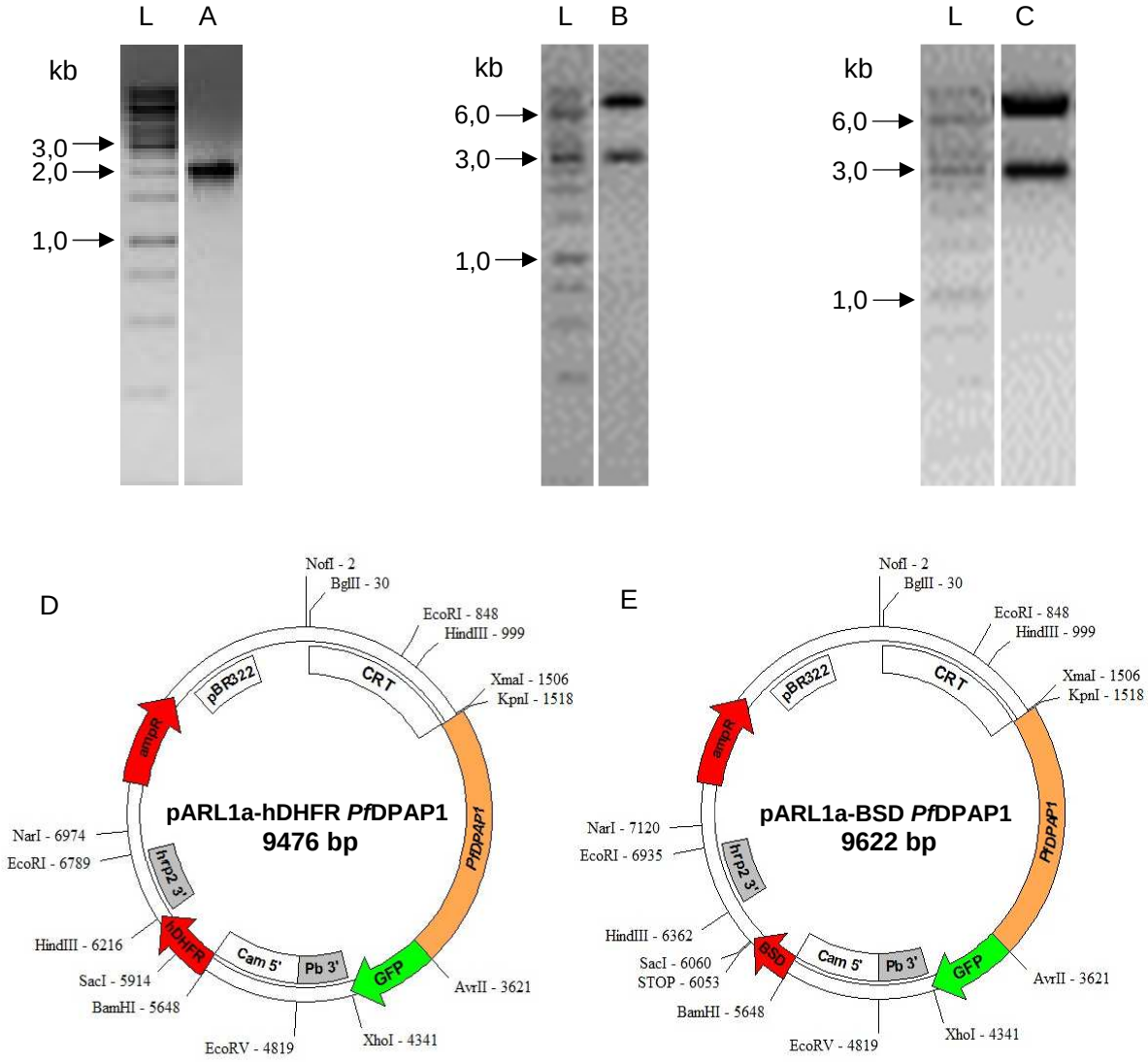

Figure 28 - Results of the cloning of *Pf*DPAP1 into the pARL1a-hDFHR vector and pARL1a-BSD vector. **L -** GeneRulerTM 1 kb DNA Ladder (Fermentas), **A -** 1/10 volume of the PCR product of *Pf*DPAP1 in 6 x DNA loading Dye, **B -** analytical digestion of the plasmid pARL1a-hDHFR-*Pf*DPAP1 with the enzymes Kpn*I* and *XhoI*. **C -** analytical digestion of the plasmid pARL1a-BSD-*Pf*DPAP1 with the enzymes Kpn*I* and *XhoI*. **D -** vector map of the resulting pARL1a-hDHFR vector with *Pf*DPAP1, **E -** vector map of the resulting pARL1a-BSD vector with *Pf*DPAP1.

4.1.11 Aminoacylproline aminopeptidase (APP)

In order to analyse the gene structure of the aminoacylproline aminopeptidase (APP), sequence investigations were performed in the *P. falciparum* genome database, which showed that this open frame (ORF) contains no introns. Therefore, the amplification of this construct was performed by polymerase chain reaction (PCR) using freshly isolated gDNA from *P. falciparum* and gene specific primers encoding for a C-terminal Strep tag. Thereby, the high-fidelity PCR supermix (Invitrogen, Karlsruhe) was used for the amplification and the quality of the resulting PCR product was checked in a 1%

agarose gel. A band between 2000 bp and 2500 bp could be detected which corresponds to the expected molecular mass of 2334 bp (Fig. 29A). After purification via an affinity column, the vector and the resulting PCR product were cleaved with *KpnI* and *AvrII* and the ligation reaction was started. Subsequently, the ligation approach was transformed into competent *E. coli* XL10-Gold competent cells and the plasmid was then isolated for test digestion. By digesting with *KpnI* and *XhoI* the insert and the GFP were cut out. The vector band (6653 bp) and the band of the insert and GFP (3054 bp) were detected in a 1% agarose gel (Fig. 29B). The sequencing of this construct revealed that there are no mutations, so that this construct can be used for the transfection experiments.

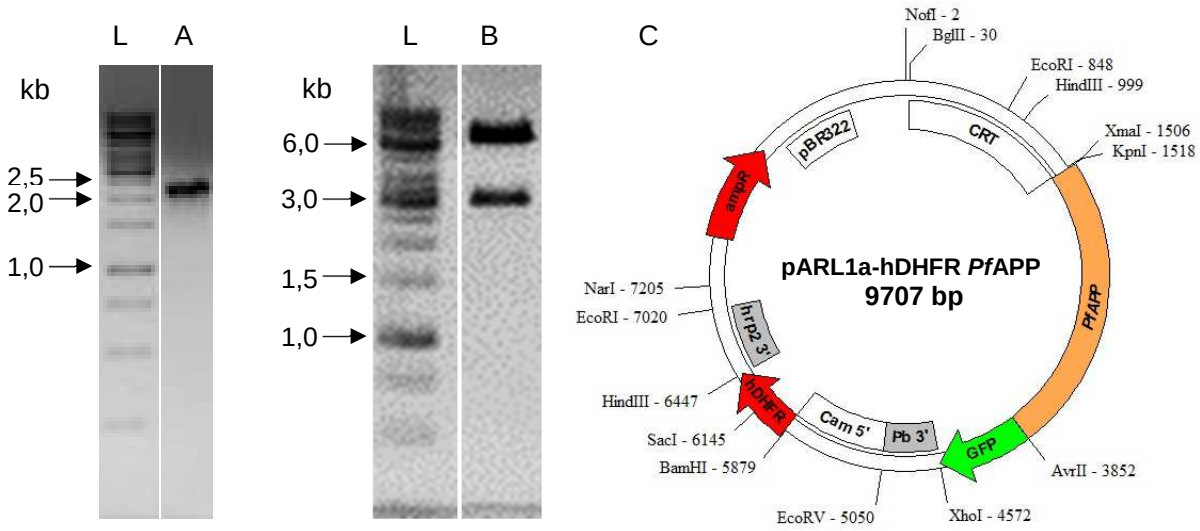

Figure 29 - Results of the cloning of *Pf*APP into the pARL1a-hDFHR vector. **L -** GeneRulerTM 1 kb DNA Ladder (Fermentas), **A -** 1/10 volume of the PCR product in 6 x DNA loading Dye, **B -** analytical digestion of a plasmid preparation with the enzymes Kpn*I* and *XhoI*. **C -** vector map of the resulting pARL1a-hDHFR vector with *Pf*APP.

4.1.12 Dipeptidyl aminopeptidase 2 (DPAP2)

In contrast to the previous constructs, sequence analyses in the *P. falciparum* genome database showed that the dipeptidyl aminopeptidase 2 (DPAP2) contains introns. Therefore, the amplification of the ORF of DPAP2 by was obtained by RT-PCR using freshly isolated *P. falciparum* RNA and gene specific primers encoding for a C-terminal Strep tag. The amplification was performed using the Super ScriptIII One Step RT-PCR System with Platinum® Taq DNA polymerase (Invitrogen, Karlsruhe, Germany) according to the manufacturer's instructions. It was used 1 µg RNA for the reaction.

The resulting PCR product was detected in a 1% agarose gel. In Figure 30A, a strong, defined band with an expected molecular weight of about 1773 bp was detected. After purification both the vector and the PCR fragment were digested with *XmaI* and *AvrII* and subsequently ligated by T4-DNA-Ligase. The succeeding transformation into *E. coli* XL10-Gold was followed by the isolation and test digestion of plasmid DNA. The analytical digestion with *XmaI* and *XhoI* was separated in an 1% agarose gel which showed two bands, one about 6653 bp (vector without GFP) and the other about 2493 bp (insert + GFP) (Fig. 30B). The sequencing of this construct revealed that there are no mutations, so that this construct can be used for the transfection experiments.

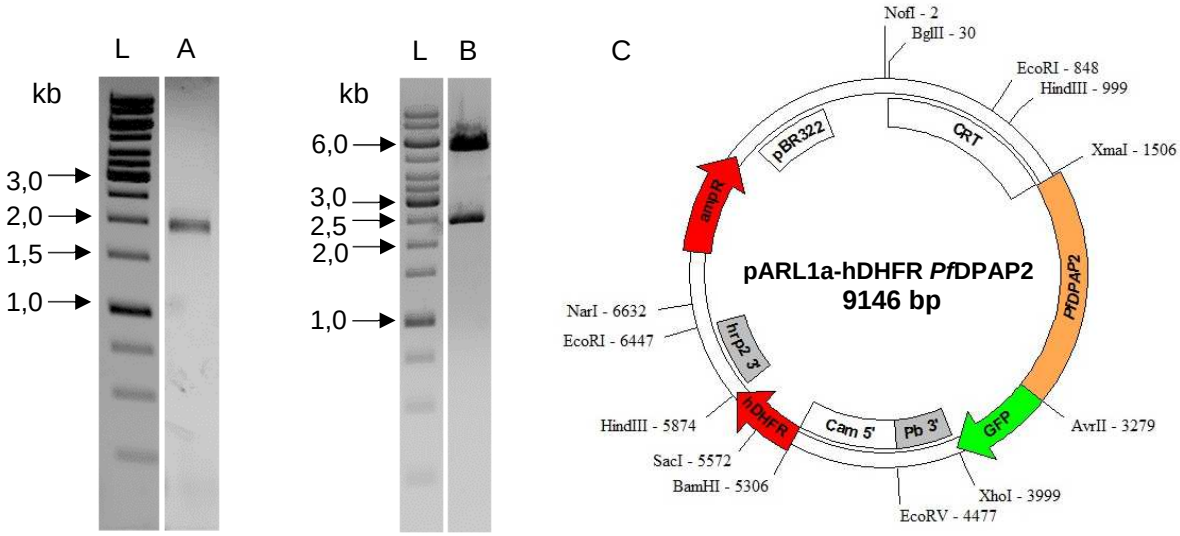

Figure 30 - Results of the cloning of *Pf*DPAP2 into the pARL1a-hDFHR vector. **L -** GeneRulerTM 1 kb DNA Ladder (Fermentas), **A -** 1/10 volume of the PCR product in 6 x DNA loading Dye, **B -** analytical digestion of a plasmid preparation with the enzymes Xma*I* and *XhoI*. **C -** vector map of the resulting pARL1a-hDHFR vector with *Pf*DPAP2.

4.1.13 Heme Detoxification protein (HDP)

As in the previous construct, introns were revealed in this case by means of sequence analyses in the plasmodial genome database, so that the amplification of the ORF was carried out by RT-PCR using freshly isolated RNA from *Plasmodium falciparum* and gene specific primers encoding for a C-terminal Strep tag. Correspondingly, the SuperScript III One Step RT-PCR system with Platinum Taq DNA Polymerase (Invitrogen) was used for the amplification as described above (3.2.2). One tenth of the PCR product was subsequently separated in size in a 1% agarose gel. A band between 500 and 750 bp was detected. The ORF of the 618 bp small HDP could thus be

successfully amplified (Fig. 31A). Subsequent purification via an affinity column frees the DNA from salts, enzymes and free nucleotides. After digestion with the restriction enzymes *KpnI* and *AvrII*, the vector and the PCR product are purified another time and can subsequently be ligated to each other. After the transformation into *E. coli* XL10-Gold, plasmid DNA was isolated and test digested by *KpnI* and *XhoI.* The analytical digestion was separated in an 1% agarose gel which exhibited two bands, one about 6653 bp (vector without GFP) and the other about 1338 bp (insert only) (Fig. 31B). The sequencing of this construct revealed that there are no mutations, so that this construct can be used for the transfection experiments.

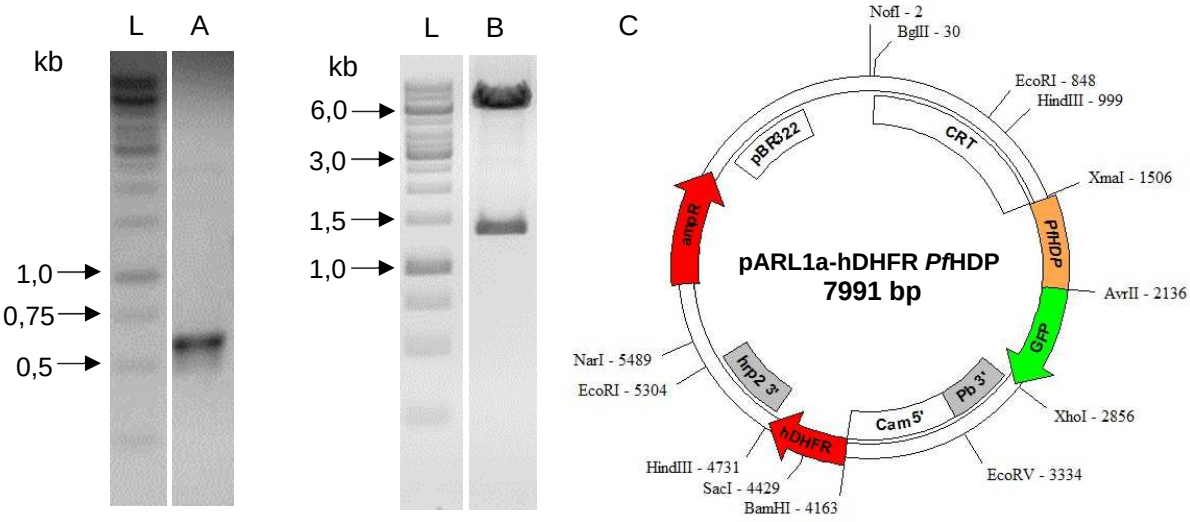

Figure 31 - Results of the cloning of *Pf*HDP into the pARL1a-hDFHR vector. **L -** GeneRulerTM 1 kb DNA Ladder (Fermentas), **A -** 1/10 volume of the PCR product in 6 x DNA loading Dye, **B -** analytical digestion of a plasmid preparation with the enzymes Kpn*I* and *XhoI*. **C -** vector map of the resulting pARL1a-hDHFR vector with *Pf*HDP.

To conclude, all constructs are cloned successfully, there is only Falcilysin missing. Furthermore, every cloned construct has already been transfected into *Pf*3D7 (Tab. 5).

Table 5 - Overview of all constructs

Proteins	Accession-no.	Status	Vectors
Plasmepsin I (PMI)	PF14_0076	transfected	pARL1a+-WR
Plasmepsin II (PMII)	PF14_0077	transfected	pARL1a+-BSD
Plasmepsin III (HAP)	PF14_0078	transfected	pARL1a+-WR
Plasmepsin IV (PMIV)	PF14_0075	transfected	pARL1a+-BSD
Falcipain-2 (FP2)	PF11_0165	transfected	pARL1a+-WR
Falcipain-3 (FP3)	PF11_0162	transfected	pARL1a+-BSD
Falcipain-2 b (FP2b)	PF11_0161	transfected	pARL1a+-WR
Falcilysin (Fl)	PF13_0322	missing	pARL1a+-WR
Alanyl aminopeptidase (AAP)	MAL13P1.56	transfected	pARL1a+-WR/BSD
Dipeptidyl aminopeptidase (DPAP1)	PF11_0174	transfected	pARL1a+-WR/BSD
Dipeptidyl aminopeptidase (DPAP2)	PFL2290w	transfected	pARL1a+-WR
Aminoacylproline aminopeptidase (APP)	PF14_0517	transfected	pARL1a+-WR

4.2 Proliferation Assays in sickle cell blood

4.2.1 Sickle cell analysis

Sickle cell anaemia occurs heterozygote and the causative mutation is always placed at position 6 of the beta chain, wherein a glutamic acid is transformed into a valine. The quantity of sickle cells in the blood varies widely from person to person. Therefore, the percentage of sickle cells in the blood used in this work was first determined by means of a sickling test using sodium metabisulphite. The blood bank, from which the blood was obtained, has assured that the blood donation always came from the same person. After 4 hours of treatment with sodium metabisulphite, 1000 cells were counted by hand and a proportion of 55% sickle cells was determined (Fig. 32).

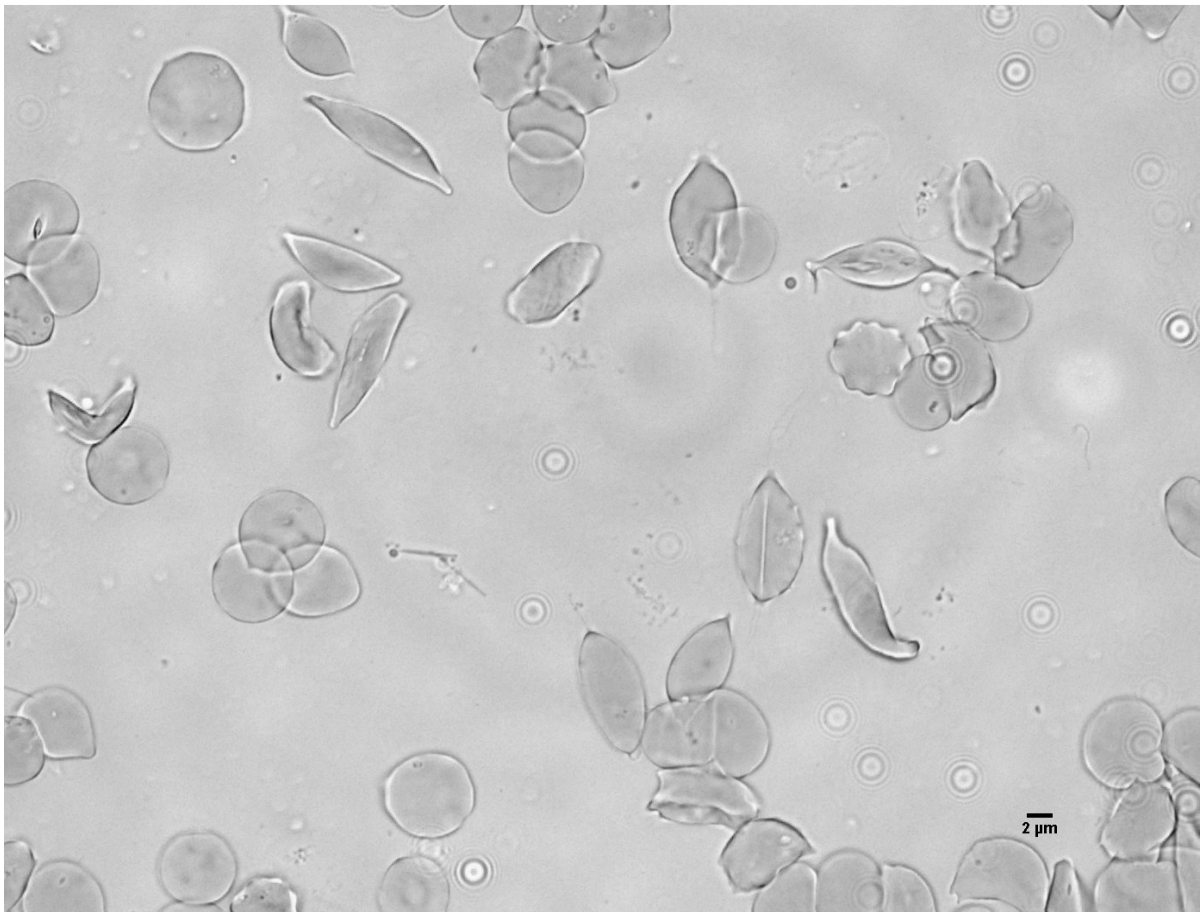

Figure 32 - Sickle cell blood treated with sodium metabisulphite for 4 hours revealed a percentage of about 55% sickled erythrocytes.

Furthermore, it is still highly controversial, whereby the sickle cell mutation has a protective role against malaria. There are three hypotheses, of which one says that the parasites cannot infect sickle cells. So first of all, it was necessary to check whether *P. falciparum* is able to infect sickle cells. Therefore, it was tried to cultivate the 3D7 in sickle cell blood and samples were taken daily and exposed to sodium metabisulphite for four hours. Immediately before microscopy the cells were treated with Hoechst (Invitrogen) according to MÜLLER et al., 2010, in order to stain parasite's nucleus. In the upper row in figure 33 an infected sickle cell surrounded by normal round erythrocytes is demonstrated. The pictures below also display an infected sickle cell, whereas this one shows more than one nuclear staining which indicates a later stage of parasite development. One more example for an infected sickle cell by *P. falciparum* is given in figure 34.

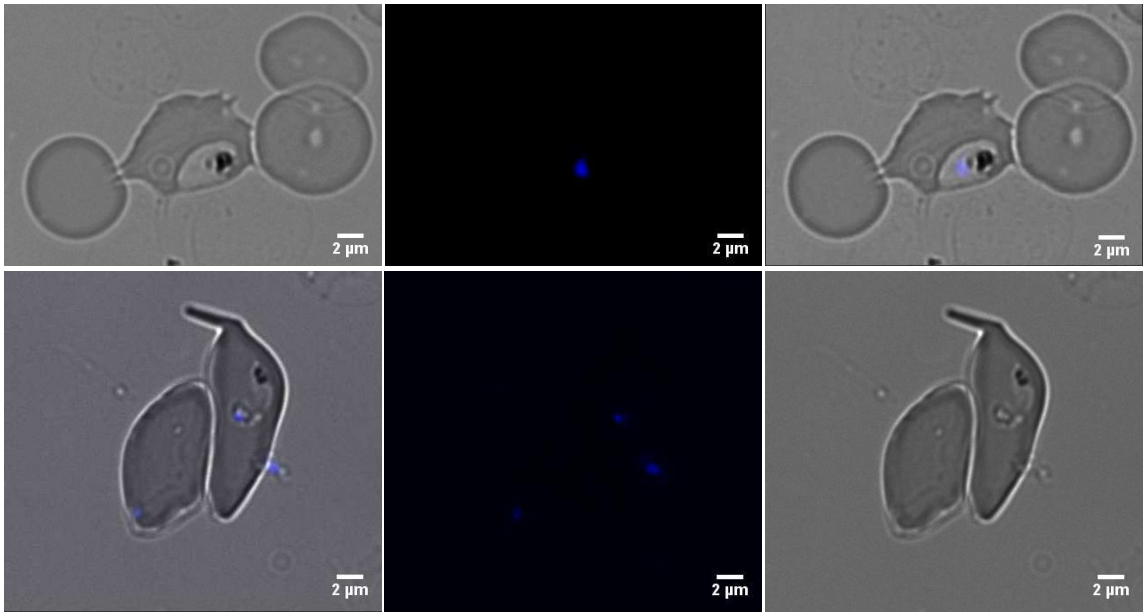

Figure 33 - Fluorescence microscopy image 100 x magnified of the *Pf*3D7 within a sickle cell. Phase: parasite in transmitted light, Hoechst: nuclear staining, Merge: merge of all images.

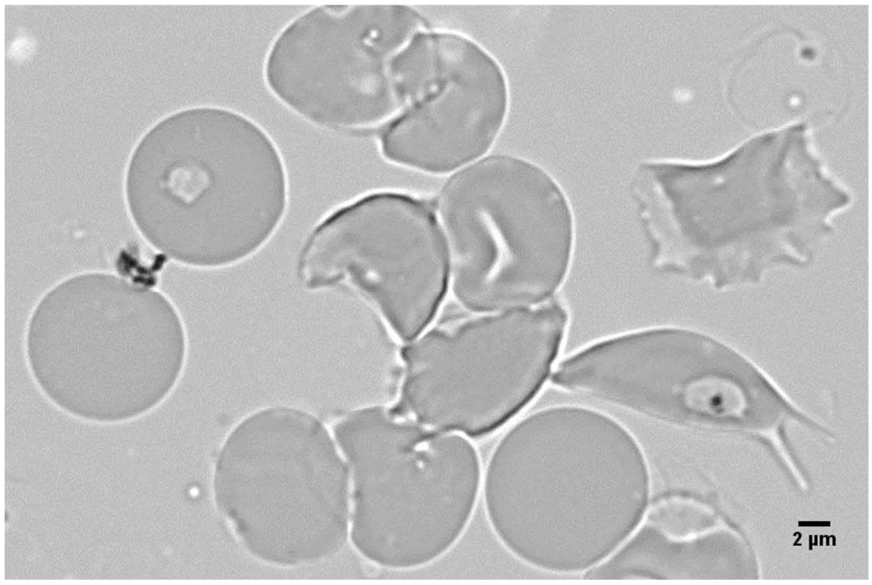

Figure 34: Phase microscopy image 100x magnified of the *Pf*3D7 within a sickle cell.

4.2.2 Proliferation assay of Pf3D7 in sickle cell blood

Having verified that the 3D7 indeed can infect sickle cells, its growth behaviour in sickle cell blood was examined. The assay was set at 1% parasitaemia and 2% haematocrit in RPMI medium. Samples were taken in two-day rhythm over three weeks and stained with ethidium bromide to subsequently determine the parasitaemia using a cytometer. *P. falciparum* 3D7 shows similar growth behaviour in wild type as well as in sickle cell blood up to the 14th day approximately. After two weeks, 3D7 cultured in sickle cell

blood demonstrates initially a moderate and - later after nearly three weeks - a rapid decrease in parasitaemia, whereas the parasite maintained in wild type blood keeps proliferating exponentially (Fig. 35).

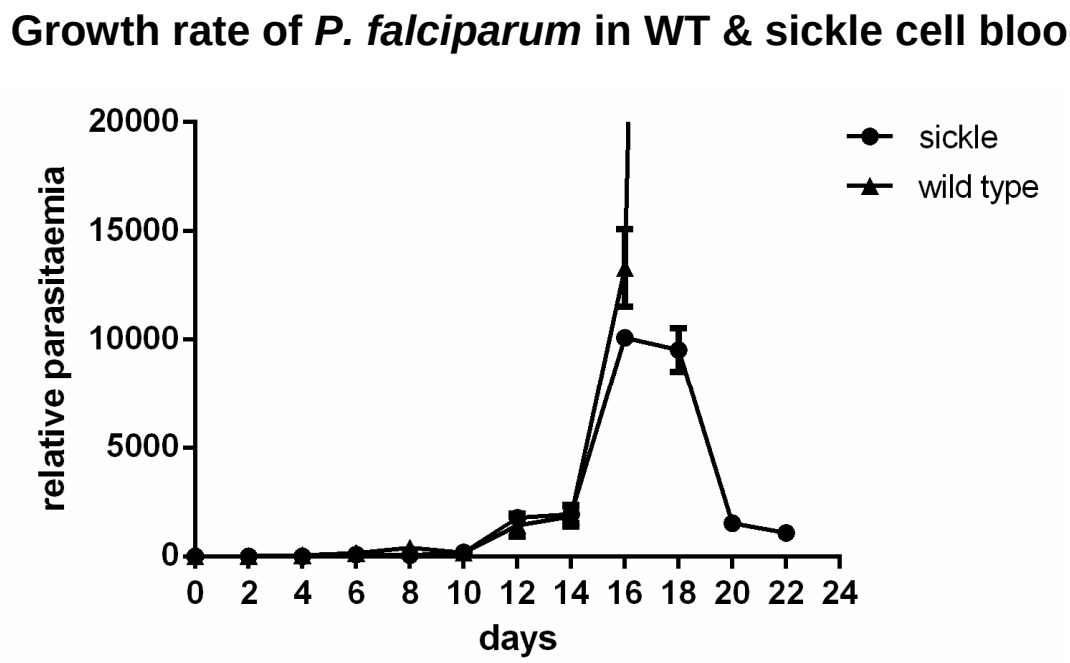

Figure 35 - Proliferation assay of *P. falciparum* (3D7) in wild type (WT) and sickle cell blood (SCT). 3D7 *P. falciparum* keeps growing continuously in wild type blood while dying in sickle cell blood after about three weeks.

Since the values are so far apart, the logarithmic scale was chosen as the most representative one. First of all, it was revealed that the 3D7 is able to grow in sickle cell blood. In contrast to the growth in wild-type blood, the 3D7 does not reach the exponential growth phase in the sickle cell blood and after three weeks it shows clearly a diminished parasitaemia (Fig. 36).

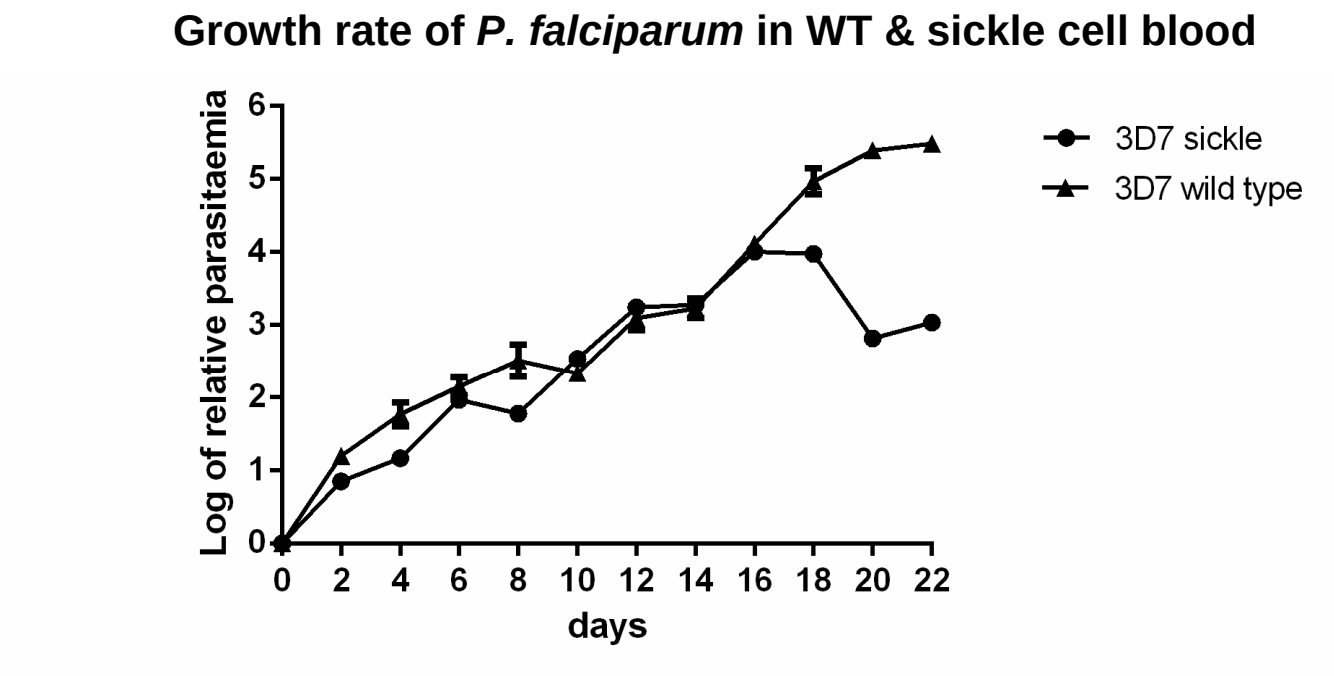

Figure 36 - Proliferation assay of *Pf*3D7 in wild type (WT) and sickle cell blood (SCT) in logarithmic scale.

4.2.3 Proliferation Assay of PfDPAP1 in sickle cell blood

To determine the influence of the genetically modified parasites on the growth in sickle cell blood, it will be normalised against parasites carrying the MOCK plasmid as already previously generated (KNÖCKEL et al., 2012; MÜLLER et al., 2009) and the resulting growth curves were analysed by Microsoft Excel and GraphPadPrism 6.0. The assay was prepared under the same conditions as previously described for the 3D7 (4.2.2). A sample was taken every two days and the measurement was carried out in a cytometer after previous staining with ethidium bromide. The first tested construct was selected randomly. During the first ten days, no significant difference in growth behaviour was detected. Therefore, the following results were normalised against the respective value from day ten. Surprisingly, there was detected a negative effect in the proliferation of DPAP1 and after three weeks the parasitaemia of both the WR Mock cell line and the DPAP1 diminished rapidly (Fig. 37).

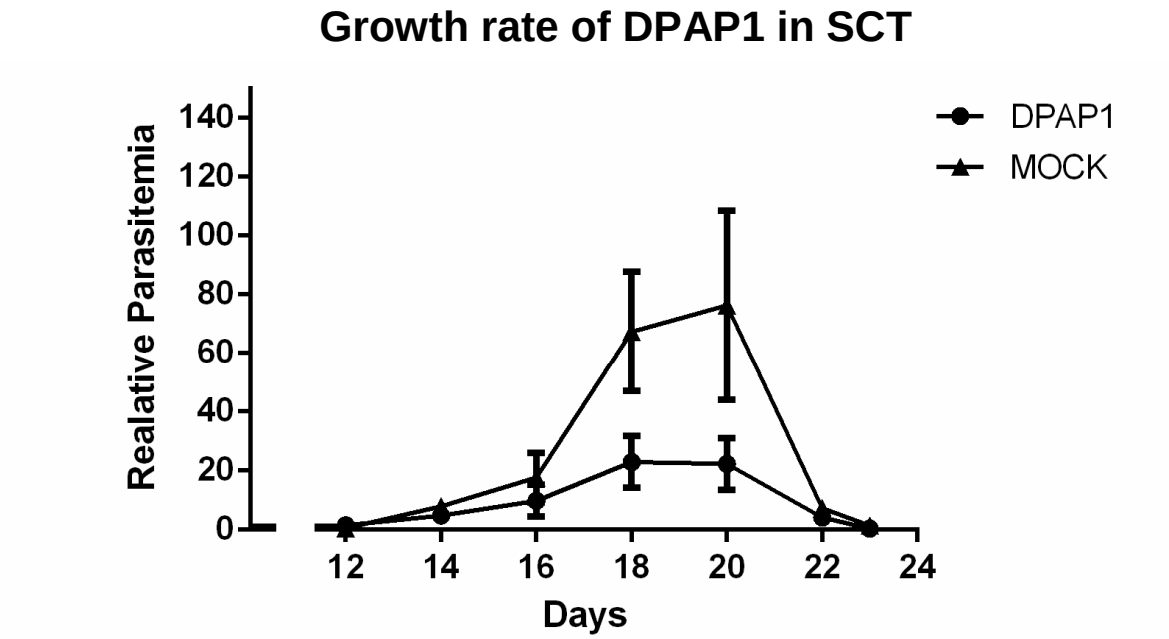

Figure 37 - Proliferation assay of *Pf*DPAP1 in sickle cell blood (SCT). Both *Pf*DPAP1 and Mock are dying after two weeks.

A plasmid rescue could verify that it was indeed DPAP1 and MOCK WR examined in the proliferation assay. In order to understand better this shocking result, localisation studies were performed. Transgenic parasites were cultured as described above (3.5.1) and subsequently applied to fluorescence microscopy in order to visualise GFP fluorescence of the respective plasmodial protein and the counterstaining HOECHST (Invitrogen) in vivo according to MÜLLER et al. (2010). The fusion protein *Pf*DPAP1-GFP was localised to either the food vacuole and the cytosol (Fig. 38, upper picture). In the lower series of GFP pictures a different localisation in other structures, supposed to be vesicles, is detected. These results are consistent with the observations from KLEMBA et al. (2004) and suggest an alternative trafficking route for DPAP1 in *P. falciparum*.

Nevertheless, the overexpression of DPAP1 does not lead to a positive proliferation curve in sickle cell blood and a protease that catalyses the two first steps in the haemoglobin degradation cascade and which was already clearly localised to only one compartment, the food vacuole, was tested next (DAHL; ROSENTHAL, 2004).

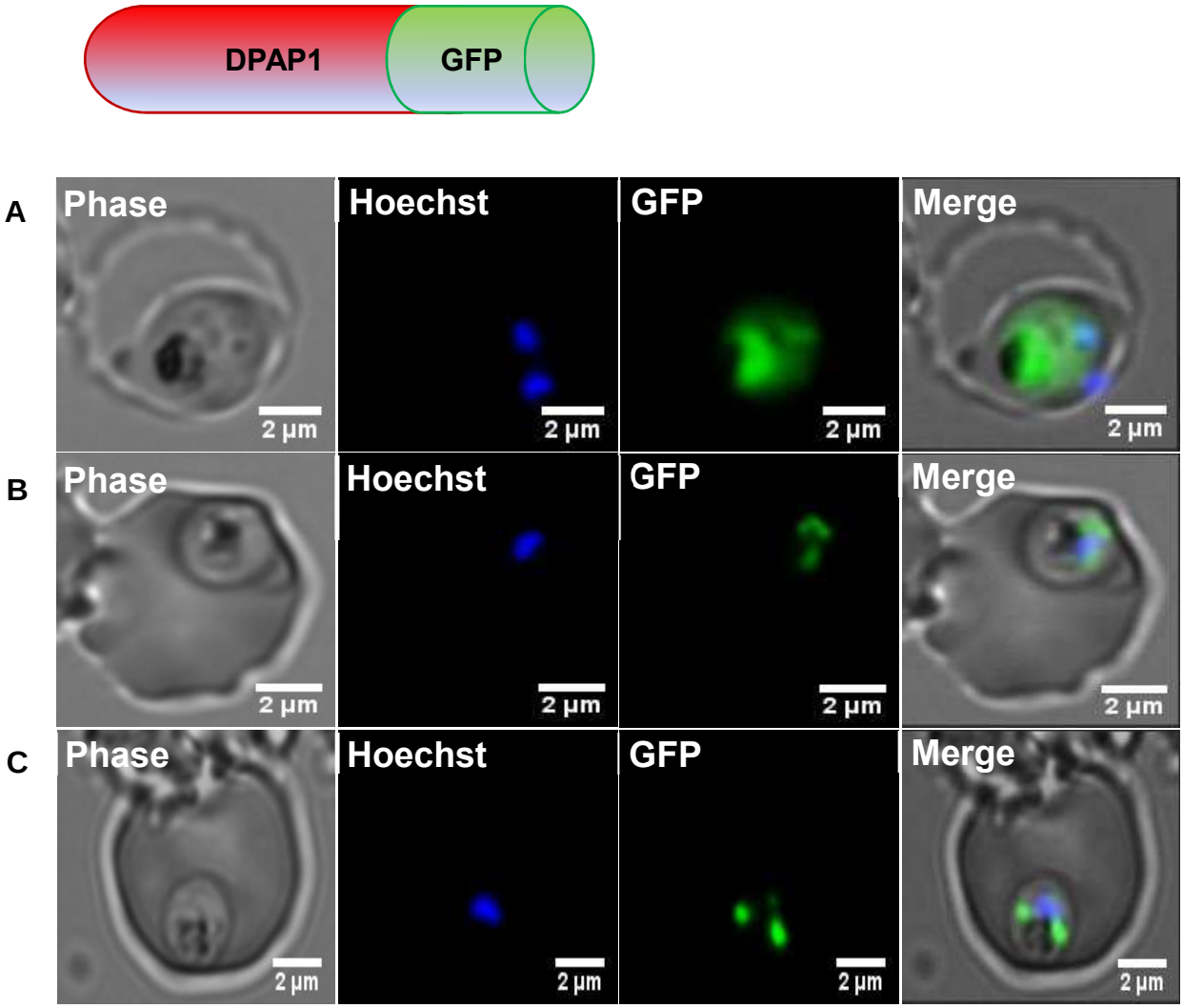

Figure 38 - Fluorescence microscopy image 100 x magnified of the dipeptidylaminopeptidase 1 (*Pf*DPAP1-GFP). **A** Colocalization to the food vacuole and cytosol, **B** punctuated localization supposed to be vesicles, **C** punctuated localization supposed to be vesicles. Phase: parasite in transmitted light, Hoechst: nuclear staining, GFP: the fluorescence of the GFP fusion proteins, Merge: merge of all images.

4.2.4 Proliferation Assay of PfFP2 in wild type blood

First of all, the cysteine protease Falcipain 2 (FP2) and the MOCK cell line were analysed regarding to their growth behaviour in wild type blood (O+) expecting a similar growth curve. The assay was performed under the exactly same conditions as in 4.2.3. Indeed, FP2 and WR showed a similar, exponential growth (Fig. 39) suggesting that the system is functioning and that there is no difference in proliferation due to the transfection event. Thus, it could be concluded that every difference in growth of FP2 in sickle cell blood can be attributed to the activity of the investigated enzyme.

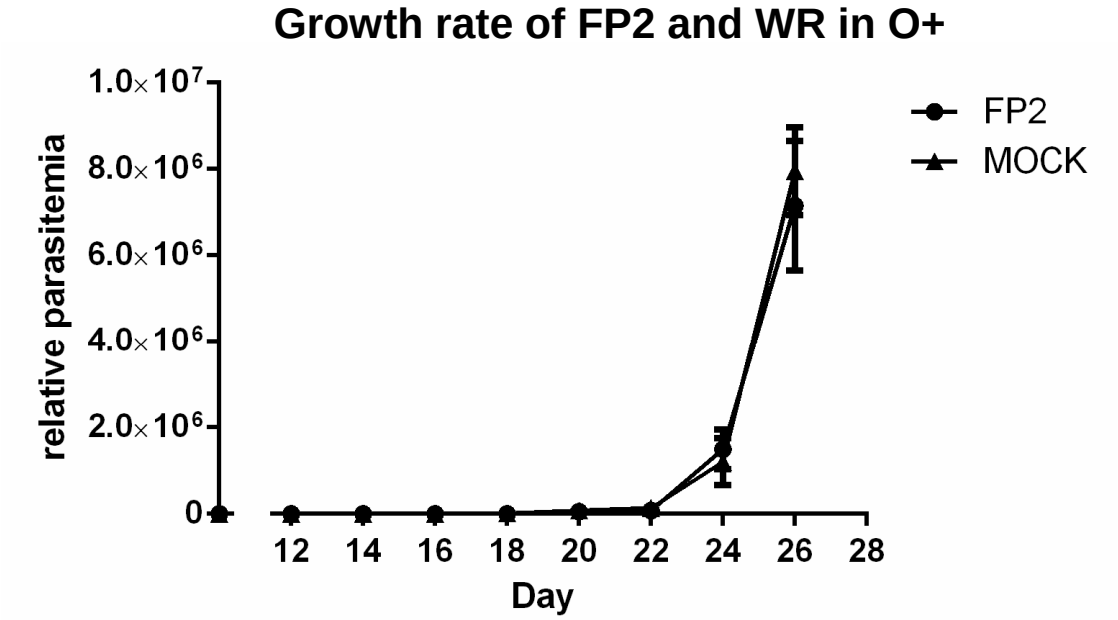

Figure 39 - Proliferation assay of *Pf*FP2 in wild type blood (O+), normalised to day 10. Similar, exponential growth behavior of FP2 and the Mock in wild type blood.

4.2.5 Proliferation Assay of PfFP2 in sickle cell blood (SCT)

The proliferation assay with FP2 and the Mock cell line WR was prepared under the same conditions as previously described (4.2.3). During the first ten days, no significant difference in growth behaviour was detected. Therefore, the following results were normalised against the respective value form day ten. FP2 and the Mock cell line WR keep growing comparable until day 6. From day 8 on the proliferation of Mock WR is decreasing which results in a less steelier growth curve compared to FP2 and three times lower relative parasitaemia (Fig. 40).

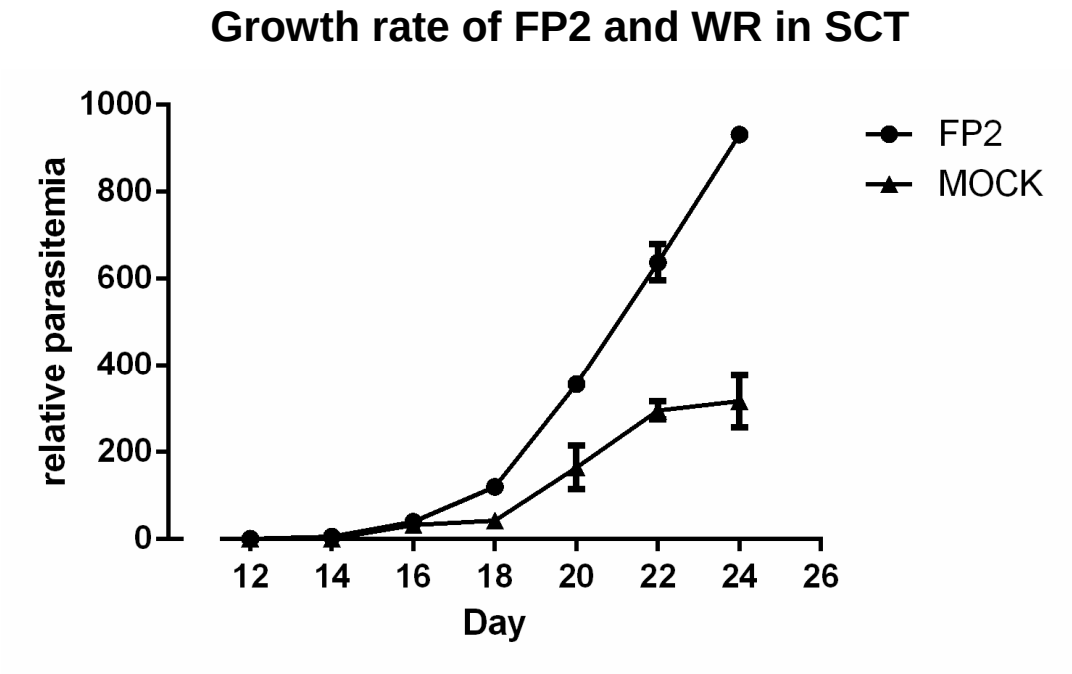

Figure 40 - Proliferation assay of *Pf*FP2 in sickle cell blood (SCT), normalised to day 10.
Similar growth behavior over the first two weeks, but after three weeks the Mock revealed a three times lower relative parasitaemia.

4.2.6 Western Blot analysis of PfFP2

In order to prove that the transfection construct which was used for the proliferation assays, was still expressing the FP2 fusion protein, western blot analysis was performed as described in 3.3.7. Premature FP2 has a molecular mass of about 56 kDa and after processing a mature form of about 27 kDa is generated. In Figure 42, either the pro and mature form as well as two intermediate forms were detected.

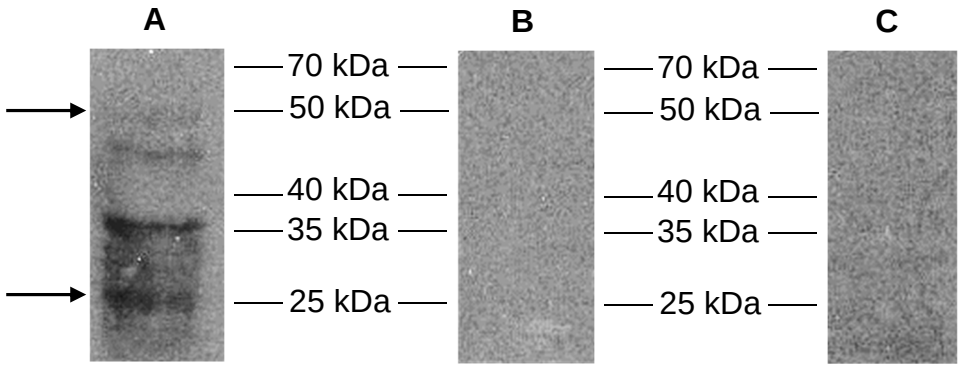

Figure 41 A - Verification of the expression of the fusion protein FP2 by western blot analysis using monoclonal antibodies directed either against the Strep-tag (IBA, Germany) and a secondary anti-mouse peroxidase coupled antibody (Dianova) according to SAMBROOK et al. (1989). **1**0 µg total cell lysate protein were applied on a 12 % SDS-PAGE**.** Arrows represent the position of pro and mature FP2, **B -** Western Blot analysis of Mock WR, **C:** Western Blot analysis of 3D7.

4.2.7 quantitative Real time PCR of PfFP2

Real time PCR was used for transcript quantification according to the department's standard (ICB-USP) procedure. A primer previously designed by Carsten Wrenger and Kamila Anna Meissner, which amplifies within the GFP and can thus be used for all constructs, was applied in this experiment. Normalisation was carried out against the housekeeping gene K1 (seryl tRNA ligase), which is expressed equally in all stages of *P. falciparum*. Each sample was run in a triplicate. In this experiment, increased expression of FP2 compared to the mock cell line was expected at the transcriptional level. An astonishing 1000-fold higher (968,76) transcription level of this cysteine protease was detected (Fig. 42).

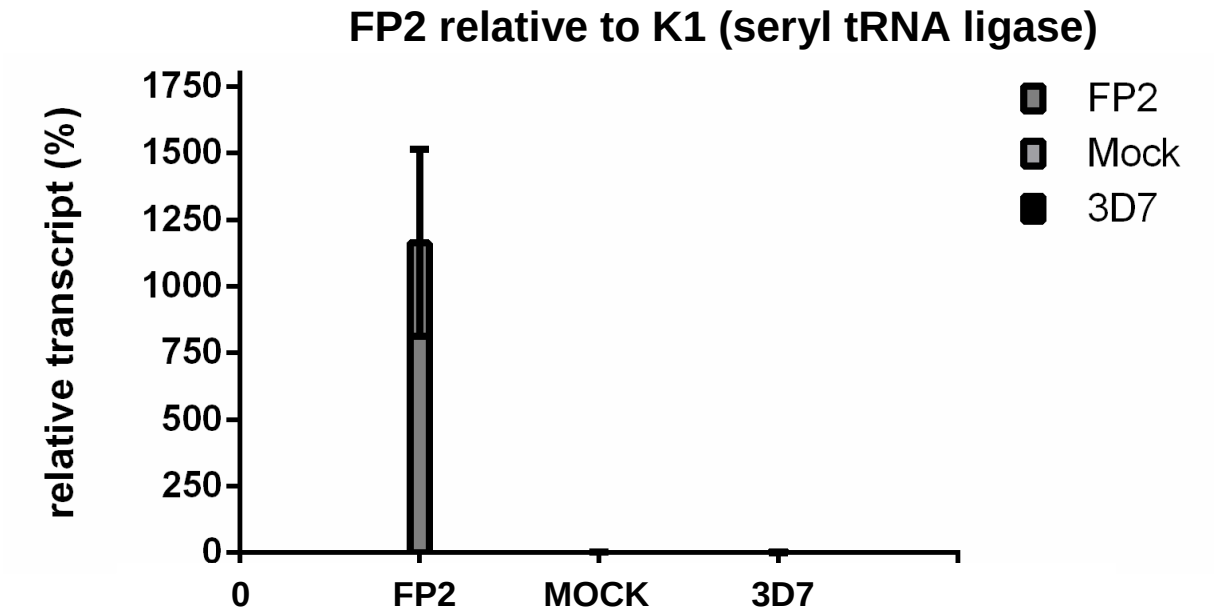

Figure 42 - Quantitative Real-time PCR of *Pf*FP2 using a general qRT primer which amplified from the GFP. A 1000-fold higher transcription level of *Pf*FP2 was detected.

As the result of the real-time PCR using the general GFP primer was so amazing, FP2 gene specific primers were designed by means of the program Primer 3 for comparison. The reaction was performed under the same conditions and an about 3-times higher (2,82) transcription level was detected for FP2 (Fig. 43). This result is consistent with the result from the growth assay in sickle cell blood.

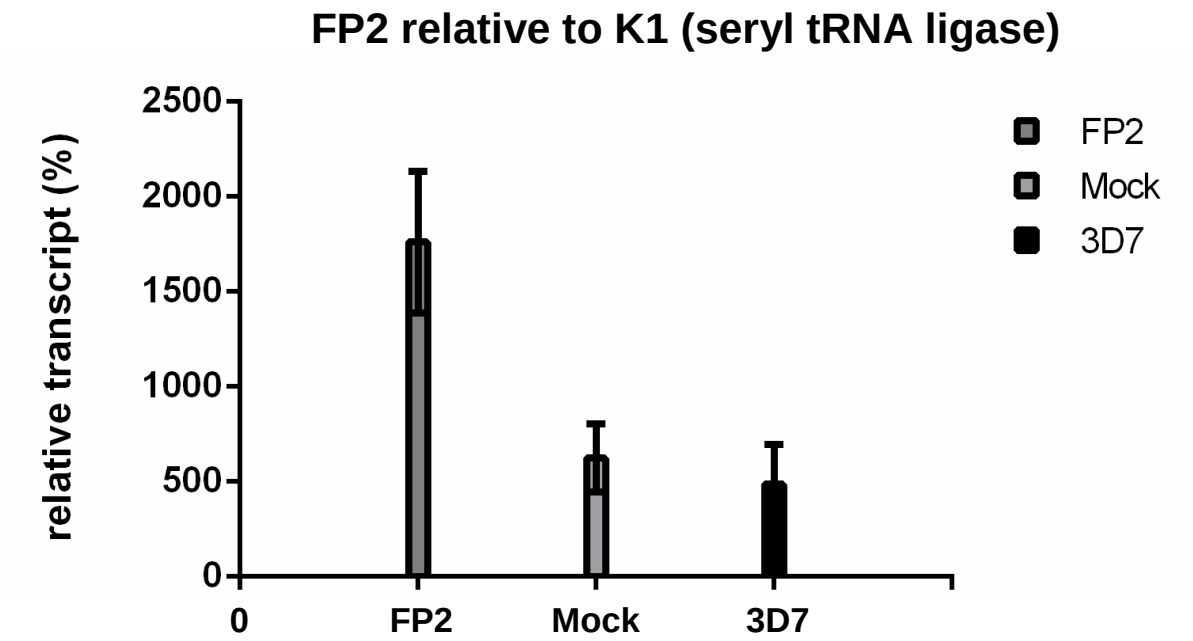

Figure 43 - Quantitative Real-time PCR of *Pf*FP2 using gene specific primers designed by means of Primer 3. An about three-times higher transcription level was detected for *Pf*FP2.

4.3 Structural analysis

4.3.1 Cysteine protease Falcipain 2b (FP2b)

4.3.1.1 Cloning in pASK-IBA3 plus

In order to analyse the gene structure of the cysteine protease Falcipain 2b (FP2b), sequence investigations were performed in the *P. falciparum* genome database, which showed that this open frame (ORF) contains no introns. However, a transmembrane domain within the first 60 amino acids was detected using the program TMHMM2.0. Therefore, the amplification of this construct was started after the transmembrane domain and polymerase chain reaction (PCR) using freshly isolated gDNA from *P. falciparum* and gene specific primers encoding for a C-terminal Strep tag were performed in order to amplify the respective open reading frame. The reaction mixture was pipetted exactly according to the pipetting scheme in 3.2.1 (Table 1) and the PCR product was exponentially amplified by means of the PCR program in 3.2.1 (Table 2). The PCR product for *Pf*FP2b has a molecular mass of 1271 bp was detected by agarose gel electrophoresis (Fig. 44A). After purification both, the pASK-IBA3 plus vector and the fragment were digested with *XbaI* and *HindIII* - since FP2b has an internal restriction site for *BsaI* - and subsequently ligated. After the transformation into *E. coli* XL10-Gold, plasmid DNA was isolated and test digested by *XbaI* and *HindIII*.

The analytical digestion was separated by 1% agarose gelelectrophoresis revealing two bands, one about 3247 bp (pASK-IBA3 plus vector) and the other about 1271 bp (insert) (Fig. 44B). The sequencing of this and all further constructs was performed according to the sequencing-method of Sanger and revealed that there are no mutations, so that this construct can be used for recombinant expression. The determined sequences are listed in the appendix for all cloned constructs. Figure 44C is a schematic illustration of the obtained vector pASK-IBA3 plus *Pf*FP2b with the calculated molecular masses of the (vector 3247 bp and insert 1271 bp).

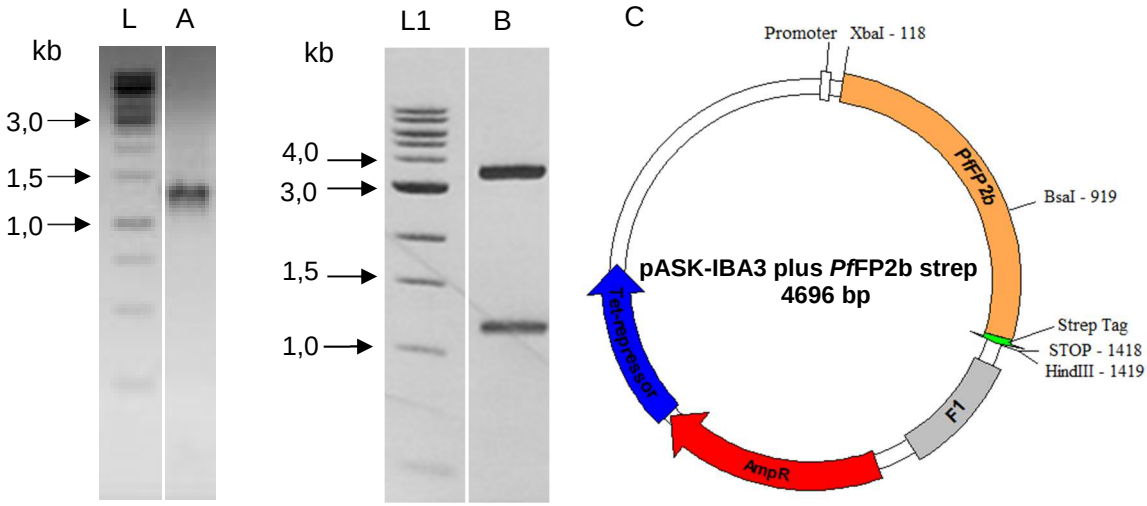

Figure 44 - Results of the cloning of *Pf*FP2b into the pASK-IBA3 plus vector. **L -** GeneRulerTM 1 kb DNA Ladder (Fermentas), **L1 -** GeneRulerTM 1 kb Plus DNA Ladder (Fermentas) **A -** 1/10 volume of the PCR product in 6 x DNA loading Dye, **B -** analytical digestion of a plasmid preparation with the enzymes *XbaI* and *HindIII*. **C -** vector map of the resulting pASK-IBA3 plus vector with *Pf*FP2b.

4.3.1.2 Expression and detection of the purified protein by SDS-PAGE

After sequencing, the plasmid was transformed into the competent expression cell line *E. coli* BLR-DE3. Once the bacterial culture had reached an A_{600} of 0,5 - 0,7, expression was induced by AHT (200 ng/ml) and recombinant expression was performed overnight and at 20 °C (3.3.1). The next day, the culture was centrifuged and the pellet resuspended in buffer W and stored at -20 °C until purification. During the purification, samples were taken from the pellet fraction, supernatant, and elution to check the solubility of the protein and the quality of purification via the strep-tag (3.3.3). The samples were subsequently separated by 12% SDS-PAGE (3.3.5). The gel was stained in Coomassie blue (3.3.6), whereby the proteins were non-specifically stained. In the eluate, a band was detected at the expected molecular mass of

approximately 50 kDa (Fig. 45A). Neither washing with $MgCl_2$ and ATP or casein and NaOH nor FPLC could eliminate the contamination band of about 70 kDa (Fig. 45B). However, for crystallisation approaches clean and pure protein is necessary.

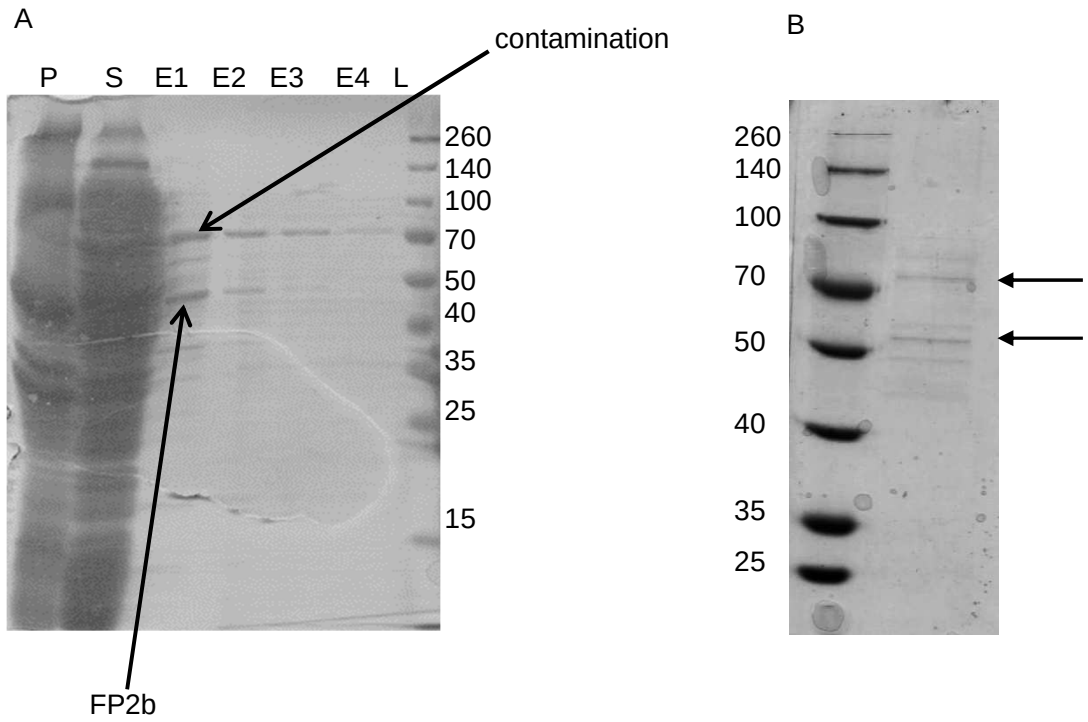

Figure 45 A - 12% SDS-PAGE for checking the purification of the expressed protein *Pf*FP2b. **P -** Pipette tip form the pellet in 100 µl buffer W, **S -** 100 µl of the supernatant after centrifugation, **L -** prestained protein molecular weight marker (Fermentas), **E -** 100 µl of elution in 1 ml desthiobiotin (diluted 1:10 in buffer W).
B - 12% SDS-PAGE for checking the purification after FPLC. Arrows represent the position of contamination and *Pf*FP2b.

4.3.2 Heme Detoxification protein (HDP)

4.3.2.1 Cloning in pASK-IBA3 plus

In contrast to the previous construct, sequence analyses in the *P. falciparum* genome database showed that the Heme detoxification protein (HDP) contains introns. Therefore, the amplification of the ORF of HDP was obtained by RT-PCR using freshly isolated *P. falciparum* RNA and gene specific primers encoding for a C-terminal Strep-tag. The amplification was performed using the Super ScriptIII One Step RT-PCR System with Platinum® Taq DNA polymerase (Invitrogen) according to the manufacturer's instructions. 1 µg RNA was used for the RT-PCR reaction. The resulting PCR product was detected in an 1% agarose gel. In Figure 46A, a strong, defined band with an expected molecular weight of about 618bp was detected. After

purification both, the pASK-IBA3 plus vector and the PCR fragment were digested with *BsaI* and subsequently ligated by T4-DNA-Ligase. The succeeding transformation into *E. coli* XL10-Gold was followed by the isolation and test digestion of plasmid DNA. The analytical digestion with *XbaI* and *HindIII* was separated in an 1% agarose gel exhibiting two bands, one about 3247 bp (pASK-IBA3 plus vector) and the other about 618 bp (insert) (Fig. 46B). The sequencing of this construct verified its correctness.

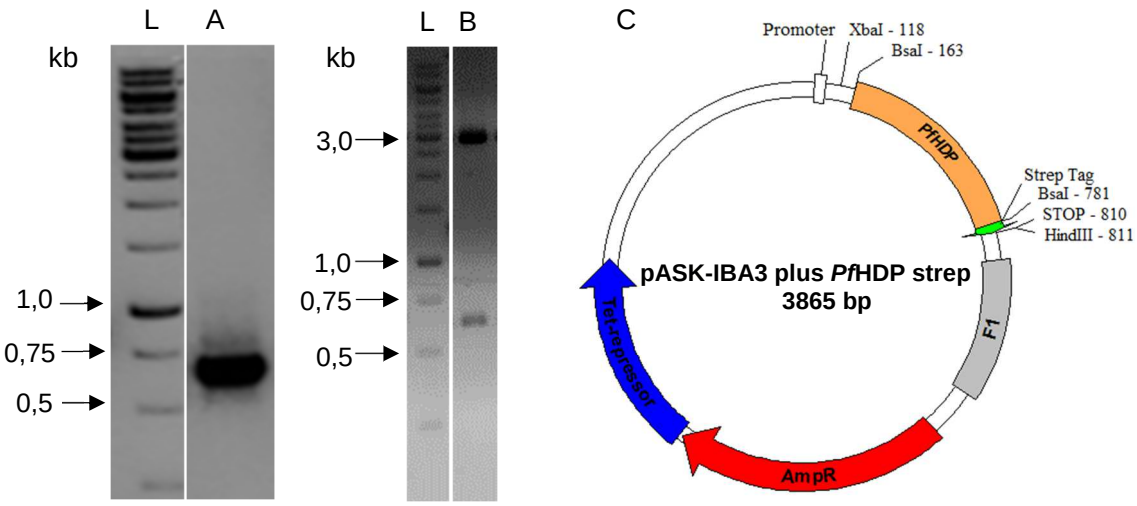

Figure 46 - Results of the cloning of *Pf*HDP into the pASK-IBA3 plus vector. **L:** -GeneRulerTM 1 kb DNA Ladder (Fermentas), **A -** 1/10 volume of the PCR product in 6 x DNA loading Dye, **B -** analytical digestion of a plasmid preparation with the enzymes *XbaI* and *HindIII.* **C -** vector map of the resulting pASK-IBA3 plus vector with *Pf*HDP.

4.3.2.2 Expression and detection of the purified protein by SDS-PAGE

Having shown above that the plasmid actually contains the desired insert, the plasmid was transformed into the expression cells BLR-DE3. Subsequent expression of the protein was induced by AHT (200 ng/ml) and carried out overnight at room temperature (3.3.1). The next day, the bacteria culture was centrifuged under refrigerated conditions, resuspended in buffer W and frozen at -20 °C. The efficiency of the purification was checked by SDS-PAGE (3.3.5). Once again, samples of the pellet fraction, the supernatant and the elution were taken to exclude protein loss in the purification or insolubility of the protein (Fig. 48). The samples were subsequently separated by SDS-PAGE analysis (3.3.5). A single band with a molecular weight of about 24,5 KDa was expected in the elution fraction. Figure 47 displays a strong, distinct band of about 24 kDa, but in the pellet fraction. Although a very weak band can

also be seen at the same height in the elution 2, these expression conditions have not led to any soluble protein.

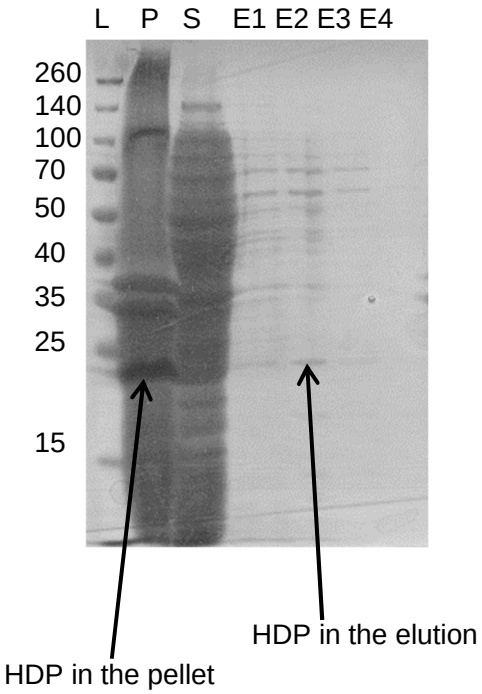

Figure 47 - 12% SDS-PAGE for checking the purification of the expressed protein PfHDP. **P -** Pipette tip form the pellet in 100 µl buffer W, **S -** 100 µl of the supernatant after centrifugation, **L -** prestained protein molecular weight marker (Fermentas), **E -** 100 µl of elution in 1 ml desthiobiotin (diluted 1:10 in buffer W).

Therefore, the plasmid was transformed into pGro7 competent *E. coli* cells for co-expression of the chaperone (GroES/GroEL). The expression was carried out under the same conditions as described above, however reaching the A_{600} of 0,5 the chaperones were induced by adding L-arabinose at a final concentration of 0,5 mg/ml and then the induction of our plasmid was started by adding AHT (200 ng/ml). After Strep-tag purification via chromatography the HDP was eluted and could be expressed soluble (Fig. 49A). Nevertheless, the chaperone seems to be necessary for correct folding of HDP as both proteins could not be separated from the respective protein neither by FPLC nor by washing with the detergent Triton X 100 and 1% Glycerol (Figure 48A, 48B).

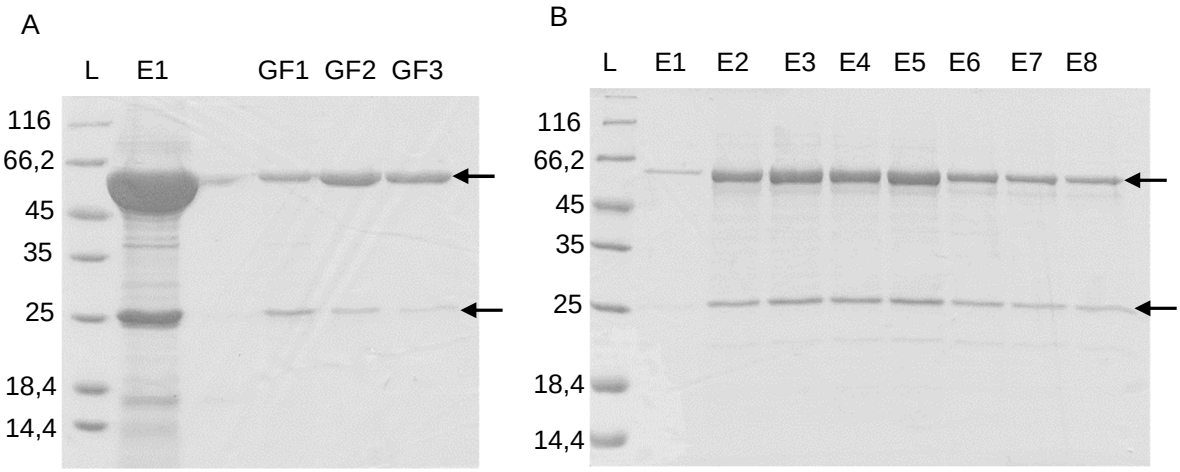

Figure 48 A - 12% SDS-PAGE for checking the purification of the expressed protein *Pf*HDP in PGRO7. **L -** Pierce™ Unstained Protein MW Marker (Thermo Fisher Scientific), **E1 -** HDP-GroEL complex purified via Strep tag chromatography, **GF1-GF3 -** Elutions after FPLC. **B -** 12% SDS-PAGE for checking the purification of the expressed PfHDP in PGRO7 after Strep-tag purification and washing by Triton X100 and 1% Glycerol. **L -** Pierce™ Unstained Protein MW Marker (Thermo Fisher Scientific), **E1-E8 -** elutions. Arrows represent the chaperone GroEL (approximately 60 kDa) and HDP.

4.3.3 Aminoacylproline aminopeptidase (APP)

4.3.3.1 Cloning in pASK-IBA3 plus

BLAST analyses disclosed that this construct contains no introns. Therefore, the amplification of this construct was performed by PCR using freshly isolated gDNA from *P. falciparum* and gene specific primers encoding for a C-terminal Strep-tag. The reaction mixture was pipetted exactly according to the pipetting scheme in 3.2.1 (Table 1) and the PCR product was exponentially amplified by means of the PCR program in 3.2.1 (Table 2). One tenth of the PCR product was subsequently separated by agarose electrophoresis (Fig. 49A). A band at the molecular mass of about 2300 bp was detected. The ORF of the large amoniopeptidase (MW 2334bp) could thus be successfully amplified. After purification both the vector and the fragment were digested with *BsaI* and subsequently ligated by T4-DNA-Ligase. After the transformation into *E. coli* XL10-Gold, plasmid DNA was isolated and test digested by *XbaI* and *HindIII.* The analytical digestion was separated in an 1% agarose gel which exhibited two bands, one about 3247 bp (pASK-IBA3 plus vector) and the other about 2334 bp (insert) (Fig. 49B). The sequencing of this construct revealed that there are no mutations, so that this construct can be used for recombinant expression.

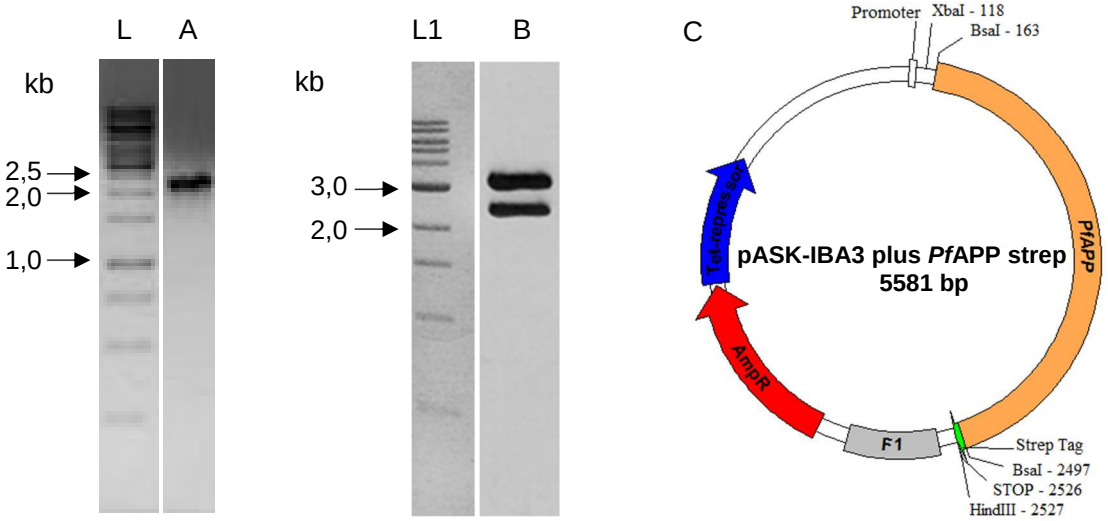

Figure 39 - Results of the cloning of *Pf*APP into the pASK-IBA3 plus vector. **L -** GeneRulerTM 1 kb DNA Ladder (Fermentas), **A -** 1/10 volume of the PCR product in 6x DNA loading Dye, **L1 -** GeneRulerTM 1 kb plus DNA Ladder (Fermentas) **B -** analytical digestion of a plasmid preparation with the enzymes *XbaI* and *HindIII*. **C:** vector map of the resulting pASK-IBA3 plus vector with *Pf*APP.

4.3.3.2 Expression and detection of the purified protein by SDS-PAGE and Western Blot

For successful expression, the isolated plasmid was transformed into the expression strain BLR-DE3. Expression of the protein *Pf*APP was initiated by AHT (200 ng/ml) and performed overnight at 20 °C (3.3.1). The purification of the protein from the disrupted bacteria took place via Strep-tag affinity chromatography (3.3.3) and was subsequently verified by SDS-PAGE (3.3.5). Figure 51 shows the SDS gel stained with Coomassie blue (3.3.6). A protein with the expected molecular mass of approximately 73 kDa could be detected (Fig. 50A). The protein was thus not only successfully expressed, but also successfully purified via the Strep-tag. A second SDS-PAGE with identical loading was used for Western-Blot analysis using a monoclonal anti-strep-tag antibody (3.3.7). A strong and distinct band at the level of 73 kDa was detected in the elution fraction (Fig. 50B).

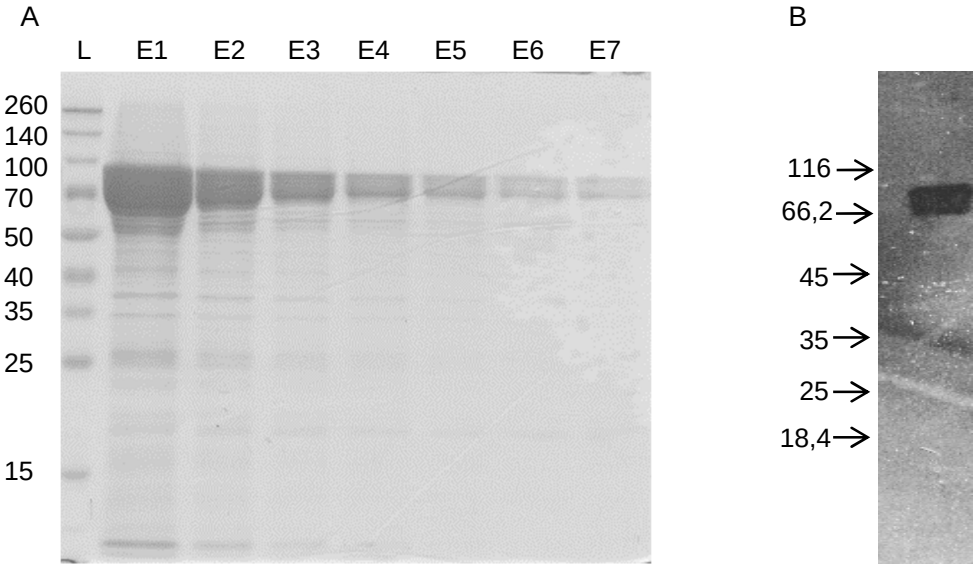

Figure 50 A - 10% SDS-PAGE for checking the purification of the expressed protein *Pf*APP in BLR-DE3. **L -** prestained protein molecular weight marker (Fermentas), **E1-E7 -** elutions.
B - Verification of the expression of the fusion protein APP by western blot analysis using monoclonal antibodies directed either against the Strep-tag (IBA, Germany) and a secondary anti-mouse peroxidase coupled antibody (Dianova) according to SAMBROOK et al. (1989).

In order to purify APP up to crystallisation level, a FPLC analysis on a calibrated Superdex S200 column was carried out (Fig. 51).

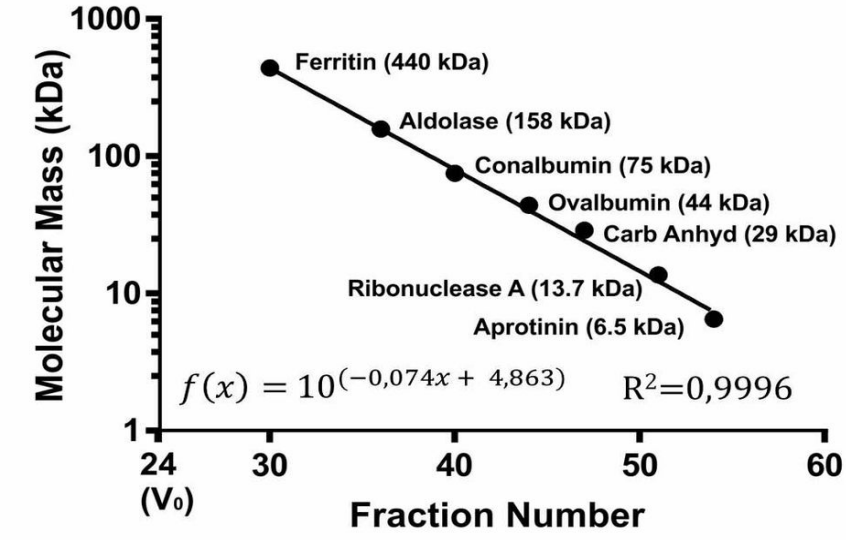

Figure 401 - Calibration curve of the gelfiltration column Superdex 200.

The chromatogram of the FPLC turned out that APP is predominantly present in its dimeric state (Fig. 52).

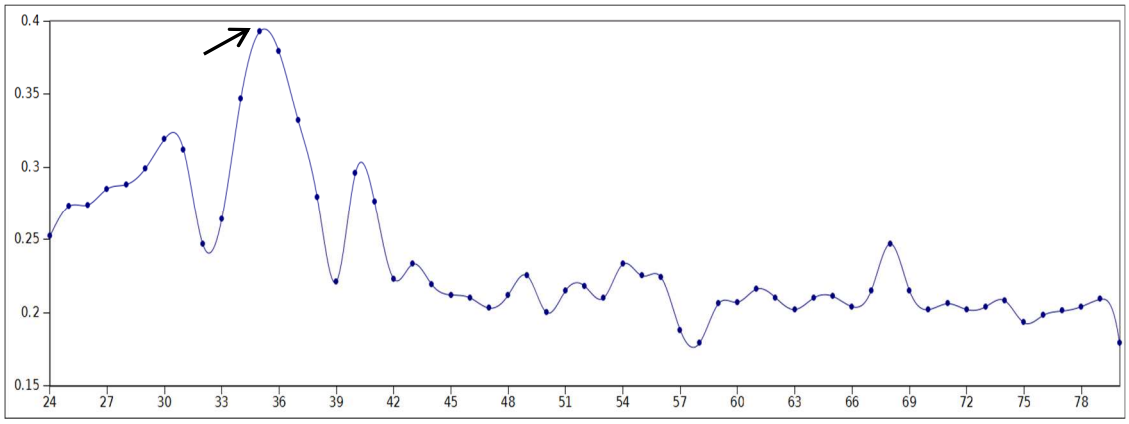

Figure 52 - Chromatogram of the APP run on the gelfiltration column Superdex 200. The arrow represents the peak of the dimeric state of APP in its native state.

Dynamic light scattering (DLS) revealed that APP gets aggregated after concentration and there is only a small amount left of the dimeric state (Fig. 53). But for a crystallisation approach pure as well as high concentrated protein (at least 10 mg/ml) is requested.

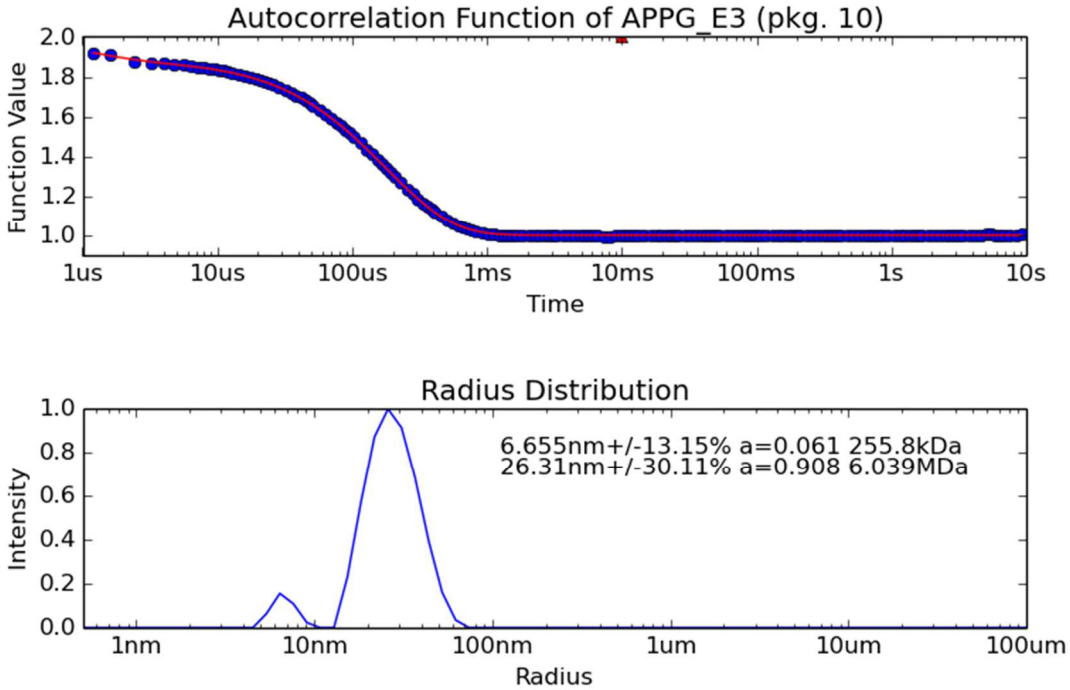

Figure 413 - Dynamic light scattering (DLS) of APP.
The small peak represents the tetrameric state of *Pf*APP whereas the huge peak embodies highly accumulated APP.

In order to analyse the sequence homology of *P. falciparum* APP, sequence analyses were performed by BLAST searches (ALTSCHUL et al., 1990), which showed that the

first 128 amino acids from the N-terminus are not conserved and absent in any homologue protein. Furthermore, this N-terminal region is predicted by the server XtalPred (SLABINSKI et al., 2007), to possess a long, disordered region, which greatly reduces the probability of crystallisation. Premature APP is supposed to be processed to its mature form within the food vacuole. Signalling of the premature form to the food vacuole might be signalised by the N-terminal extension. Additionally, the original APP DNA sequence was examined regarding the presence of codons which are rare to *E. coli*. Based on these new findings, a truncation of APP removing 128 amino acids from the N-terminal and 6 amino acids from the C-terminal, and codon optimisation was carried out by GenScript, USA (Fig. 54).

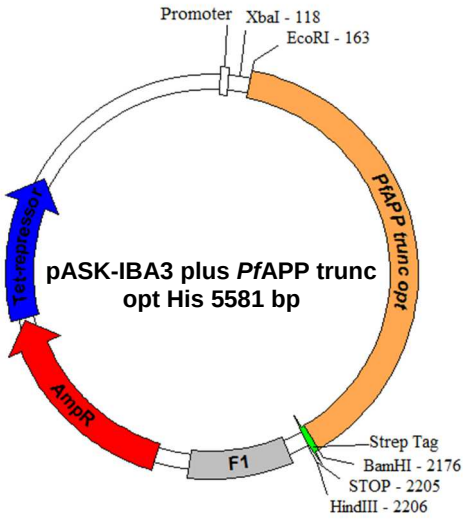

Figure 54 - Vector map of the pASK-IBA3 plus vector with *Pf*APP trunc opt.

Subsequently, the modified ORF of APP was transformed into *E. coli* BLR-DE3 competent cells and recombinant expression performed under the same conditions as describes above, with one single change: $MnCl_2$, which has been shown to be essential for the activity of this aminopeptidase, was added to the expression mixture as well as protein buffer. The purification was carried out via Ni-NTA affinity chromatography and the elution fractions were separated in a 10% SDS PAGE (Fig. 55).

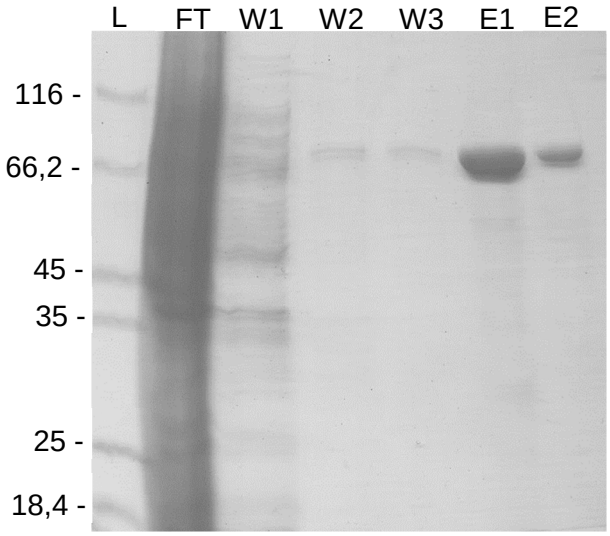

Figure 55 - 10% SDS-PAGE of the Ni-NTA affinity chromatography of *Pf*APP. **L -** Pierce™ Unstained Protein MW Marker (Thermo Fisher Scientific), **FT -** flow through, **W -** washing step, **E -** elution step.

In the next step, size exclusion chromatography was performed in order to remove remaining impurities and to separate different oligomeric states of APP from each other. Three distinct peaks have been detected of which the first peak (I) represents the void fraction containing aggregated APP as well as other impurities (Figure 56) and peak II and III were further investigated by native page (Figure 57). Predominantly dimeric APP (155,6 kDa) was sensed in the third peak along with traces of monomeric (77,8) and tetrameric APP (311,2 kDa). The second peak of the size exclusion chromatography Icontained a mixture of dimeric and tetrameric APP, as well as higher oligomeric states, presumably hexamers and octamers.

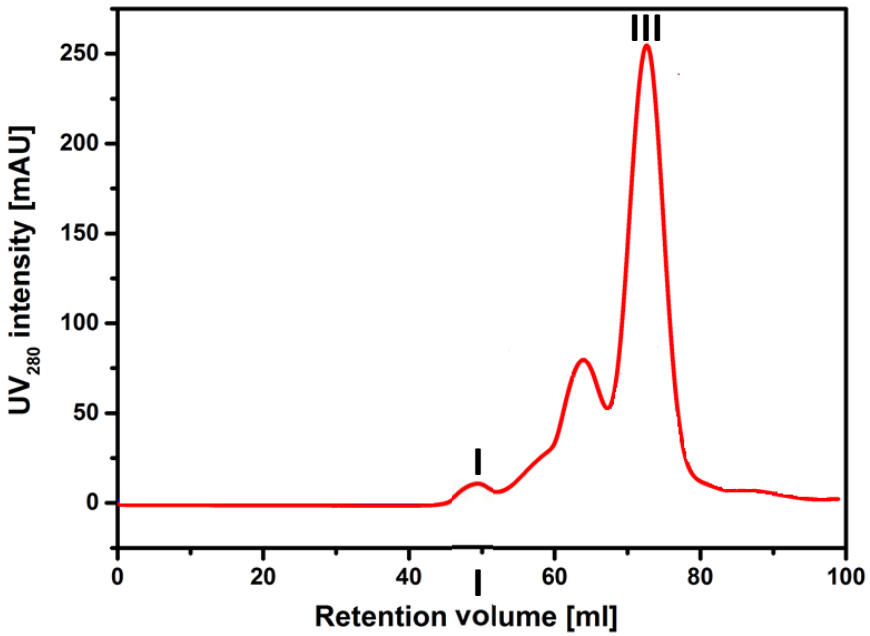

Figure 426 - Chromatogram of the size exclusion chromatography (FPLC). I: Small void peak, II: retention volume of 64 ml, III: retention volume of 75 ml.

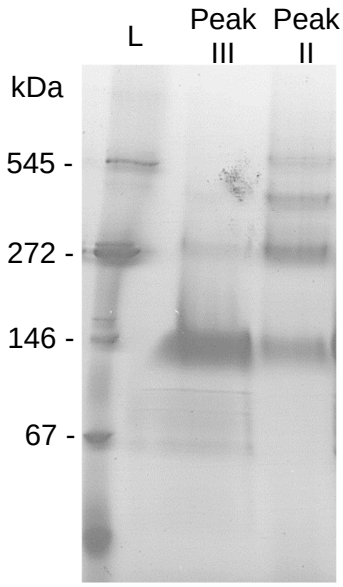

Figure 437 - Native Page of Peak II and III of the APP separated by size exclusion chromatography. Peak III contained predominantly dimeric APP and traces of monomeric and tetrameric APP, whereas peak II contained a mixture of dimeric and tetrameric APP, as well as higher oligomeric states, presumably hexamers and octamers.

The fractions from the middle of peak III were joined together and concentrated for further structural characterisation. In order to verify the dispersity and status of aggregation of the concentrated protein, DLS (Dynamic light scattering) analysis was performed using a sample concentrated of up to 5,3 mg/ml. A representative radius

distribution pattern as well as a hydrodynamic radius of 4,8 nm (≈ 125 kDa) calculated from 20 measurements and indicating a highly monodisperse solution (PDI = 18 %) are shown in figure 58. As already reported for other aminopeptidases, APP also preferentially forms dimers (LI et al., 2008; LYER et al., 2015). Circular Dichroism (CD) spectroscopy involving circularly polarised light is used to investigate the secondary structure of proteins. The recorded CD-spectrum displays two distinct minima at 220 nm and 208 nm, a zero crossing at 203 nm and a maximum towards 195 nm (Fig. 59). These results suggest that APP is well folded and a secondary structure content of 40% α-helices, 23% β-sheets, 13% turns and 24% random coil was approached using a set of reference spectra and the algorithm developed by VENYAMINOV et al. (1991).

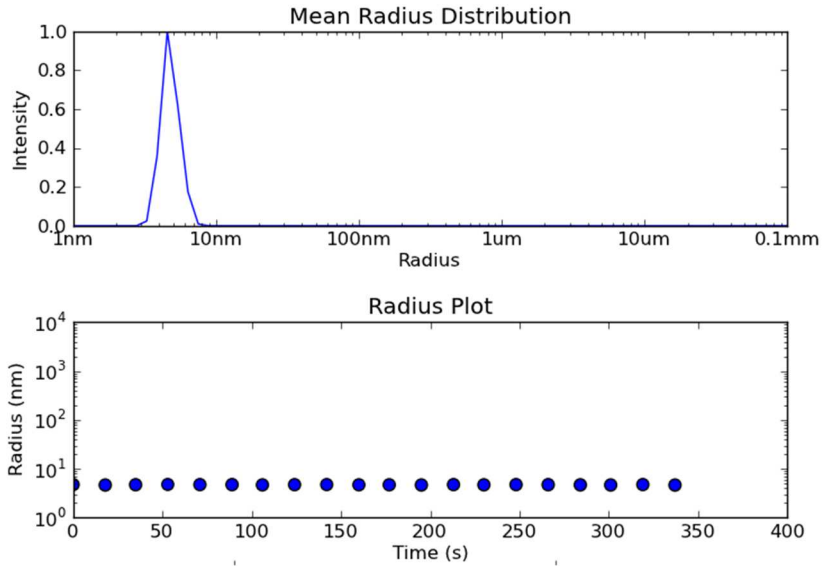

Figure 58 - DLS measurement of APP concentrated up to 5,3 mg/ml shows a highly monodisperse solution.

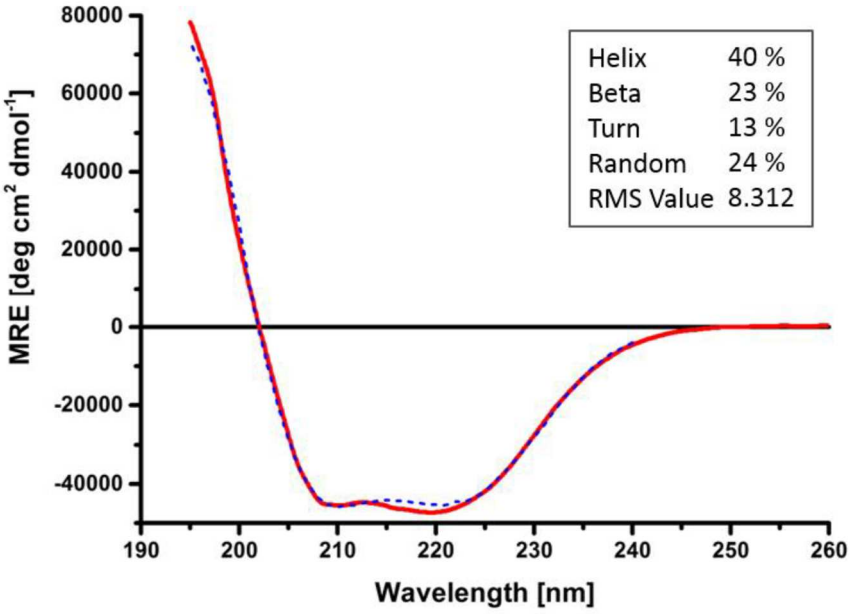

Figure 59 - CD-spectrum of concentrated APP illustrates typical characteristics for a well-folded protein and allows a secondary structure content approximation.

In order to verify whether the expressed, truncated and optimised form of APP is still active, an activity assay was performed in cooperation with CEFAP at USP using specifically designed penta-peptides according to RAGHEB et al. (2009). The substrate and APP were incubated at 37 °C in a ratio of 1:20 using a Tris-HCl buffer supplemented with $MnCl_2$. After two hours, the reaction was stopped by adding 10% Acetic acid and the amount of uncleaved peptide was identified by mass-spectrometry. A penta-peptide, which has a glycine in P1 ' position instead of the proline (Tyr-Pro-Trp-Thr-Gln → Tyr-Gly-Trp-Thr-Gln), was used as a control to verify the substrate specificity of the enzyme. APP is digesting its substrate within one hour completely, whereas the modified substrate is not catalysed (Fig. 60).

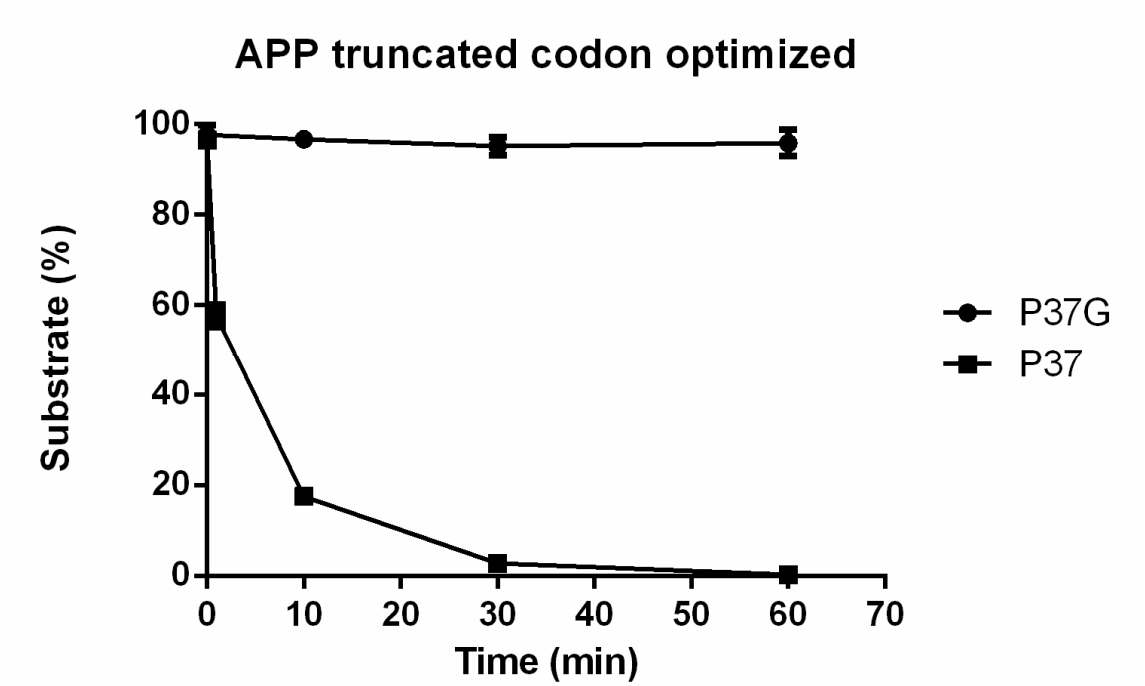

Figure 60 - Activity assay of APP using specifically designed peptides. P37: H-Tyr-Pro-Trp-Thr-Gln-OH, P37G: mutant where the proline was substituted by a glycine: H-Tyr-Gly-Trp-Thr-Gln-OH. APP is

The commercial crystallization screens PACT premier (MD1-36), JCSGplus (MD1-40), Morpheus (MD1-47), Stura FootPrint (MD1-20) (all Molecular Dimensions, Suffolk, UK) and AmSO4 (Quiagen) were tested and pipetted by a Honeybee 961 pipetting robot (Genomic Solutions, Huntingdon, UK). After a few days, APP protein crystals were found in various crystallization conditions, predominantly at high molecular weight PEG (>1500) and pH values between 7 and 8. The obtained crystals have been set up with a protein concentration ranging from 7,4 to 11,6 mg/ml. The colourless APP crystals possessed a rhombical shape with side dimensions up to 200 µm, while the thickness remained significantly smaller. Best diffracting crystals were obtained in a condition containing 0,2 M sodium fluoride, 0,1 M Bis-Tris propane pH 6,5 and 20% PEG 3350 with a protein concentration of 11,6 mg/mL (Fig. 61 A). Crystals were complemented with 26% (v/v) glycerol, fished in a nylon loop, flash cooled in gaseous nitrogen at -173,15 °C and mounted at the P14 EMBL beamline at the PETRA III synchrotron for X-ray diffraction analysis. APP crystal diffracted up to a resolution of 1,7 Å (Fig. 61 B). The data collection statistics are shown in Table 6.

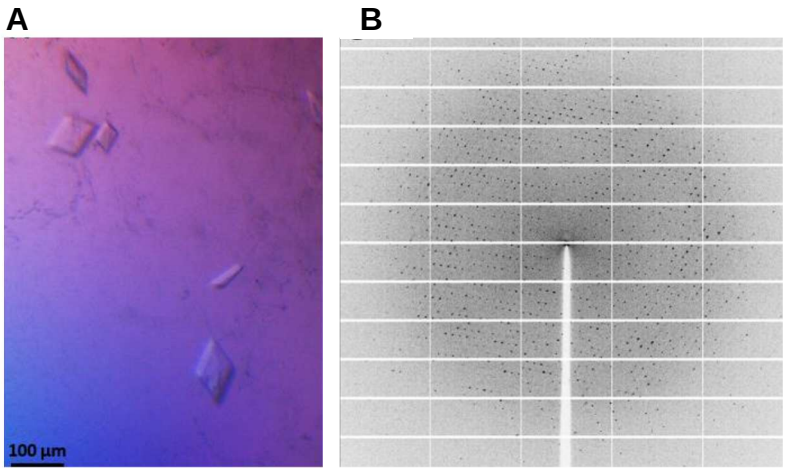

Figure 691 A - APP crystals grown in 0,2 M sodium fluoride, 0,1 M Bis-Tris propane pH 6,5 and 20% PEG 3350 with a protein concentration of 11,6 mg/mL possessed a rhombical shape.
B - Diffraction pattern of APP crystal showing a resolution up to 1,7 Å.

The crystal structure of APP was solved by performing molecular replacement using one monomer from human APP (PDB: 3CTZ) as a search model resulting in a contrast value of 7,44, a correlation coefficient of 60% and a R-factor of 44,5% (WISEDCHAISRI; GONEN, 2013). Isotropic B factors were calculated by REFMAC5 (MURSHUDOV et al., 2011) resulting in two TLS group and the TLS contribution was included in the final structural model of APP. Amino acids 1-28, 101-102, 178-180, 199-205, 328-333 from chain A are absent in the structural model due to their invisibility in the electron density. The increased B-factor compared to domain II and III correlates with the fact that most missing loops are located in the N-terminal domain I suggesting a higher flexibility. In chain B, a large fraction of domain I is not discernible excluding the amino acids 1 - 53, 72 - 73, 97 - 135, 172 – 187, 195 - 202 and 332 - 333 from the structural model. Chain A has less amino acid misplacement as a result of stabilising crystal contacts which are absent to chain B. The resulting model demonstrates excellent geometry and no Ramachandran outliers identified by PROCHECK (LASKOWSKI et al., 1993).

Table 6 - Data collection and refinement statistics for APP

Data collection statistics[a]	
Beamline	P14
Wavelength [Å]	0.96863
Space group	C2
Unit cell parameters: a, b, c [Å]	146.09, 93.86, 103.03
α, β, γ [°]	90.0, 105.33, 90.0
Resolution [Å]	30 - 1.89 (1.99 – 1.89)
Temperature [K]	100
Rmergeb	6.5 (61.3)
Rmeasc	7.8 (72.7)
Measured reflections	364885 (53166)
Unique reflections	106236 (15406)
Average I/σ(I)	13.1 (2.2)
Mn(I) half-set correlation CC(1/2)	99.9 (65.0)
Completeness [%]	99.2 (99.1)
Average mosaicity	0.10
Redundancy	3.4 (3.5)
Refinement statistics	
Resolution range [Å]	30 - 1.89
R/ Rfree [%]	18.67 / 22.54
Protein atoms	9561
Water molecules	284
Ions	4
Ligands	4
Rms deviation	
Bond-length [Å]	0.0186
Bond angle [°]	18.810
B factor [Å2]	
Protein	34.7
Water	27.9
Ions	19.2
Ligands	37.3
Ramachandran plot analysis	
Most favored regions [%]	88.3
Allowed regions [%]	11.2
Generously allowed regions [%]	0.5

a: Values in parentheses are for the highest resolution shell.

b R*merge* =Σ$\Sigma i|Ii(hkl)-\langle I(hkl)\rangle|hkl\Sigma\Sigma Ii(hkl)ihkl$,

c R*meas* =Σ$\sqrt{nn-1}\Sigma|Ii(hkl)-\langle I(hkl)\rangle|ni=1hkl\Sigma\Sigma Ii(hkl)ihkl$,

where *I (hkl)* is the mean intensity of the reflections hkl, Σhkl is the sum over all reflections and Σi is the sum over i measurements of reflection hkl.

APP sequence identity with other known homolog structures was determined by the server Clustal Omega (SIEVERS et al., 2011) performing sequence alignment and

revealed a sequence identity of 35% for human APP and 30% identity for *C. elegans* APP (data not shown). Surprisingly, the Cα RMSD value from the structure comparison with *C. elegans* APP is lower (1,7 Å) than that one for human APP (2,1 Å)

As expected from the data of the biophysical characterization, APP forms a homodimer in the crystal (Fig. 62). The overall size of the dimer is approximately 85 x 70 x 55 $Å^3$. Several hydrophobic interactions and four hydrogen bonds ensure stabilization of the dimer.

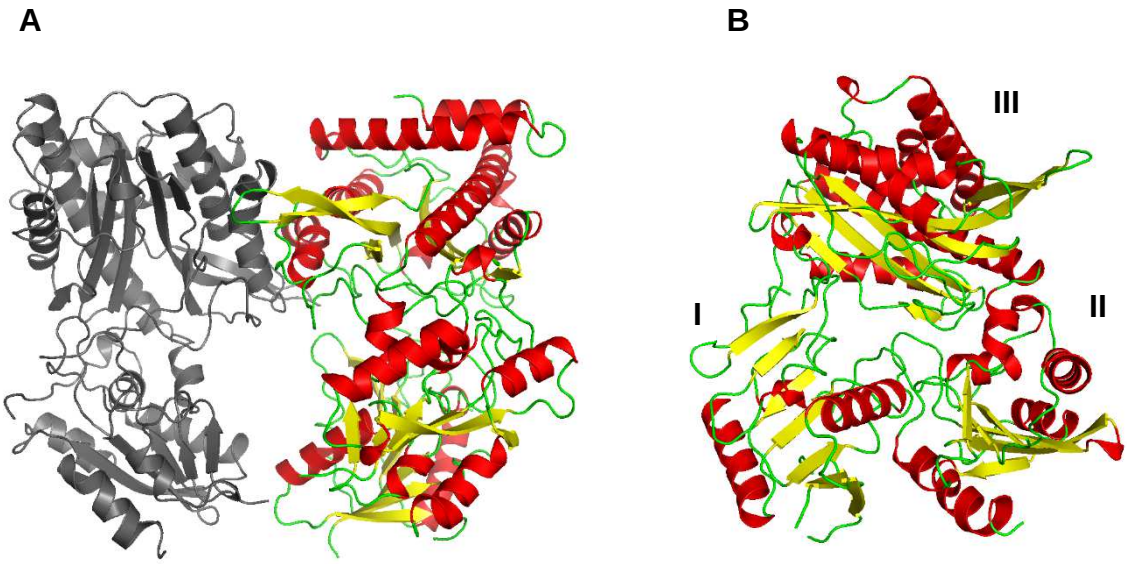

Figure 62 - Cartoon representation of the structural model of *P. falciparum* APP. **A -** APP is found in a homodimer assembly in the crystal. **B -** One APP monomer consist of three domains, domain I from the N-terminus to residue 203, domain II from residue 204 to 374 and domain III from residue 375 to the C-terminus. In the cartoon representation β-strands are coloured yellow, α-helices in red and green is used for turns and loops. The figure was created with PyMOL (Schrödinger, LLC).

P. falciparum APP possesses a three-domain structure likewise the analysed homologs. Domain I range from the N-terminus to residue 203, domain II from residue 204 to 374 and domain III from residue 375 to the C-terminus. There are six conserved amino acids constituting the active site, named D_{469}, D_{480}, H_{542}, H_{543}, E_{575} and E_{589}. The metal ions of the dinuclear center are coordinated by all six amino acids and are most likely manganese ions as already identified for the human APP (LI et al., 2008) and shown to be required for activity in *P. falciparum* APP (RAGHEB et al., 2009). In previous studies of human and *E. coli* APP it was hypothesized that the manganese cluster is connected to a water molecule and thereby is able to perform a nucleophilic attack on the X-pro bond of the substrate peptide (GRAHAM et al., 2004); LI et al., 2008).

4.3.3.3 Localisation analyses of *Pf*APP

Transgenic parasites were cultured and subsequently applied to fluorescence microscopy in order to visualise GFP fluorescence of the respective plasmodial protein and the counterstaining HOECHST (Invitrogen) *in vivo* according to MÜLLER et al., 2010. Figure 63 shows a parasite which is expressing the fusion protein *Pf*APP-GFP. This construct could be unambiguously localised in the parasite´s cytosol. Interestingly, the research group of Michael Klemba could detect a co-localisation of the aminopeptidase P (APP) in the food vacuole as well as the cytosol (DALAL; KLEMBA, 2007; RAGHEB et al., 2009). The expression of the fusion protein has been verified by western blot analysis using harvested parasites (Fig. 64).

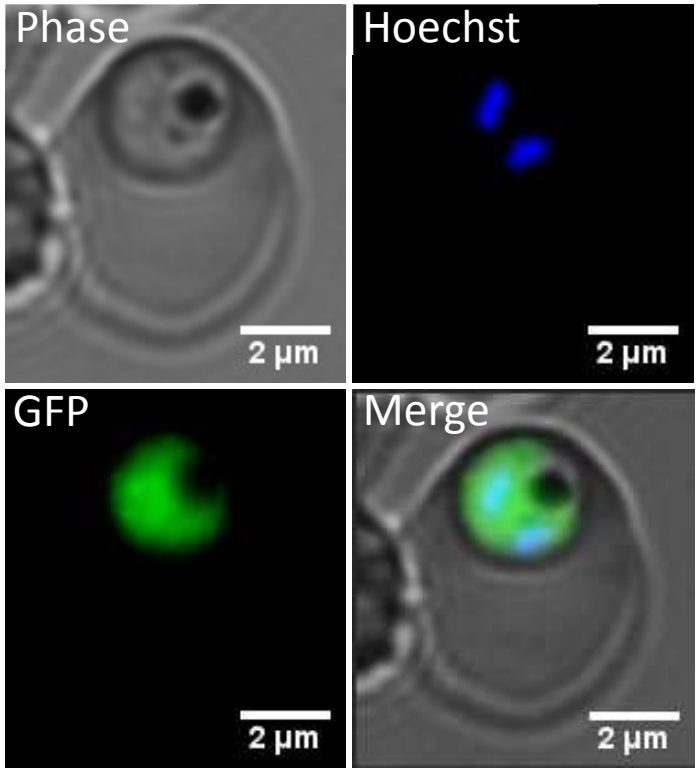

Figure 3403 - Fluorescence microscopy image 100 x magnified of the aminopeptidase P (*Pf*APP-GFP). *Pf*APP is a cytosolic protease. Phase: parasite in transmitted light, Hoechst: nuclear staining, GFP: the fluorescence of the GFP fusion proteins, Merge: merge of all images.

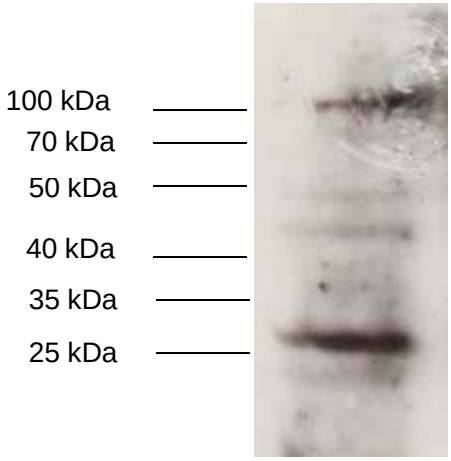

Figure 453 - Verification of the recombinant aminopeptidase P (APP) in *P. falciparum* by western blot analysis using monoclonal antibodies directed either against the GFP-tag (IBA, Germany) and a secondary anti-mouse peroxidase coupled antibody (Dianova) according to SAMBROOK et al, 1989. 10 µg total cell lysate protein were applied on a 12 % SDS-PAGE.

5. DISCUSSION

Besides the *de novo* synthesis of selected nutrients (MÜLLER et al., 2010) the malaria parasite has to import nutrients from its host cell for metabolic purposes such as energy supply. Highly proliferating cells such as the malaria parasite *P. falciparum* require an accelerated level of macromolecules for the maintenance of cellular structure and function. The unique life cycle and resulting microenvironments of the parasite has led to the evolution of metabolic pathways which differ from the human host (MÜLLER et al., 2010; WRENGER et al., 2008). It may be possible to exploit these unique pathways and enzymes in the design of therapeutic strategies. For instance, many anti-malarials are known to affect the food vacuole in which the digestion of the host haemoglobin occurs. Due to the high mutational rate of the parasite and its resulting rapid adaptation to environmental changes, drug resistance and its geographic distribution are increasing. Epidemiological studies revealed that there is a high correlation between abnormalities of erythrocytes such as sickle cell trait and *falciparum* endemic countries (PIEL et al., 2010).

5.1 Cloning and transfection

Sequence comparisons with already known proteases from other organisms and predictions of the open reading frame in the genome database of *P. falciparum* revealed 12 gene sequences which are participating in haemoglobin degradation (GARDNER et al., 2002). Additionally, an open reading frame was found that encodes a protein which detoxifies heme by forming hemozoin crystals, the heme detoxification protein (HDP) (JANI et al., 2008). However, two open reading frames were interrupted by introns, so that in addition to an amplification of total DNA (gDNA), RT-PCRs of total RNA (gRNA) had to be performed in order to clone the corresponding DNA sequences of the proteases into either the pASK-IBA3 vector and the pARL1a-hDHFR or rather pARL1a-BSD vector.

Of the original 13 constructs to be examined, 12 were successfully cloned (4.1 - 4.13). The metalloprotease falcilysin (Fl), which could not be cloned, had a molecular mass of more than 3,5 kb. Cloning of this fragment might be problematic since the empty transfection vector pARL1a- hDHFR is only slightly bigger in size. Therefore, attempts were made to compensate this problem by applying different ligation conditions. To

solve this problem, the amounts of PCR product and vector used, the duration and temperature of the ligation reaction were modified, among other things such as ATP or magnesium concentrations, competent cells or cloning strategies.
However, all cloned constructs were successfully transfected into the transfection vector pARL1a-hDHFR and pARL1a-BSD respectively (Table 5).

5.2 Proliferation assays in sickle cell blood

Haemoglobin S ("the sickle cell haemoglobin") is a structurally variant of normal haemoglobin (HbA) that result from a mutation in which glutamic acid at position 6 of the beta chain of HbA is changed to valine (BUNN, 1997; RAPHAEL, 2005; ROSENTHAL, 2011). This substitution leads to morphological different polymerised haemoglobin by which sickle red blood cells may adhere to endothelial cells or other normal erythrocytes resulting in aggregates and microvascular obstruction. (NAGEL; PLATT, 2001). It is still highly controversial, whether the sickle cell mutation has a protective role against malaria. There are three hypotheses, of which one says that both erythrocytes containing HbS are less supportive for *P. falciparum* growth under low oxygen tensions as well as a reduced parasite invasion event into HbS carrying erythrocytes under low oxygen levels (FRIEDMAN, 1978; PASVOL et al., 1978). The uncertainty whether *P. falciparum* can indeed infect sickle red blood cells could be clarified demonstrating with Hoechst stained parasites within sickle red blood cells (Fig. 33, 34).
Although sickle cell disease is always caused by the same mutation, there are differences in the HbA/HbS ratio. A proportion of 55% sickle cells was determined for the blood used within this work by means of a sickling test (Figure 32).
Furthermore, 3D7 shows exponential growth behaviour in wild type blood whereas the parasitaemia decreased rapidly after three weeks in sickle cell blood. Additionally*, P. falciparum* culture was maintained for almost two weeks in sickle cell blood. The percentage of sickle red blood cells increased rapidly within the first five days, but afterwards decreased even below the starting value (data not shown). This suggests that the parasites preferentially infect normal erythrocytes and only when hardly or no normal ones are present anymore, they infect sickle red blood cells.
The first enzyme to be tested in a proliferation assay in sickle cells was randomly selected. *Pf*DPAP1 generates dipeptides from haemoglobin-derived oligopeptides and

is a plasmodial ortholog of the lysosomal exopeptidase cathepsin C which cleaves dipeptides from the N-terminus of its oligopeptide substrates (KIRSCHKE; BARRETT,1987). Both enzymes share a sequence identity of 30% and a similarity of 45%. Cathepsin C is also an important protein in the activation of some serine proteases of immune effector cells (ADKISON et al., 2002; WOLTERS et al., 2001). Furthermore, the protein plays an important role in lysosomal protein degradation so that the plasmodial enzyme might have a similar function in the food vacuole.

Surprisingly, a negative effect in the proliferation of DPAP1 was detected and after three weeks the parasitaemia of both the WR Mock cell line and the DPAP1 diminished rapidly (Fig. 37). In order to get more information about the mode of action of this enzyme, localisation studies were performed. The fusion protein *Pf*DPAP1-GFP was localised to the food vacuole and the cytosol (Figure 38, upper picture). Additionally, *Pf*DPAP1 was also detected in other structures supposed to be vesicles. A putative signal sequence at the N-terminus indicates that this protein transits to the *P. falciparum* secretory pathway. Klemba et al. (2004) found premature DPAP1 accumulated in the parasitophorous vacuole (PV) suggesting an alternative trafficking route for DPAP1 through the PV to the FV. Co-localisation of proteins present in the cytosol as well as in an intracellular organelle bares always the risk of misinterpretations since the cytosolic localization can dramatically quench the fluorescence signal in the respective organelle. Highest activity was measured at pH 5,5 - 6,0 against the dipeptide Pro-Arg which is consistent with its function within the acidic FV. Additionally, inactivation of DPAP1 leads either to death or is highly deleterious to the blood stage parasite. Fractionation and immuno-gold labelling experiments allow to conclude that the structures/punctuated spots found within the parasite are not involved in trafficking of DPAP1 outside of the parasite (KLEMBA et al., 2004). Moreover, DPAP1 requires a reducing environment to be active. Finally, there are at least two cathepsin C homologs in the genome of the intestinal parasite *Cryptosporidium parvum* (ABRAHAMSEN et al., 2004) leading to the assumption that these enzymes as well as the plasmodial DPAP1 could play a role outside the haemoglobin catabolism.

The next enzyme to be examined in a proliferation assay in sickle cell blood was *Pf*FP2, a cysteine protease whose mature form is unambiguously localised to the food vacuole

(SUBRAMANIAN et al., 2007). Previously, however the growth behaviour of both the FP2 and the respective Mock cell line (3D7 containing the pARL1a-hDFHR plasmid, WR) was investigated in wild type blood. FP2 and WR showed a similar, exponential growth (Fig. 40) suggesting that there is no difference in proliferation due to the transfection event. Thus, it could be concluded that every difference in growth of FP2 in sickle cell blood can be attributed to the activity of the investigated enzyme. FP2 and the Mock cell line WR kept growing similar. But after two weeks and a half WR decreased which results in a less steelier growth curve compared to FP2 and three times lower relative parasitaemia (Fig. 41). The result of the quantitative Real-time PCR performed with gene specific primers (Fig. 42) is consisting with the result from the growth assay in sickle cell blood. Cysteine protease inhibitors block haemoglobin hydrolysis and parasite development indicating that parasite cysteine protease activity is required for this essential process (ROSENTHAL et al., 1988; ROSENTHAL et al., 1991). Furthermore, inhibition of FP2 by Leupeptin or E-64 lead to a swelling of the food vacuole filled with dark-staining material which was demonstrated to be an accumulation of undegraded haemoglobin (BAILLY et al., 1992; DLUZEWSKI et al., 1986; ROSENTHAL et al., 1988). Surprisingly, DPAP1 has still a sequence identity of 20 - 25% to FP2 (ROSENTHAL, 2004).

5.3 Recombinant expression and structural analysis

The cysteine protease Falcipain 2b (FP2b) possesses a transmembrane domain within the first 60 amino acids. Full-length FP2b could not be expressed soluble (data not shown) for which reason a construct truncated by the transmembrane domain was cloned. This truncated enzyme could be expressed soluble in BLR-DE3, however a contamination presumably an *E. coli*- derived protein could not be removed. A problem with the expression of host-different proteins in prokaryotic cells is the missing post-translational modification of eukaryotic proteins, which can lead to the formation of inclusion bodies. The particular problem in the production of proteases in this expression system is that these enzymes do not occur in *E. coli*. In addition, proteins having catalytic activity, such as e.g. cysteine proteases, which affect the expression cell and an overproduction of this protein can cause toxicity in *E. coli*. A further method for increasing the solubility of recombinant proteins and thus avoiding the formation of

inclusion bodies is in the purification by "solubility tags", such as GST (glutathione-S-transferase) or MBP (maltose-binding protein).
During haemoglobin degradation heme is going to be released which is extremely toxic to the parasite. Thus, a detoxification of heme is essential for an uninterrupted growth and proliferation of the parasite. Primarily detoxification takes place by conversion of heme into an insoluble crystalline material called hemozoin (Hz) or the malaria pigment (JANI et al., 2008). In humans heme is detoxified by a combination of proteins like hemopexin and heme oxygenase (KIKUCHI et al., 2005) which are absent from the parasite genome. JANI et al. (2008) found a novel protein, the heme detoxification protein (HDP), which polymerises heme into hemozoin. Functionality of HDP seems to be conserved across *Plasmodium* genus. It was not possible to express HDP soluble in BLR-DE3. Therefore, the plasmid was transformed into pGro7 competent cells which encodes for a chaperone (GroES/GroEL) that is required for the proper folding of many protein. Indeed, HDP could be expressed soluble and purified via Strep-tag chromatography together with the chaperone. Nevertheless, the chaperone seems to be necessary for correct folding of HDP as it could not be separated from the respective protein. HDP is a crucial protein to the parasite and possesses an “outbound-inbound” trafficking route that has not been observed for any of the known malaria proteins.

Aminopeptidases catalyse the hydrolysis of amino acids from the amino termini of proteins and peptides. So far, 8 amino acids are identified in the *P. falciparum* genome: 4 methionine aminopeptidases, 2 neutral aminopeptidases (*Pf*M1AAP and *Pf*M17LAP), a prolyl aminopeptidase (*Pf*APP) and an aspartyl aminopeptidase (*Pf*AAP) (TEUSCHER et al., 2007). APP is a protein with a molecular mass of 90 kDa in its premature, inactive form and is processed into a 73 kDa mature form. In the first go entire APP was successfully expressed in BLR-DE3, however the protein gets aggregated after concentration and the quantity of left dimeric APP is too small for any crystallisation approach.
The N-terminal extension of 128 amino acids might possess a putative signal peptide for import to the endoplasmic reticulum (ER) and does not seem to be present in mature APP. Furthermore, this N-terminal region is predicted by the server XtalPred (SLABINSKI et al., 2007), to possess a long, disordered region, which greatly reduces the probability of crystallisation. Additionally, the original APP DNA sequence was

examined regarding the presence of codons which are rare to *E. coli*. Based on these new findings, a truncation of APP removing 128 amino acids from the N-terminal and 6 amino acids from the C-terminal, and codon optimisation was carried out. Moreover, Mn^{2+} is necessary for proper APP folding and was thereby supplemented in both the expression media and protein buffer. These variations led to expression and purification of highly pure and active APP predominantly present in its dimeric form. DLS measurements verified a highly monodisperse solution of dimeric APP which could be subsequently used for random crystallisation screenings. Colourless, rhombic crystals were obtained and diffracted up to 1,7 Å. As expected, APP is as a homodimer and has a three-dimensional architecture just as human APP 1 and *E. coli* APP (GRAHAM et al., 2004; LI et al., 2008). However, the structure was solved at the same time by Drinkwater and colleagues and published in the Biochemical Journal in September 2016. In the future, we will be highly interested to co-crystallise APP with a non-cleavable peptide substrate in order to get more insides in substrate specificity. Currently, APP is the only aminopeptidase known to hydrolyse N-terminal amino acid from X-Pro-containing peptides (CUNNINGHAM; O'CONNOR, 1997; RAGHEB et al., 2009).

GFP localisation studies revealed an unambiguously occurrence in parasite´s cytosol. Interestingly, the research group of Michael Klemba could detect a co-localisation of the aminopeptidase P (APP) in the food vacuole as well as the cytosol (DALAL; KLEMBA, 2007; RAGHEB et al., 2009) suggesting a role in both haemoglobin degradation as well as peptide turnover and amino acid recycling. Consistent with this suggestion active APP was observed at both pH 7,5 and 6,5 as well as pH 5,5 and 5,0, albeit with a loss of activity of 20% in the latter case (RAGHEB et al., 2009).

6. CONCLUSION

- Further proliferation assays of haemoglobin degradative enzymes or enzyme combinations in sickle cell blood
- Screening for small molecule compounds against FP2
- co-crystallisation of APP with a non-cleavable peptide substrate & apstatin/bestatin → substrate specificity and identify new peptide inhibitors
- ONGOING: FP2DE4-GFP, a pH sensitive variant of GFP facilitates single trafficking to the food vacuole and can be used for ratiometric pH recordings.

7. REFERENCES*

ABRAHAMSEN, M.S.; TEMPLETON, T.J.; ENOMOTO S.; ABRAHANTE, J.E.; ZHU, G.; LANCTO, C.A.; DENG, M.; LIU, C.; WIDMER, G.; TZIPORI, S.; BUCK, G.A.; XU, P.; BANKIER, A.T.; DEAR, P.H.; KONFORTOV, B.A.; SPROGGS, H.F.; IYER, L.; ANANTHARAMAN, V.; ARAVIND, L.; KAPUR, V. Complete genome sequence of the apicomplexan, Cryptosporidium parvum. **Science,** v. 304, p. 441–445, 2004.

ABU-ZEID, Y.A.; ABDULHADI, N.H.; HVIID, L.; THEANDER, T.G.; SAEED, B.O.; JEPSEN, S.; JENSEN, J.B.; BAYOUMI, R.A. Lymphoproliferative responses to Plasmodium falciparum antigens in children with and without the sickle cell trait. Scand. **J. Immunol.**, v. 34, n. 2, p. 237-242, 1991.

ADKISON, A.M.; RAPTIS, S.Z.; KELLEY, D.G.; PHAM, C.T. Dipeptidyl peptidase I activates neutrophil-derived serine proteases and regulates the development of acute experimental arthritis. **J. Clin. Investig.**, v. 109, p. 363–371, 2002.
ALLISON, A.C. Notes on sickle-cell polymorphism. **Ann. Hum. Genet.**, v. 19, n.1, p. 39-51, 1954.

ANDERSON, T.J.C.; HAUBOLD, B.; WILLIAMS, J.T.; ESTRADA-FRANCO, J.G.; RICHARDSON, L.; MOLLINEDO, R.; BOCKARIE, M.; MOKILI, J.; MHARAKUWA, S.; FRENCH, N.; WHITWORTH, J.; VELEZ, I.D.; BROCKMAN, A.H.; NOSTEN, F.; FERREIRA, M.U.; DAY, K.P. Microsatellite Markers Reveal a Spectrum of Population Structures in the Malaria Parasite Plasmodium falciparum. **Mol. Biol. Evol.**, v. 17, p. 1467–1482, 2000.

ANDREWS, K.T.; TRAN, T.N.; FAIRLIE, D.P. Towards histone deacetylase inhibitors as new antimalarial drugs. **Curr. Pharm. Des.**, v. 18, p. 3467–3479, 2012.

ASHLEY, E.A.; DHORDA, M.; FAIRHURST, R.M.; AMARATUNGA, C.; LIM, P.; SUON, S.; SRENG, S.; ANDERSON, J.M.; MAO, S.; SAM, B.; SOPHA, C.; CHUOR, C.M.; NGUON, C.; SOVANNAROTH, S.; PUKRITTAYAKAMEE S, JITTAMALA, P.; CHOTIVANICH, K.; CHUTASMIT, K.; SUCHATSOONTHORN, C.; RUNCHAROEN, R.; HIEN, T.T.; THUY-NHIEN, N.T.; THANH, N.V.; PHU, N.H.; HTUT, Y.; HAN, K.-T.; AYE, K.H.; MOKUOLU, O.A.; OLAOSEBIKAN, R.R.; FOLARANMI, O.O.; MAYXAY, M.; KHANTHAVONG, M.; HONGVANTHONG, B.; NEWTON, P.N.; ONYAMBOKO, M.A.; FANELLO, C.I.; TSHEFU, A.K.; MISHRA, N.; VALECHA, N.; PHYO, A.P.; NOSTEN, F.; YI, P.; TRIPURA, R.; BORRMANN, S.; BASHRAHEIL, M.; PESHU, J.; FAIZ, M.A.; GHOSE, A.; HOSSAIN, M.A.; SAMAD, R.; RAHMAN, M.R.; HASAN, M.M.; ISLAM, A.; MIOTTO, O.; AMATO, R.; MACINNIS, B.; STALKER, J.; DKWIATKOWSKI, D.P.; BOZDECH, Z.; JEEYAPANT, A.; CHEAH, P.Y.; SAKULTHAEW, T.; CHALK, J. INTHARABUT, B.; SILAMUT, K.; LEE, S.J.; VIHOKHERN, B.; KUNASOL, C.; IMWONG, M.; TARNING, J.; TAYLOR, W.J.; YEUNG, S.; WOODROW, C.J.; FLEGG, J.A.; DAS, D.; SMITH, J.; VENKATESAN, M.; PLOWE, C.V.; STEPNIEWSKA, K.; GUERIN, P.J.; DONDORP, A.M.; DAY, A.P.; WHITE, N.J. Spread of Artemisinin Resistance in Plasmodium falciparum Malaria. **N. Engl. J. Med.**, v. 371, p. 411-423, 2014.

---

* According to ASSOCIAÇÃO BRASILEIRA DE NORMAS TÉCNICAS. NBR 6023: informação e documentação: referências: elaboração. Rio de Janeiro, 2002.

BAILLY E.; JAMBOU, R.; SAVEL, J.; JAUREGUIBERRY, G. *Plasmodium falciparum:* differential sensitivity in vitro to E-64 (cysteine protease inhibitor) and Pepstatin A (aspartyl protease inhibitor). **J. Protozool.**, v. 39, p. 593-599, 1992.

BANERJEE, R.; LIU, J.; BEATTY, W.; PELOSOF, L.; KLEMBA, M.; GOLDBERG, D.E. Four plasmepsins are active in the Plasmodium falciparum food vacuole, including a protease with an active-site histidine. **Proc. Natl. Acad. Sci. U.S.A.**, v. 99, n. 2, p. 990-995, 2002.

BEAUDOIN, R.L.; AIKAWA, M. Primaquine-induced changes in morphology of exoerythrocytic stages of malaria. **Science**, v. 160, p. 1233–1234, 1968.

BECKER, K.; TILLEY, L.; VENNERSTROM, J.L.; ROBERTS, D.; ROGERSON, S.; GINSBURG, H. Oxidative stress in malaria parasite-infected erythrocytes: host-parasite interactions. **Int. J. Parasitol.**, v. 34, n. 2, p. 163-189, 2004.

BEET, E.A. Sickle cell disease in the Balovale District of Northern Rhodesia. **East. Afr. Med. J.**, v. 23, p. 75-86, 1946.

BHISUTTHIBHAN, J.; PAN, X.; HOSSLER, P.A.; WALKER, D.J.; YOWELL, C.A. et al. The plasmodium falciparum translationally controlled tumor protein homolog and its reaction with the antimalarial drug artemisinin. **J. Biol. Chem.**, v. 273, p. 16192–16198, 1998.

BRADFORD, M.M. A Rapid and Sensitive Method for the Quantitation of Microgram Quantities or Protein Utilizing the Principle of Protein-Dye Binding. **Anal. Biochem.**, v. 72, p. 248-254, 1976.

BROWNE, P.; SHALEV, O.; HEBBEL, R.P. The molecular pathobiology of cell membrane iron: the sickle red cell as a model. **Free. Radic. Biol. Med.**, v. 24, n. 6, p. 1040-1048,1998.

BOYER, S.H.; BELDING, T.K.; MARGOLET, L.; NOYES, A.N. Fetal hemoglobin restriction to a few erythrocytes (F cells) in normal human adults. **Science**, v. 188, p. 361–363, 1975.

BUNN, H.F. Pathogenesis and treatment of sickle cell disease. **N. Engl. J. Med.**, v. 337, n. 11, p. 762–769,1997.

CALDAS DE CASTRO, M.; SINGER, B.H. Was malaria present in the Amazon before the European conquest? Available evidence and future research agenda. **Journal of Archaeological Science**, v. 32, p 337-340, 2004.

CALDERON-PEREZ, B.; XOCONOSTLE-CAZARES, B.; LIRA-CARMONA, R.; HERNANDEZ-RIVAS, R.; ORTEGA-LOPEZ, J.; RUIZ-MEDRANO, R. The Plasmodium falciparum translationally controlled tumor protein (TCTP) is incorporated more efficiently into B cells than its human homologue. **PLoS ONE**, v. 9, e85514 10.1371, 2014.

CALMETTE, A. Obituary for A Laveran. **Bull. Soc. Pathol. Exot.**, v. 6, p. 373-378, 1922.

CHOLERA, R.; BRITTAIN, N.J.; GILLRIE, M.R.; LOPERA-MESA, T.M.; DAIKITÉ, S.A.; ARIE, T.; KRAUSE, M.A.; GUINDO, A.; TUBMAN, A.; FUJIOKA, H.; DIALLO, D.A.; DOUMBO, O.K.; HO, M.; WELLEMS, T.E.; FAIRHURST, R.M. Impaired cytoadherence of Plasmodium falciparum-infected erythrocytes containing sickle hemoglobin. **Proc. Natl. Acad. Sci. U.S.A.**, v. 105, n. 3, p. 991-996, 2008.

COMPTON, S.J.; JONES, C.G. Mechanism of dye response and interference in the Bradford protein assay. **Anal. Biochem.**, v. 151, p. 369–374, 1985.

CONWAY, D.J.; FANELLO, C.; LLOYD, J.M.; AL-JOUBORI, B.M.A.-S.; BALOCH, A.H.; SOMANATH, S.D.; ROPER, C.; ODUOLA, A.M.J.; MULDER, B.; POVOA, M.M.; SINGH, B.; THOMAS, A.W. Origin of *Plasmodium falciparum* malaria is traced by mitochondrial DNA. **Mol. Biochem. Parasitol.**, v. 111, p. 163–171, 2000.

CONWAY, D.J. Tracing the dawn of *Plasmodium falciparum* with mitochondrial genome sequences. **Trends in Genetics**, v. 19, p. 671–674, 2003.

COX-SINGH, J.; DAVIS, T.M.; LEE, K.S.; SHAMSUL, S.S.; MATUSOP, A.; RATNAM, S.; RAHMAN, H.A.; CONWAY, D.J.; SINGH, B. Plasmodium knowlesi malaria in humans is widely distributed and potentially life threatening. **Clin. Infect. Dis.**, v. 46, p. 165-171, 2008.

COURA, J.R.; SUÁREZ-MUTIS, M.; LADEIA-ANDRADE, S. A new challenge for malaria control in Brazil: asymptomatic*Plasmodium* infection - A Review. **Mem. Inst. Oswaldo Cruz**, v. 101*,* p. 229-237, 2006.

CUNNINGHAM, D.F.; O´CONNOR, B. Proline specific peptidases. **Biochem. Biophys. Acta**, v. 1343, p. 160-186, 1997.

CURLEY, G.P.; O'DONOVAN, S.M.; MCNALLY, J.; MULLALLY, M.; O'HARA, H.; TROY, A.; O'CALLAGHAN, S.A.; DALTON, J.P. Aminopeptidases from Plasmodium falciparum, Plasmodium chabaudi chabaudi and Plasmodium berghei. **J. Eukaryot. Microbiol.**, v. 41, n. 2, p. 119-123, 1994.

CYRKLAFF, M.; SANCHEZ, C.P.; KILIAN, N.; BISSEYE, C.; SIMPORE, J.; FRISCHKNECHT, F.; LANZER, M. Hemoglobins S and C interfere with actin remodeling in Plasmodium falciparum-infected erythrocytes. **Science**, v. 334, n. 6060, p. 1283-1286,2011.

DAHL, E.L.; ROSENTHAL, P.J. Biosynthesis, localization, and processing of falcipain cysteine proteases of Plasmodium falciparum. **Mol. Biochem. Parasitol.**, v. 139, n. 2, p. 205-212., 2004.

DALAL, S.; KLEMBA, M. Roles for two aminopeptidases in vacuolar hemoglobin catabolism in Plasmodium falciparum. **J. Biol. Chem.**, v. 282, n. 49, p. 35978-35987, 2007.

DAS GUPTA, R.; KRAUSE-IHLE, T.; BERGMANN, B.; MÜLLER, I.B.; KHOMUTOV, A.R.; MÜLLER, S.; WALTER, R.D.; LÜERSEN, K. 3-Aminooxy-1-aminopropane and derivatives have an antiproliferative effect on cultured Plasmodium falciparum by decreasing intracellular polyamine concentrations. **Antimicrob Agents Chemother.**, v. 49, n. 7, p. 2857-2864, 2005.

DEANE, L.M. Malaria vectors in Brazil. **Mem. Inst. Oswaldo Cruz**, v. *81*, p. 5-14,1986.
DELVES, M.; PLOUFFE, D.; SCHEURER, C.; MEISTER, S.; WITTLIN, S.; WINZELER, E.A.; SINDNEN, R.E.; LEROY, D. The Activities of Current Antimalarial Drugs on the Life Cycle Stages of Plasmodium: A Comparative Study with Human and Rodent Parasites. **PLoS Med.**, v. 9, n. 2, e1001169, 2012.

DELVES, M.J.; RUECKER, A.; STRASCHIL, U.; LELIÈVRE, J.; MARUQES, S.; LÓPEZ-BARRAGÁN, M.J.; HERREROS, E.; SINDENA, R.E. Male and Female Plasmodium falciparum Mature Gametocytes Show Different Responses to Antimalarial Drugs. **Antimicrobial Agents and Chemotherapy**, v. 57, p. 3268–3274, 2013.

DEU, E.; LEYVA, M.J.; ALBROW, V.E.; RICE, M.J.; ELLMAN, J.Á.; BOGYO, M. Functional studies of Plasmodium falciparum dipeptidyl aminopeptidase I using small molecule inhibitors and active site probes. **Chem. BioL.**, v. 17(8), p. 808-819, 2010.
DLUZEWSKI, A.R.; RANGACHARI, K.; WILSON, R.G.; GRATZER, W.B. *Plasmodium falciparum*: protease inhibitors and inhibition of erythrocyte invasion. **Exp. Parasitol.**, v. 62, p. 416-422, 1986.

DONDORP, A.M.; FANELLO, C.I.; HENDRIKSEN, I.C.E.; GOMES, E., SENI, A.; et al. Artesunate versus quinine in the treatment of severe falciparum malaria in African children (AQUAMAT): an open-label, randomised trial. **Lancet**, v. 376, p. 1647–1657, 2010.

DRINKWATER, N.; SIVARAMAN, K.K.; BAMERT, R.S.; RUT, W.; MOHAMED, K.; VINH, N.B.; SCAMMELLS, P.J.; DRAG, M.; MCGOWAN, S. Structure and substrate fingerprint of aminopeptidase P from Plasmodium falciparum. **Biochem.**, v. 473 (19), p. 3189-3204, doi: 10.1042/BCJ20160550.

ECKERT, W.A.; KARTENBECK, J. Quantitative Bestimmung von Proteinen. In Eckert WA, **Kartenbeck J Proteine**: Standardmethoden der Molekular- und Zellbiologie. 1. Edition, Springer-Verlag, Berlin, p. 62-66, 1997.

ELLIOTT, D.A.; MCINTOSH, M.T.; HOSGOOD, H.D.3rd; CHEN, S.; ZHANG, G.; et al. Four distinct pathways of hemoglobin uptake in the malaria parasite Plasmodium falciparum. **Proc. Natl. Acad. Sci. U.S.A.**, v. 105, p. 2463–2468, 2008.

EVANS, P. Scaling and assessment of data quality. **Acta crystallographica. Section D, Biological crystallography**, v. 62, p. 72–82, doi:10.1107/S0907444905036693, 2006

FAIRHURST, R.M.; BARUCH, D.I.; BRITTAIN, N.J.; OSTERA, G.R.; WALLACH, J.S.; HOANG, H.L.; HAYTON, K.; GUINDO, A.; MAKOBONGO, M.O.; SCHWARTZ, O.M.; TOUNKARA, A.; DOUMBO, O.K.; DIALLO, D.A.; FUJIOKA, H.; HO, M.; WELLEMS,

T.E**.** Abnormal display of PfEMP-1 on erythrocytes carrying haemoglobin C may protect against malaria. **Nature**, v. 435, n. 7045, p. 1117-1121, 2005.

FARID, M. Stroke in sickle cell anemia patients: A need for multidisciplinary approaches. **Atherosclerosis**, v. 229, n. 2, p. 496–503, 2013.
FERREIRA, A.; MARGUTI, I.; BECHMANN, I.; JENEY, V.; CHORA, A.; PALHA, N.R.; REBELO, S.; HENRI, A.; BEUZARD, Y.; SOARES, M.P. Sickle hemoglobin confers tolerance to Plasmodium infection. Cell, v. 145, n. 3, p. 398-409, 2011.

FLORENT, I.; DERHY, Z.; ALLARY, M.; MONSIGNY, M.; MAYER, R.; SCHRÉVEL, J. A Plasmodium falciparum aminopeptidase gene belonging to the M1 family of zinc-metallopeptidases is expressed in erythrocytic stages. **Mol. Biochem. Parasitol.**, v. 97, n. 1-2, p. 1491-60, 1998.

FRANCIS, S.E.; SULLIVAN, D.J.Jr; GOLDBERG, D.E**.** Hemoglobin metabolism in the malaria parasite Plasmodium falciparum. **Annu. Rev. Microbiol.** 51, 97–123, 1997.
FRANKLIN, R.M.; BRUN, R.; GRIEDER, A.Z. Microscopic and flow cytophotometric analysis of parasitemia in cultures of Plasmodium falciparum vitally stained with Hoechst 33342 —application to studies of antimalarial agents. **Parasitenkd.**, v. 72, p. 201, doi:10.1007/BF00931147, 1986.

FRIEDMAN, F.J. Erythrocytic mechanism of sickle cell resistance to malaria. **Proc. Natl. Acad. Sci. U. S. A.**, v. 75, n. 4, p. 1994-1997, 1978.

GEARY, T.G.; JENSEN, J.B. Effects of antibiotics on Plasmodium falciparum in vitro. **Am. J. Trop. Med. Hyg.**, v. 32 p. 221–225, 1983.

GLUZMAN, I.Y.; FRANCIS, S.E.; OKSMAN, A.; SMITH, C.E.; DUFFIN, K.L.; GOLDBERG, D.E. Order and specificity of the Plasmodium falciparum hemoglobin degradation pathway. **J. Clin. Invest.**, v. 93, n. 4, p. 1602-1608, 1994.

GOLDBERG, D.E**.** Hemoglobin degradation. **Curr. Top. Microbiol. Immunol.,** v. 295, p. 275-291, 2005.

GRAHAM, S.C.; MAHER, M.J.; SIMMONS, W.H.; FREEMAN, H.C.; GUSS, J.M. Structure of Escherichia Coli Aminopeptidase P in Complex With the Inhibitor Apstatin. **Acta crystallographica Section D, Biological crystallography.**, v. 60, p. 1770–1779, doi:10.1107/S0907444904018724, 2004.

GREENWOOD, B.M.; FIDOCK, D.A.; KYLE, D.E.; KAPPE, S.H.I.; ALONSO, P.L.; COLLINS, F.H.; DUFFY, P.E. Malaria: progress, perils, and prospects for eradication. **J. Clin. Invest.,** v. 118, p. 1266-1276, 2008.

HANSON, G.T.; MCANANEY, T.B.; PARK, E.S.; RENDELL, M.E.P.; YARBROUGH, D.K.; CHU, S.; XI, L.; BOXER, S.G.; MONTROSE, M.H.; REMINGTON, S.J. Green Fluorescent Protein Variants as Ratiometric Dual Emission pH Sensors. 1. Structural Characterization and Preliminary Application. **Biochem.**, v. 41, n. 52, p. 15477–15488. doi: 10.1021/bi026609p, 2002.

HAQUE, A.; ENGWERDA, C.R. An antioxidant link between sickle cell disease and severe malaria. **Cell**, v. 145, n. 3, p. 335-336, 2011.

HEBBEL, R.P.; MOHANDAS, N. **Cell adhesion and micro rheology in sickle cell disease.** In Steinberg MH, Forget BG, Higgs DR, eds. Disorders of Hemoglobin. Cambridge: Cambridge University Press: p. 527–549, 2001.
HEBBEL, R.P. Sickle hemoglobin instability: a mechanism for malarial protection. **Redox. Rep.**, v. 8, n. 5, p. 238-240, 2003.

HERRICK, J.B. Peculiar elongated and sickle-shaped red corpuscles in a case of severe anemia. **Arch. Intern. Med.**, v. 6, p. 517, 1910.

IYER, S.; LA-BORDE, P.J.; PAYNE, K.A.P.; PARSONS, M.R.; TURNER, A.J.; ISAAC, R.E.; ACHARYA, K.R. Crystal structure of X-prolyl aminopeptidase from Caenorhabditis elegans: A cytosolic enzyme with a di-nuclear active site. **FEBS open bio.**, v. 5, p. 292–302, doi: 10.1016/j.fob.2015.03.013, 2015.

JANI, D.; NAGARKATTI, R.; BEATTY, W.; ANGEL, R.; SLEBODNICK, C.; ANDERSEN, J.; KUMAR, S.; RATHORE, D. HDP-a novel heme detoxification protein from the malaria parasite. **PLoS Pathog.**, v. 4(4), e1000053, 2008.

JENSEN, J.B.; TRAGER, W. Plasmodium falciparum in culture: use of outdated erthrocytes and description of the candle jar method. **J. Parasitol.**, v. 63, n. 5, p. 883-886, 1977.

JEONG, J.-J.; KUMAR, A.; HANADA, T.; SEO, P.-S.; LI, X.; HANSPAL, M.; CRISHTI, A.H. Cloning and characterization of Plasmodium falciparum cysteine protease, falcipain 2B. **Blood Cells Mol. Dis.**, v. 36, p. 429-435, 2006.

JIN, H.; XU, Z.; CUI, K.; ZHANG, T.; LU, W.; HUANG, J. Dietary flavonoids fisetin and myricetin: dual inhibitors of Plasmodium falciparum falcipain-2 and plasmepsin II. **Fitoterapia**, v. 94, p. 55-61, 2014.

JOY, D.A.; FENG, X.; MU, J.; FURUYA, T.; CHOTIVANICH, K.; KRETTLI, A.U.; HO, M.; WANG, A.; WHITE, N.J.; SUH, E.; BEERLI, P.; SU, X.Z. Early Origin and Recent Expansion of Plasmodium falciparum. **Science**, v. 300, p. 318-321, 2003.

KABSCH, W. XDS. **Acta Crystallographica Section D - Biological Crystallography**, v. 66, p. 125–132. doi:10.1107/S0907444909047337, 2010.

KIKUCHI, G.; YOSHIDA, T.; NOGUCHI, M. Heme oxygenase and heme degradation. **Biochem. Biophys. Res. Commun.**, v. 338, p. 558-567, 2005.

KIRSCHKE, H.; BERRETT, A.J. in Lysosomes: Their Role in Protein Breakdown (Glaumann, H., and Ballard, J., eds) p. 192–238, **Academic Press Inc.**, London, 1987.
KISZEWSKI, A.E. Blocking Plasmodium falciparum malaria with drugs: the gametocytocidal and sporontocidal properties of current and prospective antimalarials. **Pharmaceuticals**, v. 4, p. 44–68, 2011.

KLEMBA, M.; GLUZMAN, I.; GOLDBERG, D.E. A Plasmodium falciparum dipeptidyl aminopeptidase I participates in vacuolar hemoglobin degradation. **J. Biol. Chem.**, v. 279, n. 41, p. 43000-43007, 2004.

KLONIS, N.; CRESPO-ORITZ, M.P.; BOTTOVA, I.; ABU-BAKAR, N.; KENNY, S.; et al. Artemisinin activity against Plasmodium falciparum requires hemoglobin uptake and digestion. **Proc. Natl. Acad. Sci. U. S. A.**, v. 108, p. 11405–11410, 2011.

KNÖCKEL, J.; MÜLLER, I.B.; BUTZLOFF, S.; BERGMANN, B.; WALTER, R.D.; WRENGER, C. The antioxidative effect of de novo generated vitamin B6 in Plasmodium falciparum validated by protein interference. **Biochem. J.**, v. 443, n. 2, p. 397-405, 2012.

KOLAKOVICH, K.A.; GLUZMAN, I.Y.; DUFFIN, K.L.; GOLDBERG, D.E. Generation of hemoglobin peptides in the acidic digestive vacuole of Plasmodium falciparum implicates peptide transport in amino acid production. **Mol. Biochem. Parasitol.**, v. 87, 2, p. 123-135, 1997.

KONOTEY-AHULU, F.I.D. Hereditary qualitative and quantitative erythrocyte defects in Ghana. An historical and geographical survey. **Ghana Med. J.**, v. 7, p. 118–119, 1968.

KUMURA, N.; FURUKAWA, H.; ONYANGO, A.N.; IZUMI, M.; NAKAJIMA, S.; et al. Different behavior of artemisinin and tetraoxane in the oxidative degradation of phospholipid. **Chem. Phys. Lipids**, v. 160, p. 114–120, 2009.

KYES, S.; PINCHES, R.; NEWBOLD, C. A simple RNA analysis method shows var and rif multigene family expression patterns in Plasmodium falciparum. **Mol. Biochem. Parasitol.**, v. 105, p. 311-315, 2000.

LAEMMLI, U.K. Cleavage of structural proteins during the assembly of the head of bacteriophage T4. **Nature**, v. 227, p. 680-685, 1970.

LASKOWSKI, R.A.; MACARTHUR, M.W.; MOSS, D.S.; THORNTON, J.M. PROCHECK: a program to check stereochemical quality of protein structures. **J. Appl. Crystallogr.**, v. 26, p. 283–291, doi:10.1107/S0021889892009944, 1993.

LI, X.; LOU, Z.; LI, X.; ZHOU, W.; MA, M.; CAO, Y.; GENG, Y.; BARTLAM, M.; ZHANG, X.C.; RAO, Z. Structure of Human Cytosolic X-prolyl Aminopeptidase - A double Mn(II)-dependent dimeric enzyme with a novel three-domain subunit. **The Journal of biological chemistry***,* v. 283, p. 22858–22866, doi:10.1074/jbc.M710274200, 2008.

LINDNER, J.; MEISSNER, K.A.; SCHETTERT, I.; WRENGER, C. Trafficked Proteins-Druggable in Plasmodium falciparum? **Int. J. Cell. Biol.**, 2013:435981, doi: 10.1155/2013/435981, 2013.

LÓPEZ, C.; SARAVIA, C.; GOMEZ, A.; HOEBEKE, J.; PATARROYO, M.A. Mechanisms of genetically-based resistance to malaria. **Gene**, v. 467, n. 1-2, p. 1-12, 2010.

LUCIUS, R.; LOOS-FRANK, B. **Biologie von Parasiten.** 2. Auflage. Springer-Verlag Heidelberg, p. 218-220, 2008.

MARENGO-ROWE, A.J. Haemoglobinopathies. **Br. J. Hosp. Med.**, v. 6, p. 617–630, 1971.

MARENGO-ROWE, A.J. Structure-function relations of human hemoglobins. **Proc. (Bayl. Univ. Med. Cent.)**, v. 19, p. 239–245, 2006.
MCANANEY, T.B.; PARK, E.S.; HANSON, G.T.; REMINGTON, S.J.; BOXER, S.G. Green Fluorescent Protein Variants as Ratiometric Dual Emission pH Sensors. 2. Excited-State Dynamics. **Biochem.**, v. 41, p. 15489-15494, 2002.

MEHLHORN, H.; PIEKARSKI, G. **Grundriß der Parasitenkunde.** 6. Edition. Spektrum Akademischer Verlag, Heidelberg, 2002. p. 106-129.

MULLER-EBERHARD, U.; JAVID, J.; LIEM, H.H.; HANSTEIN, A.; HANNA, M. Plasma concentrations of hemopexin, haptoglobin and heme in patients with various hemolytic diseases. **Blood**, v. 32, n. 5, p. 811-815, 1968.

MÜLLER, I.B.; WU, F.; BERGMANN, B.; KNÖCKEL, J.; WALTER, R.D.; GEHRING, H.; WRENGER, C. Poisoning Pyridoxal 5-Phosphate-Dependent Enzymes: A New Strategy to Target the Malaria Parasite Plasmodium falciparum. **PLoS ONE**, v. 4, n. 2, e4406, 2009.

MÜLLER, I.B.; KNÖCKEL, J.; ESCHBACH, M.L.; BERGMANN, B.; WALTER, R.D.; WRENGER, C. Secretion of an acid phosphatase provides a possible mechanism to acquire host nutrients by Plasmodium falciparum. **Cell. Microbiol.**, v. 12, n. 5, p. 677–691, 2010.

MURSHUDOV, G.N.; SKUBA, P.; LEBEDEV, A.A.; PANNU, N.S.; STEINER, R.A.; NICHOLLS, R.A.; WINN, M.D.; LONG, F.; VAGIN, A.A. REFMAC5 for the refinement of macromolecular crystal structures. **Acta Crystallographica Section D - Biological Crystallography**, v. 67, p. 355–367, doi:10.1107/S0907444911001314, 2011.

NAGEL, R.L.; PLATT, O.S. **General pathophysiology of sickle cell anemia.** In Steinberg MH, Forget BG, Higgs DR, eds. Disorders of Hemoglobin. Cambridge: Cambridge University Press, 2001. p. 494–526.

NEAFSEY, D.E.; SCHAFFNER, S.F.; VOLKMAN, S.K.; PARK, D.; MONTGOMERY, P.; MILNERJR, D.A.; LUKES, A.; ROSEN, D.; DANIELS, R.; HOUDE, N.; CORTESE, J.F.; TYNDALL, E.; GATES, C.; STANGE-THOMANN, N.; SARR, O.; NDIAYE, D.; NDIR, O.; MBOUP, S.; FERREIRA, M.U.; DO LAGO MORAES, S.; DASH, A.P.; CHITNIS, C.E., WIEGAND, R.C.; HARTL, D.L.; BIRREN, B.W.; LANDER, E.S.; SABETI, P.C.; WIRTH, D.F. Genome-wide SNP genotyping highlights the role of natural selection in *Plasmodium falciparum* population divergence. **Genome Biology**, v. 9, R171, 2008.

OLOTU, A.; FEGAN, G.; WAMBUA, J.; NYANGWESO, G.; LEACH, A.; LIEVENS, M.; KASLOW, D.C.; NJUGUNA, P.; MARSH, K.; BEJON, P. Seven-Year Efficacy of

RTS,S/AS01 Malaria Vaccine among Young African Children. **N. Engl. J. Med.**, v. 374, p. 2519-2529, 2016.

O'NEILL, P.M.; BARTON, V.E.; WARD, S.A. The molecular mechanism of action of Artemisinin - the debate continues. **Molecules**, v. 15, p. 1705–1721, 2010.

PANDEY, K.C.; SINGH, N.; ARASTU-KAPUR, S.; BOGYO, M.; ROSENTHAL, P.J. Falstatin, a cysteine protease inhibitor of Plasmodium falciparum, facilitates erythrocyte invasion. **PLoS Pathog.**, v. 2, n. 11, e117, 2006.
PASVOL, G.; WEATHERALL, D.J.; WILSON, R.J. Cellular mechanism for the protective effect of haemoglobin S against P. falciparum malaria. **Nature**, v. 274, n. 5672, p. 701-703, 1978.

PAULING, L.; ITANO, H.A.; SINGER, S.J.; WELLS, I.C. Sickle cell anemia, a molecular disease. **Science**, v. 110, p. 543–548, 1949.

PIEL, F.B.; PATIL, A.P. HOWES, R.E. NYANGIRI, O.A.; GETHING, P.W.; WILLIAMS, T.N.; WEATERHALL, D.J.; HAY, S.I. Global distribution of the sickle cell gene and geographical confirmation of the malaria hypothesis. **Nat. commun.**, v. 1, p. 104; doi: 10.1038/ncomms1104, 2010.

RAGHEB, D.; BOMPIANI, K.; DALAL, S.; KLEMBA, M. Evidence for Catalytic Roles for Plasmodium falciparum Aminopeptidase P in the Food Vacuole and Cytosol. **The Journal of biological chemistry**, v. 284, p. 24806–24815, doi: 10.1074/jbc.M109.018424, 2009.

RAMPLING, T.; EWER, K.J.; BOWYER, G.; BLISS; C.M.; EDWARDS, N.J.; WRIGHT, D.; PAYNE, R.O.; VENKATRAMAN, N.; DE BARRA, E.; SNUDDEN, C.M.; POULTON, I.D.; DE GRAAF, H.; SUKHTANKAR, P.; ROBERTS, R.; IVINSON, K.; WELTZIN, R.; RAJKUMAR, B.-Y., WILLE-REECE, U.; LEE, C.K.; OCKENHOUSE, C.F.; SINDEN, R.E.; GERRY, S.; LAWRIE, A.M.; VEKEMANS, J.; MORELLE, D.; LIEVENS, M.; BALLOU, R.W.; COOKE, G.S.; FAUST, S.N.; GILBERT, S.; HILL, A.V.S. Safety and High Level Efficacy of the Combination Malaria Vaccine Regimen of RTS,S/AS01B With Chimpanzee Adenovirus 63 and Modified Vaccinia Ankara Vectored Vaccines Expressing ME-TRAP. **The Journal of Infectious Disease**, v. 214, p. 772–781, 2016.

RAPHAEL, R.I. Pathophysiology and treatment of sickle cell disease. **Clin. Adv. Hematol. Oncol.**, v. 3, n. 6, p. 492–505, 2005.

ROSENTHAL, P.J.; MCKERROW, J.H.; AIKAWA, M.; NAGASAWA, H.; LEECH, J.H. A malaria cysteine proteinase is necessary for hemoglobin degradation by *Plasmodium falciparum.* **J. Clin. Invest.**, v. 82, p. 1560-1566, 1988.

ROSENTHAL, P.J.; WOLLISH, W.S.; PALMER, J.T.; RASNICK, D. Antimalarial effects of peptide inhibitors of a *Plasmodium falciparum* cysteine proteinase. **J. Clin. Invest.**, v. 88, p. 1467-1472, 1991.

ROSENTHAL, P.J. Lessons from sickle cell disease in the treatment and control of malaria. **N. Engl. J. Med.**, v. 364, n. 26, p. 2549-2551, 2011.

SAMBROOK, J.; FRITSCH, E.F.; MANIATIS, T. **Molecular Cloning: A Laboratory Manual.** 2. Edition. Cold Spring Harbor Laboratory Press, New York, 1989.

SANGER, F.; NICKLEN, S.; COULSON, A.R. DNA sequencing with chain-terminating inhibitors. **Proc. Natl. Acad. Sci. U. S. A.**, v. 74, p. 5463-5467, 1977.

SCHECHTER, A.; ELION, J. Cold. Spring. **Harb. Perspect. Med.**, 2012. In Press.
SCHROEDER, W.A.; HUISMAN, T.H.; SHELTON, J.R.; SHELTON, J.B.; KLEIHAUER, E.F.; DOZY, A.M.; ROBBERSON, B. Evidence for multiple structural genes for the gamma chain of human fetal hemoglobin. **Proc. Natl. Acad. Sci. U. S. A.**, v. 60, n. 2, p. 537–544, 1968.

SERJEANT, G.R. The Natural History of Sickle Cell Disease. **Cold Spring Harb. Perspect Med.**, v. 3, a011783, 2013.

SHENAI, B.R.; SIJWALI, P.S.; SINGH, A.; ROSENTHAL, P.J. Characterization of native and recombinant falcipain-2, a principal trophozoite cysteine protease and essential hemoglobinase of Plasmodium falciparum. **J. Biol. Chem.**, v. 275, n. 37,p. 29000-29010, 2000

SHENG, K.; SHARIFF, M.; HEBBEL, R.P. Comparative oxidation of hemoglobins A and S. **Blood**, v. 91, n. 9, p. 3467-3470, 1998.

SIJWALI, P.S.; SHENAI, B.R.; GUT, J.; SINGH, A.; ROSENTHAL, P.J. Expression and characterization of the Plasmodium falciparum haemoglobinase falcipain-3. **Biochem. J.**, v. 360, n. 2, p. 481-489, 2001.

SIEVERS, F.; WILM, A.; DINEEN, D.; GIBSON, T.J.; KARPLUS, K.; LI, W.; LOPEZ, R.; MCWILLIAM, H.; REMMERT, M.; SODING, J.; THOMPSON, J.D.; HIGGINS, D.G. Fast, scalable generation of high-quality protein multiple sequence alignments using Clustal Omega. **Molecular systems biology**, v. 7, p. 539, doi:10.1038/msb.2011.75, 2011.

SKINNER-ADAMS, T.S.; STACK, C.M.; TRENHOLME, K.R.; BROWN, C.L.; GREMBECKA, J.; LOWTHER, J.; MUCHA, A.; DRAG, M.; KAFARSKI, P.; MCGOWAN, S.; WHISSTOCK, J.C.; GARDINER, D.L.; DALTON, J.P. Plasmodium falciparum neutral aminopeptidases: new targets for anti-malarials. **Trends in Biochemical Sciences**, v. 35, p. 53-61, 2009.

SLOMIANNY, C. Three-dimensional reconstruction of the feeding process of the malaria parasite. **Blood Cells**, v. 16, p. 369–378, 1990.

STEINBERG, M.H.; BARTON, F.; CASTRO, O.; PEGELOW, C.H.; BALLAS, S.K.; KUTLAR, A.; ORRINGER, E.; BELLEVUE, R.; OLIVIERI, N.; ECKMAN, J.; VARMA, M.; RAMIREZ, G.; ADLER, B.; SMITH, W.; CARLOS, T.; ATAGA, K.; DE CASTRO, L.; BIGELOW, C.; SAUNTHARARAJAH, Y.; TELFER, M.; VICHINSKY, E.; CLASTER, S.; SHURIN, S.; BRIDGES, K.; WACLAWIW, M.; BONDS, D.; TERRIN, M. Effect of hydroxyurea on mortality and morbidity in adult sickle cell anemia: risks and benefits up to 9 years of treatment. **JAMA**, v. 289, n. 13, p. 1645–1651, 2003.

STURM, A.; AMINO, R.; VAN DE SAND, C.; REGEN, T.; RETZLAFF, S.; RENNENBERG, A.; KRUEGER, A.; POLLOK, J.M.; MENARD, R.; HEUSSLER, V.T. Manipulation of host hepatocytes by the malaria parasite for delivery into liver sinusoids. **Science**, v. 313, p. 1287-1290, 2006.

SUBRAMANIAN, S.; SIJWALI, P.S.; ROSENTHAL, P.J. Falcipain cysteine proteases require bipartite motifs for trafficking to the *Plasmodium falciparum* food vacuole. **J. Biol. Chem.**, v. 282, n. 34, p. 24961-24969, 2007.

TAYLOR, J.E.; PACHECO, M.A.; BACON, D.J.; BEG, M.A.; MACHADO, R.L.; FAIRHURST, R.M.; HERRERA, S.; KIM, J.-Y.; MENARD, D.; PÓVOA, M.M.; VILLEGASM, L.; MULYANTO; SNOUNOU, G.; CUI, L.; ZEYREK, F.Y.; ESCALANTE, A.A. The evolutionary history of Plasmodium vivax as inferred from mitochondrial genomes: parasite genetic diversity in the Americas. **Mol. Biol. Evol.**, v. 30, n. 9, p. 2050–2064, 2013.

TEUSCHER, F.; LOWTHER, J.; SKINNER-ADAMS, T.S.; SPIELMANN, T.; DIXON, M.W.A.; STACK, C.M.; DONNELLY, S.; MUCHA, A.; KAFARSKI, P.; VASSILIOU, S.; GARDINER, D.L.; DALTON, J.P.; TRENHOLME, K.R. The M18 Aspartyl Aminopeptidase of the Human Malaria Parasite *Plasmodium falciparum*. **J. Biol. Chem.**, v. 282, n. 42, p. 30817-30826, 2007.

TRAGER, W.; JENSEN, J.B. Human malaria parasites in continuous culture. **Science**, v. 193, p. 673-675, 1976.

TREUEL, L.; MALISSEK, M.; GEBAUER, J.S.; ZELLNER, R. The influence of surface composition of nanoparticles on their interactions with serum albumin. **Chem. Phys. Chem.**, v. 11, n. 14, p. 3093-3096, doi: 10.1002/cphc.201000174, 2010.

THE RTS,S CLINICAL TRIALS PARTNERSHIP. A Phase 3 Trial of RTS,S/AS01 Malaria Vaccine in African Infants. **N. Engl. J. Med.**, v. 367, p. 2284-95, 2012.

THE RTS,S CLINICAL TRIALS PARTNERSHIP. Efficacy and safety of RTS,s/S01 malaria vaccine with or without a booster dose in infants and children in Africa: final results of a phase 3, individually randomised, controlled trial. **Lancet**, v. 386, p. 31-45, 2015.

THOM, C.S.; DICKSON, C.F.; GELL, D.A.; WEISS, M.J. Hemoglobin Variants: Biochemical Properties and Clinical Correlates. **Cold Spring Harb. Perspect Med.**, v. 3, a011858, 2013.

VAGIN, A.; TEPLYAKOV, A. Molecular replacement with MOLREP. **Acta Crystallographica Section D - Biological Crystallography**, v. 66, p. 22–25. doi:10.1107/S0907444909042589, 2012.

VAID, A.; RANJAN, R.; SMYTHE, W.A.; HOPPE, H.C.; SHARMA, P. PfPI3K, a phosphatidylinositol-3 kinase from Plasmodium falciparum, is exported to the host erythrocyte and is involved in hemoglobin trafficking. **Blood**, v. 115. p. 2500–2507, 2010.

VAN DEN HOFF, M.J.B.; MOORMAN, .A.F.M.; LAMERS, W.H. Electroporation in 'intracellular' buffer increases cell survival. **Nucleic Acids Res.**, v. 20, n. 11, p. 2902, 1992.

VENYAMINOV, S.; BAIKALOV, I.A.; WU, C.-S.C.; YANG, J.T. Some problems of CD analyses of protein conformation. **Analytical biochemistry**, v. 198, p. 250–255, 1991.

VERMYLEN, C.; CORNU, G. Hematopoietic stem cell transplantation for sickle cell anemia. **Curr. Opin. Hematol.**, v. 4, n. 6, p. 377–380, 1997.

WALLIKER, D.; BEALE, G. in Methods in Molecular Biology: **Protocols in Molecular Parasitology**, ed. Hyde, J. E. (Humana, Totowa, NJ); 1993. p. 57-66.

WAZIR, H. The Types Of Haemoglobin Throughout Human Life. **Young Scientists Journal**, March 28, 2015 Biology, 2015.

WESTHEIDE, W.; RIEGER, R. Spezielle Zoologie. Teil 1: **Einzeller und Wirbellose Tiere.** 1. Edition, Gustav Fischer Verlag, Stuttgart, 1996.

WHITE, N.C. Assessment of the pharmacodynamics properties of antimalarial drugs in vivo**. Antimicrob Agents Chemother**, v. 41, p. 1413–1422, 1997.

WINN, M.D.; BALLARD, C.C.; COWTAN, K.D.; DODSON, E.J.; EMSLEY, P.; EVANS, P.R.; KEEGAN, R.M.; KRISSINEL, E.B.; LESLIE, A.G.W.; MCCOY, A.; MCNICHOLAS, S.J.; MURSHUDOV, G.N.; PANNU, N.S.; POTTERTON, E.A.; POWELL, H.R.; READ, R.J.; VAGIN, A.; WILSON, K.S. Overview of the CCP4 suite and current developments. **Acta Crystallographica Section D - Biological Crystallography**, v. 67, p. 235–242. doi:10.1107/S0907444910045749, 2011.

WISEDCHAISRI, G.; GONEN ,T. Phasing Electron Diffraction Data by Molecular Replacement: Strategy for Structure Determination and Refinement. **Methods in molecular biology (Clifton, N.J.)**, v. 955, p. 243–272, doi:10.1007/978-1-62703-176-9_14, 2013.

WOLTERS, P.J.; PHAM, C.T.; MUILENBURGm D.J.; LEY, T.J.; CAUGHEY, G.H. Dipeptidyl Peptidase I Is Essential for Activation of Mast Cell Chymases, but Not Tryptases, in Mice. **J. Biol. Chem.**, v. 276, p. 18551–18556, 2001.

WRENGER, C.; KNÖCKEL, J.; WALTER, R.D.; MÜLLER, I.B. Vitamin B1 and B6 in the malaria parasite: requisite or dispensable? **Brazilian Journal of Medical and Biological Research**, v. 41, p. 82-88, 2008.

WU, Y.; SIFRI, C.D.; LEI, H.H.; SU, X.Z.; WELLEMS, T.E. Transfection of Plasmodium falciparum within human red blood cells. **Proc. Natl. Acad. Sci. U. S. A.**, v. 92, n. 4, p. 973-977, 1995.

YANG, J.T.; WU, C.S.; MARTINEZ, H.M. Calculation of protein conformation from circular dichroism. **Methods Enzymol.**, v. 130, p. 208–269, 1986.

YAYON, A.; TIMBERG, R.; FRIEDMAN, S.; GINSBURG, H. Effects of chloroquine on the feeding mechanism of the intraerythrocytic human malarial parasite Plasmodium falciparum. **J. Protozool.**, v. 31, p. 367–372, 1984.

I. Appendix

*PF*3D7_1407900 – Plasmepsin I - no introns

ATGGCTTTATCAATTAAAGAAGATTTTTCAAGCGCTTTTGCGAAAAATGAATCAGCTGTGAA
TAGCTCTACATTTAATAATAATATGAAAACATGGAAGATTCAGAAACGATTTCAAATATTAT
ACGTGTTTTTTTTCTTATTGATTACCGGAGCATTATTTTATTATCTTATAGATAATGTATTA
TTCCCAAAAAATAAAAAGATAAATGAAATTATGAATACCTCAAAACATGTAATAATTGGATT
TAGTATTGAAAATTCTCATGACAGAATTATGAAAACAGTAAAACAACACAGATTAAAAAATT
ATATTAAAGAATCCTTGAAATTTTTCAAAACAGGACTTACACAAAAACCACATTTAGGTAAT
GCTGGTGATAGTGTAACATTAAATGATGTAGCTAATGTAATGTATTATGGAGAAGCTCAAAT
TGGAGATAATAAACAAAAGTTTGCTTTTATTTTTGATACAGGATCAGCAAATTTATGGGTTC
CAAGTGCTCAATGTAATACTATTGGCTGTAAAACAAAAAATCTTTATGATTCTAATAAATCC
AAAACATATGAAAAAGATGGTACTAAAGTAGAAATGAATTATGTATCTGGAACAGTAAGCGG
ATTTTTTAGTAAAGATATAGTTACTATAGCAAATTTATCATTTCCATATAAATTTATTGAAG
TTACAGATACCAATGGTTTCGAACCAGCTTATACCTTAGGACAATTTGATGGTATAGTAGGT
TTAGGATGGAAAGATTTGTCTATAGGTTCAGTAGATCCTGTTGTTGTCGAATTAAAAAATCA
AAATAAAATCGAACAAGCCGTTTTTACCTTTTATTTACCATTTGATGATAAACACAAAGGTT
ATTTAACCATAGGAGGTATTGAAGATAGATTTTATGAAGGTCAATTAACTTATGAAAAATTA
AACCACGATTTATATTGGCAAGTTGATTTAGATCTACATTTTGGTAATTTAACTGTAGAAAA
AGCTACTGCAATTGTTGACAGTGGTACTAGTTCTATAACGGCACCAACTGAATTCCTTAACA
AATTCTTTGAAGGTTTAGATGTTGTTAAAATACCTTTCTTACCATTATATATAACTACATGT
AATAACCCTAAATTACCAACTCTAGAATTCAGATCAGCAACAAATGTTTATACCTTAGAACC
AGAATACTACTTACAACAAATATTCGATTTTGGTATATCATTATGTATGGTATCTATAATAC
CTGTTGATTTGAACAAAAATACCTTCATATTAGGTGACCCATTCATGAGAAAATATTTCACC
GTCTTTGATTATGATAATCACACTGTTGGTTTCGCCCTTGCCAAAAAAAAATTGTAA

Sequence length: 1359 bp

PF3D7_1408000 – Plasmepsin II - no introns

ATGGATATTACAGTAAGAGAACATGATTTTAAACATGGCTTTATCAAAAGCAATTCAACATT
TGATGGATTAAACATTGACAATTCAAAGAACAAAAAAAAAATACAGAAAGGATTTCAAATAC
TATATGTACTTCTCTTTTGTAGTGTAATGTGTGGTTTATTTTATTATGTGTATGAAAATGTA
TGGCTTCAAAGAGATAATGAAATGAATGAAATTTTAAAAAATTCCGAACATTTAACTATTGG
ATTTAAAGTTGAAAATGCACATGATAGAATTTTGAAAACTATAAAAACACATAAATTAAAAA
ATTACATTAAAGAATCTGTCAATTTTCTTAATTCAGGACTTACTAAAACAAATTATTTAGGT
AGTTCAAATGATAATATCGAATTAGTAGATTTCCAAAATATAATGTTTTATGGTGATGCAGA
AGTTGGAGATAACCAACAACCATTTACATTTATTCTTGATACAGGATCTGCTAATTTATGGG
TCCCAAGTGTTAAATGTACAACTGCAGGATGTTTAACTAAACATCTATATGATTCATCTAAA
TCAAGAACATATGAAAAAGATGGAACCAAAGTAGAAATGAATTATGTGTCAGGAACTGTTAG
TGGATTTTTCAGTAAAGATTTAGTAACTGTTGGTAATTTATCTCTTCCATATAAATTTATTG
AAGTAATAGATACTAATGGATTCGAACCAACTTATACTGCTTCAACATTTGATGGTATCCTT
GGTTTAGGATGGAAAGATTTATCAATAGGTTCAGTAGATCCAATTGTTGTTGAATTAAAAAA
CCAAAACAAAATTGAAAATGCTCTTTTCACCTTTTACTTACCTGTACATGATAAACATACAG
GATTCTTAACCATTGGTGGTATTGAAGAAAGATTTTATGAAGGACCACTAACTTACGAAAAA

TTAAACCACGATTTATATTGGCAAATAACTTTAGATGCACACGTTGGAAATATAATGTTAGA
AAAAGCAAACTGTATTGTAGATAGTGGTACTAGTGCCATTACTGTACCAACTGACTTTTTAA
ATAAAATGTTGCAGAATTTAGATGTTATCAAAGTCCCATTCTTACCTTTCTATGTAACTCTT
TGTAACAACAGCAAATTACCAACTTTTGAATTTACCTCAGAAAATGGTAAATACACATTAGA
ACCTGAATACTACCTTCAACACATAGAAGATGTTGGTCCAGGATTATGTATGCTTAATATCA
TAGGATTAGATTTTCCAGTACCAACCTTTATTCTAGGTGACCCATTCATGAGAAAATATTTT
ACCGTCTTTGATTATGATAATCAGAGTGTTGGTATTGCTCTTGCTAAAAAGAATTTATAA

Sequence length: 1362 bp

PF3D7_1408100 – Plasmepsin III - no introns

ATGAATTTAACCATTAAAGAAGAAGATTTTACCAACACCTTCATGAAAAATGAAGAATCCTT
TAACACGTTTCGAGTAACTAAAGTAAAAAGATGGAATGCTAAAAGATTATTTAAAATATTAT
TTGTGACAGTTTTCATAGTTTTGGCAGGAGGTTTTTCTTATTATATTTTTGAAAATTTCGTT
TTTCAAAAGAACCGTAAAATTAATCACATAATTAAGACTTCAAAATATTCGACAGTAGGATT
TAATATTGAAAATTCTTATGATAGACTTATGAAAACAATTAAAGAGCATAAATTAAAAAATT
ATATAAAAGAATCAGTAAAACTTTTTAATAAAGGTTTAACCAAAAAAAGTTATTTAGGTAGT
GAGTTTGATAATGTGGAATTAAAAGATTTAGCAAATGTATTATCTTTTGGAGAGGCAAAGCT
TGGAGATAATGGTCAAAAATTTAATTTCTTATTCCATACAGCTTCATCTAATGTATGGGTAC
CCAGTATAAAATGTACATCAGAGTCTTGTGAAAGTAAAAATCATTATGATTCATCAAAATCA
AAAACATATGAAAAAGATGATACGCCTGTTAAATTGACAAGTAAAGCTGGTACAATAAGTGG
AATATTTAGTAAAGATTTAGTAACTATTGGTAAATTATCAGTACCCTATAAATTTATTGAAA
TGACGGAAATTGTTGGATTTGAACCTTTTTATTCTGAATCAGACGTTGATGGTGTTTTCGGT
TTAGGATGGAAAGATTTATCCATAGGCTCTATAGATCCATATATTGTAGAATTAAAAACACA
AAATAAAATTGAACAAGCCGTTTATTCCATTTATTTACCACCAGAAAACAAAAATAAAGGTT
ATTTAACCATAGGAGGTATCGAAGAAAGATTCTTTGATGGACCATTGAACTATGAAAAATTA
AATCACGATTTAATGTGGCAAGTTGATTTAGATGTACATTTTGGTAATGTATCTTCCAAAAA
AGCAAACGTTATTTTAGATAGTGCCACCAGTGTCATAACTGTACCAACAGAATTTTTTAATC
AATTCGTAGAATCTGCAAGTGTTTTCAAAGTTCCATTCTTATCTTTGTATGTAACCACTTGT
GGTAACACGAAATTACCAACACTCGAATATCGTTCACCAAATAAAGTATATACTTTAGAACC
TAAACAATACCTTGAACCATTAGAAAATATATTCTCAGCATTATGTATGCTTAACATTGTAC
CTATTGATTTAGAAAAAAATACCTTTGTTCTAGGTGACCCATTTATGAGAAAATATTTTACC
GTTTATGATTACGATAATCACACCGTTGGATTTGCTTTAGCCAAAAATTTATAA

Sequence length: 1356 bp

PF3D7_1407800 – Plasmepsin IV - no introns

ATGGCTCTTACCGTTAAAGAAGAAGAATTTTCGAATACATTGATTAAAAATGCTTCAGCATT
TGATCGATTGAAATTAGGTAATTTGAAGAACTTGAAAATCCAGAAAAAGCTTCAGTTTTTAT
ATTTAATATTGTTTGTCCTTATTACGGGTGTGTTTTTCTTTTTTTTGATTGGAAATTTTTAT
TCACATCGCAAGTTGTATCAAGTTATTAAAAACACAAAACACACAACTATAGGATTTAAAAT
TGATAGACCACATGATAAGGTTTTGAGCTCTGTATTGAAAAATAAATTAAGCACATATGTAA

AAGAGAGCTTCAAATTTTTTAAATCAGGTTATGCACAAAAAGGATATTTAGGAAGTGAAAAT
GACAGTATTGAATTAGATGATGTTGCTAATTTAATGTTTTATGGTGAAGGACAAATTGGAAC
TAATAAACAACCATTTATGTTTATTTTCGATACCGGTTCAGCTAATTTATGGGTTCCAAGTG
TAAATTGTGATTCCATTGGATGCAGTACTAAACATCTTTATGATGCATCTGCATCTAAATCA
TATGAAAAAGATGGAACAAAGGTAGAAATATCTTACGGTTCAGGAACTGTTAGAGGATACTT
TAGTAAAGATGTAATAAGCCTTGGAGATTTATCATTACCATACAAATTTATTGAAGTTACAG
ATGCAGATGATTTAGAACCCATATATAGTGGTTCCGAATTTGATGGTATCCTAGGTTTAGGA
TGGAAAGATTTATCCATTGGTTCTATTGATCCGGTTGTTGTTGAATTAAAGAAACAAAACAA
AATCGACAATGCTTTATTTACATTTTATTTACCTGTTCATGATAAACACGTTGGTTATTTAA
CTATAGGTGGTATCGAAAGTGATTTTTATGAAGGACCTTTAACTTATGAAAAATTAAATCAT
GACTTATATTGGCAAATAGATTTAGATATACACTTTGGTAAATATGTCATGCAAAAAGCAAA
TGCTGTTGTTGATAGTGGTACAAGTACTATAACAGCACCAACCAGTTTTCTTAATAAATTCT
TTAGAGATATGAATGTTATTAAAGTACCATTCTTACCATTATATGTAACCACCTGTGATAAC
GATGATTTACCAACACTTGAATTCCATTCAAGAAATAATAAATACACATTAGAACCTGAATT
CTATATGGACCCATTATCAGATATTGATCCAGCTCTATGTATGCTCTACATATTGCCTGTTG
ATATTGATGATAATACATTTATTTTAGGAGATCCATTTATGAGAAAATATTTCACCGTTTTT
GATTATGAAAAAGAAAGTGTTGGTTTTGCAGTAGCTAAAAATTTATAA

Sequence length: 1350 bp

PF3D7_1115700 – Falcipain 2 – no introns

ATGGATTACAACATGGATTATGCTCCCCATGAAGTAATTTCTCAACAAGGAGAAAGATTTGT
TGACAAATATGTTGATAGAAAAATTTTAAAGAATAAAAAATCATTGTTAGTTATTATTTCAT
TATCTGTACTTTCAGTTGTTGGTTTTGTTTTATTTTATTTTACTCCAAATTCTAGAAAAAGT
GATTTATTTAAAAACTCTTCAGTTGAAAATAATAATGATGACTATATAATAAATAGCTTGCT
AAAAAGCCCTAATGGCAAGAAATTTATCGTCTCAAAAATTGATGAAGCCTTATCATTCTATG
ATAGTAAAAAGAATGACATAAATAAATACAACGAAGGTAATAACAACAATAATGCTGACTTT
AAAGGTCTTAGCTTATTTAAAGAAAACACACCATCAAATAATTTTATTCATAATAAAGATTA
TTTTATAAATTTTTTTGATAATAAATTCTTAATGAATAATGCAGAACATATAAACCAATTTT
ATATGTTTATTAAAACTAATAATAAACAATATAATTCTCCAAATGAAATGAAGGAAAGATTT
CAAGTATTCTTACAAAATGCACACAAAGTAAATATGCATAACAATAATAAAAATAGTTTATA
TAAAAAAGAATTAAACAGATTTGCCGATTTAACTTATCATGAATTTAAAAACAAATATCTTA
GTTTAAGATCTTCAAAACCATTAAAGAATTCTAAATATTTATTAGATCAAATGAATTATGAA
GAAGTTATAAAAAAATATAAAGGAAATGAAAATTTTGATCATGCAGCTTATGATTGGAGATT
ACATAGTGGTGTAACACCTGTAAAGGATCAAAAAAATTGTGGATCTTGCTGGGCCTTTAGTA
GTATAGGTTCCGTAGAATCACAATATGCTATCAGAAAAAATAAATTAATAACCTTAAGTGAA
CAAGAATTAGTAGATTGTTCATTTAAAAATTATGGTTGTAATGGAGGTCTCATTAATAATGC
CTTTGAGGATATGATTGAACTTGGGGGTATATGTACAGATGATGATTATCCATATGTAAGTG
ATGCTCCAAATTTATGTAATATAGATAGATGTACTGAAAAATATGGAATCAAAAATTATTTA
TCCGTACCAGATAATAAATTAAAAGAAGCACTTAGATTCTTGGGACCTATTAGTATTAGTGT
AGCCGTATCAGATGATTTTGCTTTTTACAAAGAAGGTATTTTCGATGGAGAATGTGGTGATC
AATTAAATCATGCCGTTATGCTTGTAGGTTTTGGTATGAAAGAAATTGTTAATCCATTAACC
AAGAAAGGAGAAAAACATTATTATTATATAATTAAGAACTCATGGGGACAACAATGGGGAGA

AAGAGGTTTCATAAATATTGAAACAGATGAATCAGGATTAATGAGAAAATGTGGATTAGGTA
CTGATGCATTCATTCCATTAATTGAATAA

Sequence length: 1455 bp

PF3D7_1115300 - Falcipain 2b – no introns

ATGGATTACCACATGGATTATATTCCGAATGAGGTAATTTCTCATCAAGGAGAAAGATTTGT
CGACAAATATGTTGATAGAAAAATTTTAAAGAATAAAAAATCATTGTTAGTTATTATTTCAT
TATCAGTACTTTCAGTAGTTGGTTTTATTTTATTTTATTTTACTCCAAATTTTAGAAAAAGT
GATTTATTTAAAAACTCTTCAGTTGAAAATAATAATGATGACTATATAATAAATAGCTTGCT
AAAAAGCCCTAATGGCAAGAAATTTATCGTCTCAAAAATTGATGAAGCCTTATCATTCTATG
ATAATAAAATGAAAGATATAAATAAAAACAATAACAATAATACTTCATCCGATTTTAAAGGT
CTTAGCTTATTTAAAGAAAACAAACCATCAAATAATTTTATTCATAATGAAAATTATTTTAT
AAATGTTTTTGATCATAAATTCTTAATGAATAATGTAGAACATATAAACCAATTTTATACGT
TTATAAAAACTAATAATAAACAATATAATTCTCCGAATGAAATGAAGGAAAGATTTCAAGTA
TTCTTACAAAATGCACACAAAGTAAAAATGCATAACAATAATAAAAAGAGTTTATATAAAAA
AGAATTAAATAGATTTGCTGATTTAACTTATCACGAATTTAAAAGTAAATATCTTACTTTAA
GATCTTCGAAACCATTAAAGAATTCTAAATATTTATTAGATCAAATAAATTATGACGCCGTA
ATAAAAAAATATAAAGGAAATGAAAATTTTGATCATGCAGCTTATGATTGGAGATTACATAG
TGGTGTAACACCTGTAAAGGATCAAAAAAATTGTGGATCTTGCTGGGCCTTTAGTAGTATAG
GTTCCGTAGAATCACAATATGCTATCAGAAAAAATAAATTAATAACCTTAAGTGAACAAGAA
TTAGTAGATTGTTCATTTAAAAATTATGGTTGTAATGGAGGTCTCATTAATAATGCCTTTGA
GGATATGATTGAACTTGGGGGTATATGTACAGATGATGATTATCCATATGTAAGTGATGCTC
CAAATTTATGTAATATAGATAGATGTACTGAAAAATATGGAATCAAAAATTATTTATCTGTA
CCAGATAATAAATTAAAAGAAGCACTTAGATTCTTGGGACCTATTAGTATTAGTATAGCCGT
ATCAGATGATTTTCCGTTTTACAAAGAAGGTATTTTTGATGGAGAATGTGGTGATGAATTAA
ATCATGCCGTTATGCTTGTAGGTTTTGGTATGAAAGAAATTGTTAATCCATTAACTAAGAAA
GGAGAAAAACATTATTATTATATAATTAAGAACTCATGGGGACAACAATGGGGAGAAAGAGG
TTTCATAAATATTGAAACAGATGAATCAGGATTAATGAGAAAATGTGGACTAGGTACTGATG
CATTCATTCCATTAATTGAATAA

Sequence length: 1449 bp

PF3D7_1115400 – Falcipain 3 – no introns

ATGGAATATCATATGGAATATTCACCGAACGAGGTGATTAAACAAGAAAGAGAAGTATTTGT
AGGAAAAGAAAAAAGTGGCAGCAAATTTAAAAGAAAGAGATCTATTTTTATAGTTCTTACAG
TATCAATATGTTTTATGTTTGCTTTAATGTTATTTTATTTTACAAGAAATGAAAATAACAAG
ACCTTGTTTACTAATAGTTTATCAAATAATATAAACGATGATTACATAATAAATTCATTATT
AAAAAGTGAGAGTGGTAAAAAATTCATTGTATCAAAACTTGAAGAATTAATATCTTCTTATG
ATAAAGAGAAAAAAAATGAGAACTACTGGAGCAGAAGAAAATAACATGAATATGAATGGTATA
GACGATAAAGATAATAAAAGTGTTAGTTTTGTTAATAAAAAAAATGGGAATTTAAAAGTGAA
TAATAATAATCAAGTTTCTTATAGTAATCTTTTTGATACAAAATTTTTAATGGATAATTTAG

AGACTGTAAATTTATTTTATATCTTTTTAAAAGAGAATAATAAGAAATATGAAACATCGGAA
GAAATGCAAAAGAGATTTATAATATTTTCAGAAAATTACAGAAAGATAGAATTACATAACAA
AAAAACTAATAGTTTATATAAAAGGGGTATGAACAAATTTGGAGATTTGTCCCCCGAAGAAT
TTAGAAGTAAATATTTAAATTTAAAAACACATGGTCCATTCAAAACATTATCACCACCTGTA
TCATATGAAGCAAATTACGAAGATGTAATTAAGAAATATAAACCAGCTGATGCTAAATTAGA
TCGTATAGCATATGATTGGAGATTACATGGTGGTGTAACACCAGTTAAGGATCAAGCATTAT
GTGGATCATGTTGGGCTTTTAGTAGTGTAGGTTCTGTAGAATCACAATATGCTATAAGAAAG
AAAGCATTGTTTTTATTTAGTGAACAGGAACTAGTTGATTGTTCAGTTAAAAATAATGGTTG
TTATGGTGGATATATAACTAATGCTTTTGATGATATGATTGATCTTGGAGGATTATGTTCTC
AAGATGATTATCCATATGTTAGTAATTTACCAGAAACTTGTAATCTTAAAAGATGTAACGAG
AGATATACAATCAAATCATATGTATCTATACCAGATGATAAATTTAAAGAAGCCTTAAGATA
TCTAGGACCTATTAGTATTAGTATAGCAGCTTCAGATGATTTCGCCTTTTATAGAGGAGGTT
TTTATGATGGAGAATGTGGAGCAGCACCAAATCATGCGGTTATACTTGTAGGTTATGGTATG
AAAGATATTTATAATGAAGATACTGGAAGAATGGAAAAATTCTATTATTATATCATTAAAAA
CTCATGGGGATCTGATTGGGGAGAAGGAGGATATATTAATCTAGAAACTGATGAAAATGGAT
ACAAAAAAACTTGTTCAATTGGAACAGAAGCTTATGTACCATTACTTGAATAA

Sequence length: 1479 bp

PF3D7_1360800 – Falcilysin – no introns

ATGAATTTAACAAAATTAATGAAAGTTATTGGATATATAAATATAATCACAAATTGTGTT
CAAAGCTTTACAAATAGAGCTGATAAAAAAAGATATAATGTTTTTGCAAAAAGTTTTATA
AATACAATAAATACAAATTTATATACATTTAAAGCAGTCATGAGTAAAACACCAGAGTGG
ATACATGAGAAATCACCTAAGCACAATAGTTATGATATTATAGAAAAGAGGTATAATGAG
GAATTTAAGATGACTTATACGGTATATCAACATAAGAAGGCTAAAACACAAGTAATATCC
TTAGGTACTAATGATCCTTTAGATGTTGAACAAGCTTTTGCTTTTTATGTTAAAACGTTG
ACACATTCTGGTAAGGGTATACCTCATATTTTAGAACATTCTGTATTATCAGGATCTAAA
AATTACAATTACAAAAATTCCATAGGTTTATTAGAAAAAGGTACCTTACATACTCATTTG
AATGCATACACATTTAATGATAGGACAGTATATATGGCTGGTTCAATGAATAATAAAGAT
TTTTTTAATATTATGGGTGTATATATGGATAGTGTTTTTCAGCCGAATGTATTAGAAAAT
AAGTATATTTTTGAAACGGAAGGATGGACATATGAAGTAGAAAAATTAAAAGAAGATGAA
AAGGGGAAAGCTGAGATACCTCAAATGAAAGATTATAAAGTGTCATTTAATGGTATTGTG
TATAATGAAATGAAAGGTGCATTAAGTAGTCCTTTAGAAGATTTATATCATGAAGAAATG
AAATATATGTTTCCTGATAATGTGCATTCTAATAATAGTGGTGGGGATCCTAAAGAAATT
ACGAACTTAACATATGAAGAATTTAAAGAATTTTATTATAAGAATTATAATCCTAAAAAG
GTTAAAGTATTTTTCTTTAGTAAAAATAATCCTACTGAGTTATTAAATTTTGTAGATCAA
TATTTGGGACAATTAGATTATAGTAAATATCGTGATGATGCAGTAGAAAGTGTAGAATAC
CAAACATATAAAAAAGGACCTTTTTATATTAAGAAGAAATATGGTGACCATTCAGAGGAG
AAGGAAAATTTGGTATCAGTAGCTTGGTTATTAAATCCGAAAGTAGATAAAACTAACAAC
CACAATAATAATCATAGTAATAACCAAAGTAGTGAAAATAATGGTTATTCAAATGGTAGT
CATAGTTCAGATTTAAGTTTAGAAAATCCAACAGATTATTTTGTTCTTTTAATAATTAAT
AATTTATTAATACATACACCTGAAAGTGTTTTATATAAAGCATTAACGGATTGTGGATTA
GGAAACAATGTTATTGATAGAGGATTAAATGATAGTTTGGTACAATATATTTTTAGTATT
GGTTTGAAAGGTATTAAAAGAAATAATGAGAAAATAAAAAATTTTGATAAGGTACATTAT
GAAGTTGAAGATGTTATTATGAATGCTCTTAAGAAAGTTGTAAAAGAAGGTTTTAACAAA
TCAGCTGTTGAAGCTTCTATTAATAATATAGAATTTATATTAAAAGAAGCAAATTTGAAA
ACTTCTAAAAGTATAGATTTTGTCTTTGAAATGACATCCAAATTAAATTATAATCGTGAT

CCTTTATTAATTTTTGAATTTGAGAAATATTTAAATATTGTAAAAAATAAAATTAAAAAT
GAACCAATGTATTTAGAAAAATTTGTAGAAAAACATTTTATTAATAATGCTCATCGTTCA
GTTATTTTATTAGAAGGTGATGAGAATTATGCACAAGAACAAGAAAATTTAGAAAAGCAA
GAATTAAAAAAAAGAATAGAAAATTTTAATGAACAAGAAAAAGAACAAGTTATTAAAAAT
TTTGAAGAATTAAGTAAATATAAAAATGCAGAAGAAAGTCCTGAACATTTAAATAAATTC
CCAATTATAAGTATATCAGATTTAAATAAAAAAACATTGGAAGTACCTGTGAATGTTTAT
TTTACAAATATTAATGAAAATAATAATATAATGGAAACATATAATAAATTAAAAACTAAT
GAACATATGTTAAAAGATAATATGGATGTATTTTTAAAAAAATATGTATTAAAAAATGAT
AAACATAATACAAATAATAATAATAATAATAATAATAATATGGATTATAGTTTTACTGAA
ACCAAATATGAAGGAAATGTACCTATATTAGTTTATGAGATGCCAACAACAGGAATTGTA
TATTTACAGTTTGTGTTCTCTTTAGATCATTTAACCGTAGACGAATTAGCATATTTGAAT
TTATTCAAAACATTAATATTGGAAAATAAAACAAATAAAAGATCATCTGAAGATTTTGTT
ATCTTAAGAGAAAAAAATATTGGAAGTATGTCTGCTAATGTTGCTTTATATTCAAAAGAT
GATCATTTAAATGTAA**CCGATAAATATAATGCACAAGC**TTTATTTAATTTAGAAATGCAT
GTATTAAGTCATAAATGCAATGACGCATTAAATATAGCATTAGAAGCAGTGAAAGAATCC
GATTTTTCAAATAAGAAAAAGGTTATTGATATATTGAAAAGAAAAATTAATGGTATGAAA
ACAACATTTAGTGAAAAGGGATATGCTATATTAATGAAATATGTAAAAGCACATTTAAAT
TCTAAACATTATGCTCATAATATTATTTATGGATATGAAAATTATTTAAAATTACAAGAA
CAACTTGAATTAGCAGAAAATGATTTTAAGACATTGGAAAATATACTGGTACGTATAAGA
AATAAAATATTTAATAAGAAAAATTTAATGGTTAGTGTAACATCAGATTATGGAGCATTA
AAACATTTATTTGTTAATTCTAATGAATCATTGAAAAATTTAGTATCATATTTTGAAGAA
AATGATAAATATATAAATGACATGCAAAATAAAGTAAATGATCCAACTGTAATGGGATGG
AATGAAGAAATTAAAAGTAAGAAATTATTTGATGAAGAAAAGGTAAAGAAAGAATTTTTT
GTATTACCAACATTTGTTAATTCTGTGTCTATGTCAGGAATTTTATTTAAACCAGGAGAA
TATCTAGATCCATCCTTTACTGTCATTGTAGCCGCATTAAAAAATTCGTATTTATGGGAT
ACTGTTAGAGGATTAAATGGAGCTTATGGTGTTTTTGCTGATATTGAATATGATGGTAGT
GTAGTCTTTTTATCTGCTAGAGATCCAAATTTAGAAAAAACATTAGCTACCTTTAGAGAA
TCAGCTAAGGGTTTAAGAAAAATGGCTGATACTATGACTGAAAATGATTTGTTAAGATAT
ATTATTAATACTATAGGAACCATTGATAAACCTAGAAGAGGCATAGAATTAAGTAAACTA
TCTTTCTTAAGACTTATATCTAACGAAAGTGAACAAGACCGAGTGGAATTCAGGAAAAGA
ATTATGAACACAAAAAAAGAAGACTTTTATAAATTTGCAGACTTGTTGGAGAGCAAAGTT
AATGAATTTGAAAAAAATATTGTTATCATCACTACAAAGGAAAAGGCAAATGAATATATA
GCAAACGTAGATGGAGAATTTAAAAAGGTATTAATAGAA

Bold = forward and reverse primer of the first part (*Pf*Fl1), 2438 bp.

Underlined = forward and reverse primer of the second part (*Pf*Fl2), 1216 bp.

BclI restriction site

XmnI restriction site

PF3D7_1116700 – Dipeptidyl aminopeptidase 1 – no introns

ATGGCAAAGAGAATTTTTAGTGTAAGTTTTTTACTAGTATTGTTAAACGTTTTGCACATATG
CATTAAATTTAGTGTTGCTGATTTACCAACCCATGTAGAAACAAAGAATTTATTAGGTAAAT
GGAAAATTTTAAGGACTAAAACATCACCAAATTTGACTACTTGTGGTTCTAGTCAACCTAAT
AAGAATACATATAATGTAGGTATAACAGATTATAAAAAATATTTGCTTGAAAACAATTATGA
GTTTGTTTCAGAATTGAATGTAATATTATCAGATGATTATGTATTATATGGTGATATATATA
ATACCCAAGATAATGAGCACAGAAGTAAATGGAAAGTGTTAGCTGTGTATGATGAGAATAAG
AGAGTTATTGGTACATGGACAACTATATGTGATGAGGGTTTTGAAATAAAAATTGGGAATGA

AACGTATGCAGCTTTAATGCATTATGAACCTAATGGAAAATGTGGTCCTGTATCTGATGAAG
ATTCTTTAGATTCAAATGGAGATACTGATTGTTATACTACAAGTTTTAGTAAGATAAGATAT
GGTTGGTTAGATGTGGAGAATGAAAAAAATGAACATTTACATGGTTGTTTTTATGCAGAAAG
AATTTTTGATAATGTAAATGAAATTAAACATTTAGATTCTTTTACTATAGATAAAGATTCTC
AAAATGTTCTTCAAACATTTACTTATGACACTAAATTAAATAATATCTTAAATTCTAATAAT
ATGTTATATAAATTTGGTAATTTACAAAAACCAACATTTACCAAAAGAAACAATACAAATGT
ACAATTTAATTCTGAATTAAATTGGCACAGAATGAAACACCACGGAAAAAAAAAACCATTGA
AGAAATCCATGTTGGATGCATCAAGACAAACTTATGCATGTCCATGTAACGCTAACGAAGTT
GTTGATAATGTAATAAATAAAGGAGATTCAGATAATCCAGTATCACCAACCTTAATTCAATT
AAATAATAACCTAAAGAATACAACACAAACAGGTAATAAAGATACAAATGAAATGGATTTAG
AAAATTATGAGGATACATTAAATTCTCCTAAAAGAGAATTAGAAATAAACGAATTACCAAAG
AATTTCACTTGGGGAGACCCATGGAATAAAAATACCAGAGAATATGAGGTTACTAATCAATT
ATTATGTGGTTCATGTTATATAGCTTCACAATTATATGCATTTAAAAGAAGAATAGAAGTGG
CACTTACCAAAAAATTGGATAGAAAATATTTGAACAATTTTGATGATCAATTATCCATACAA
ACTGTTTTATCATGTTCTTTTTATGACCAAGGATGTAATGGTGGATTCCCATATTTAGTATC
TAAGCTAGCTAAATTACAAGGTATCCCATTAAATGTATATTTCCCATATAGTGCAACTGAGG
AAACTTGTCCATATAATATAAGCAAACATCCTAATGATATGAATGGTTCTGCTAAATTAAGA
GAAATCAATGCTATATTTAATAGTAACAATAATATGAGTACTTATAACAACATTAATAATGA
CCACCACCAATTAGGTGTATACGCAAATACTGCATCTTCACAAGAACAACATGGTATTTCTG
AAGAAAACAGATGGTACGCTAAAGATTTTAATTATGTAGGTGGTTGTTATGGATGTAACCAA
TGTAATGGTGAGAAAATTATGATGAATGAAATTTATAGAAATGGTCCTATCGTTTCTTCTTT
TGAAGCTTCTCCAGATTTTTATGACTATGCTGATGGTGTGTATTTTGTTGAAGATTTCCCAC
ACGCTCGTAGATGTACCATCGAACCTAAAAACGATGGTGTCTATAACATAACAGGTTGGGAT
CGTGTTAACCATGCCATTGTTTTGTTAGGATGGGGAGAAGAAGAAATTAATGGAAAATTATA
CAAATATTGGATAGGAAGAAATAGTTGGGGAAATGGTTGGGGTAAAGAAGGATACTTTAAAA
TTTTAAGAGGACAAAATTTCAGTGGTATTGAAAGTCAGAGTTTGTTTATTGAACCTGATTTT
TCAAGAGGTGCTGGTAAAATACTTTTAGAAAAAATGCAAAAGGAATTAGGAAATTAA

Sequence length: 2103 bp

PF3D7_1247800 – Dipeptidyl aminopeptidase 2 – introns spliced out

ATGAATACTTTTTATATTTTCTTTTTATTTGTGCTGACGACATGCTTCGTAAAGGGTGATTT
ACCAATACATGCTCTTATGGGAGATGTATCAGGAATATGGAAAATAAAACAAACAAAAAAGA
TGAGCCAAAAACCTGAACATTGTGGTGGGGGTATACCCAATAGAAATTTGGATAACTTAAAC
CCAAGTATAAGAAATTATCAAAGATTTTTGGAGAATGAATATGGGAACTTAGACATGATGAT
TGTGAACTTAACAATGGAAAAAGTAAAAATAATTAATCAAGAAAAGCCAAGAGATAAATGGA
CATATCTTGCTGTGAGAGATTATGAAAGGAATGAAATTATTGGTCATTGGACCATGGTATAT
GACGAAGGCTTCGAAATAAGATTGAATGGAAGCAAATATTTCGCTTTTTTCAAATATGAAAG
AAAATCAAATGCACATTGCCCTACCTCAATTGAAGACAAAAGTTATAATGATAGAGATTGTT
ACAAAACAAATCCGACGCAAACACATATTGGATGGGTACTCAATGAGAAAGTTAAAGAAAAT
ACAAAAGAAAAAATTTTTTATTGGGGATGTTTTTATGCTGAGAAGAAAGAAAGTACGCCTGT
ATCTTCTTTTGTCCTTCATAATGGGATGGAAAATAAAACGAATTTAGTAGAAAGTCATGATT
ATCATTTTGAAGAAAAAAAAAAAAAAAATCTGCCTCCTATTGGAAGGAGATCAAATTATAAA

AAGTTCCGATTTTCCAACCTACAAAAAATATATGGATCAACACAAACGCACCTGAGGGATAT
CTATGGGCGCTCAGGTGAGCGAAAGTATGGATGCAGAAAAAGAGATATTTTGAATTTAAAGA
TACGACTAACATTACCAAAACAATTTAGTTGGGGAGACCCCTTTAACGATGAAAATTTTGAA
GAAAACGTAGATGACCAAAAAGATTGTGGTAGTTGTTATTCTATATCTAGTGTGTATAGTTT
AGAAAGAAGGTTCGAAATATTATTTTGGAAGAAATATAAGAAAAAAGTAAATATGCCTAGAT
TGTCTCATCAATCAATATTAAGTTGTTCTCCATATAATCAAGGATGTGATGGAGGGTACCCA
TTTTTAGTTGGAAAACATATGTATGAATATGGTATAATACCTGAACAGTACATGCATTATGA
AAATAATGATTACAATAACTGTATTATGGATATGGGAAATTATAATCATTTAAATAAACAAA
ATAGAAATATAAAGGAAATTTATTATGTTTCAGATTATAATTATATAAATGGATGTTATGAA
TGTACTAATGAATATGAAATGATGAATGAAATTATTTTGAATGGACCAATAGTTGCAGCTAT
TAATGCTACCTCAGAATTGTTAAACTTTTATAATATAGAAGATAAAAATGTTGTTTATGATA
TCCTACCTAAAGATACTCATCAAGTATGTGATGTACCTAATAAAGGATTTAATGGATGGCAA
CAAACAAACCATGCAATTAATATTGTAGGATGGGGTGAACAAATAATTAATCAAGATAAAAT
CAAAAACGATGATGCTAACAATAATAATAATGACAATAATCATAAATTAGTAAAATATTGGA
TTATAAGAAATACATGGGGAAAAAACTGGGGATATAAAGGTTATCTCAAATTTCAAAGAGGA
ATTAATTTAGCAGGTATTGAATCTCAAGCTGTTTATATCGACCCAGATTTTTCTAGAGGATA
CCCAAAGAATATACTTCAATCCGACTCTTTGGAATAA

Sequence length: 1773 bp

PF3D7_1311800 – Alanyl aminopeptidase – no introns

ATGAAATTAACAAAAGGCTGTGCCTATAAATATATTATTTTCACAGTGTTAATTTTAGCGAA
TATTCTTTATGATAATAAAAAAAGGTGCATGATTAAAAAAAATTTACGTATTAGTTCGTGCG
GTATAATAAGTCGCTTGCTCAAATCTAATTCAAATTATAATAGTTTTAATAAGAATTATAAT
TTCACGTCTGCTATATCAGAATTACAATTTTCCAATTTTTGGAATTTAGATATTTTACAAAA
GGATATATTTAGTAATATACATAATAACAAAAACAAGCCTCAATCATATATAATACATAAAA
GACTAATGAGTGAGAAAGGAGATAATAATAATAATAATCACCAAAATAATAATGGGAATGAC
AATAAGAAAAGATTAGGATCTGTTGTAAATAATGAAGAAAATACTTGTTCAGATAAAAGAAT
GAAACCTTTTGAAGAAGGTCATGGAATTACACAAGTTGATAAGATGAATAACAACAGTGATC
ATTTACAACAAAATGGTGTTATGAATTTGAATAGTAATAATGTTGAAAATAATAATAATAAC
AATTCTGTTGTTGTTAAAAAGAACGAACCAAAAATACATTATAGGAAAGATTATAAACCAAG
TGGATTTATAATTAATAATGTAACATTAAATATTAATATCCATGACAATGAAACTATTGTAA
GATCTGTACTTGATATGGATATTAGTAAACACAATGTTGGTGAAGATTTAGTTTTTGATGGT
GTTGGATTAAAAATTAATGAGATAAGTATTAATAATAAGAAATTAGTTGAAGGAGAAGAATA
TACCTACGATAATGAATTCTTAACTATATTTTCAAAATTTGTACCAAAATCTAAATTTGCTT
TTTCATCAGAAGTTATTATACATCCAGAAACAAATTATGCTCTTACAGGTTTATATAAATCA
AAAAATATTATTGTTTCTCAATGTGAAGCTACCGGATTCCGTCGTATCACTTTTTTTATTGA
CAGACCAGATATGATGGCAAAATATGACGTTACAGTAACTGCTGATAAAGAAAAATATCCTG
TTTTATTAAGTAATGGTGATAAGGTGAATGAATTTGAAATACCAGGTGGTCGTCATGGAGCT
AGATTTAATGATCCCCATTTAAAACCATGTTATTTATTTGCTGTTGTAGCTGGTGACCTTAA
ACATTTAAGTGCTACATATATTACTAAATATACCAAAAAAAAAGTTGAATTATATGTATTTA
GTGAGGAAAAATATGTATCTAAATTACAATGGGCTTTAGAATGTCTTAAAAAATCGATGGCA
TTTGATGAAGATTATTTTGGATTGGAATATGATTTGTCTCGTTTAAATTTAGTTGCTGTTTC

TGACTTTAATGTTGGTGCTATGGAAAATAAAGGATTAAATATATTTAATGCTAATTCTTTAT
TAGCATCCAAAAAAAATTCAATTGATTTTTCATATGCAAGAATTCTAACGGTCGTAGGACAT
GAATATTTCCATAATTATACAGGAAATAGAGTTACTCTTAGAGATTGGTTTCAGTTAACATT
AAAAGAAGGTCTAACAGTACATAGAGAAAATTTGTTTTCAGAAGAAATGACGAAGACCGTAA
CTACTCGTTTATCTCATGTAGATTTATTAAGAAGTGTTCAATTTTTAGAAGATTCCTCACCA
TTATCACACCCTATTAGACCAGAATCTTATGTTAGTATGGAAAACTTTTATACTACTACTGT
TTATGATAAAGGTAGTGAAGTTATGAGAATGTATCTTACTATATTAGGTGAAGAATATTATA
AAAAAGGTTTTGATATTTATATTAAGAAAAATGATGGAAATACTGCTACTTGTGAAGATTTT
AATTATGCTATGGAACAAGCATATAAAATGAAAAAAGCAGACAATTCAGCTAACCTAAACCA
ATATTTATTATGGTTCTCACAAAGTGGTACTCCACATGTTAGTTTTAAATATAACTACGATG
CTGAAAAGAAACAATATAGTATACATGTTAATCAATATACCAAACCAGATGAAAACCAAAAA
GAAAAGAAACCTTTATTTATTCCTATAAGTGTTGGCTTAATTAATCCAGAAAACGGTAAAGA
AATGATATCACAAACCACCTTAGAATTAACAAAAGAAAGTGATACATTTGTATTTAATAATA
TAGCTGTAAAACCAATACCATCCTTATTCAGAGGATTTAGTGCACCAGTATATATTGAGGAT
AACTTAACAGATGAAGAACGTATATTATTATTGAAATATGATAGTGATGCTTTTGTTCGTTA
TAACTCATGTACCAATATATATATGAAACAAATATTAATGAATTATAATGAATTCTTAAAAG
CTAAAAATGAAAAATTAGAAAGTTTTAATCTTACACCAGTAAATGCACAATTTATAGATGCT
ATAAAATATTTATTAGAAGACCCACATGCTGATGCAGGATTTAAATCATATATAGTATCCTT
ACCACAAGATAGATATATAATAAACTTTGTAAGCAATTTAGATACAGACGTATTAGCTGATA
CTAAAGAATATATATATAAACAAATCGGAGATAAATTAAATGATGTATATTATAAAATGTTT
AAAAGTTTAGAAGCAAAAGCTGATGATTTAACATATTTTAATGATGAATCACATGTAGATTT
TGATCAAATGAATATGAGAACATTAAGAAATACATTATTATCATTATTAAGTAAAGCTCAAT
ATCCAAATATATTAAATGAAATTATTGAACATTCCAAATCACCATATCCATCCAATTGGCTA
ACTAGTTTATCAGTTTCAGCATATTTCGATAAATATTTTGAACTTTATGATAAAACTTATAA
ATTATCAAAAGATGATGAATTATTGTTACAAGAATGGTTAAAGACTGTATCAAGATCTGATC
GTAAAGATATATATGAAATACTTAAAAAATTAGAAAATGAAGTTTTGAAAGATAGTAAAAAT
CCAAATGATATTAGAGCAGTATATCTTCCATTTACAAATAATTTAAGAAGATTCCATGATAT
ATCAGGAAAAGGGTATAAATTAATTGCTGAAGTTATTACAAAAACCGATAAATTTAATCCTA
TGGTTGCAACACAATTATGTGAACCATTTAAATTATGGAATAAACTAGATACAAAAAGACAA
GAATTAATGCTTAACGAAATGAACACAATGTTACAAGAACCAAACATATCAAATAACTTAAA
GGAATATTTATTAAGATTAACAAATAAATTATAA

Sequence length: 3258 bp

PF3D7_1454400 – Aminopeptidase P – no introns

ATGCAATTGAATTTTCTTTTGTTTGTTTTTATATTTTTAATGGTATTCCATTTAAATATTTT
TAATAAGGGTAAGAGGCAAAATTTAGTATCGGCTTATTTAAATCATTTTAAAAAGTCATATT
TTAGTGGCGTTACGAGCGGATCTGATTGTGTAAATAAAAGTGAAGTGAGTAGTGATAATAAT
AATAATAATAATAATAATAATAAGATAGCACATAATTTTTTCTCCAAAAAATATCAGAG
AAATTTCGAGAATAATAATTTAAGTGAGAATCAAGAAAATAATAAGAATATAATATATAGTG
GTTCCAATATATTTAAGAATATATATAATACCGAAATGATGAGTAATAATAATACCGTTGAT
GTTAACATGATGGATAATAATCCTGCTGCTAGATTAGAAGAATTAAGAACTATTATGAAAAA
GAATAAGATTGATGTATATATTTTAATTAATAGTGATGAACACAATTCTGAAATAATAAATG

AGAAAGATAAAAAAATTGTAAAAATTACAAATTATAGTGGTGCTGATGGTATATTAATAGTA
ACAAAAGATAAACCCATATTATATGTCAATGCATTATATGAATTACAAGCTATGAATGAATT
AGATCAGAATTTATTTACATTAAGAATTAGTAGAATTGATAATAGAGATGAAATTTTTGAAA
CAATATCATCTTTAGAATTTAATACTATAGCCTTTGATGGAAAAAACACTAGTGTTGTGTTT
TATGAAAAATTAAGAAAAGCTCTTTTAAATGCATATCCAAAAAAAAAAAATTGTAGAAAAAT
TATATATAATAATAATTTTGATGATGTTAATAAAAAGGATGATGAAAATGTATTAAATTTTC
TTGTTTTGGAAAAATCATTAGTGGAAATTAAAGATTATCCTGTTAATAATAAAACTTTATAT
ATACATGATAGAAAATATAATGGTGCATGTGCAGGTGAAAAAATTGATAAATTAAAACAATC
GCTTATGTATGATATTAAAAATGTAGATAATTTACTTTTATCAGAATTAGATGAAATTGCAT
ATCTTTTAAATTTAAGAGGTTATGATTATCAATATTCACCATTATTTTATTCTTATTTATTA
TTTCAATTTGATAGAGAAGAACAAGATTTCTCTAAAATCGTATTCTTTACAACAGTAAAAAA
TTTACCAGCAGATGTTAAAAATCTTTTAGAAATTAATAAAGTTATTGTAAAAGAATATGAAG
AAATTGTACCATACCTTAGAGATGTAGTTATCCCATCCATACCAAAACATAATGATGATAAT
CCTGATTTCAAAAAATATGATATCTCATTAAGCCCATATATCAATTTAATGATATATAAACT
ATTTGATAGAAAAAATGTTCTTTTACAAAATTCACCTGTAGTTAAAATGAAAGCAGTAAAAA
ATGATGTAGAAATTGATAATATGAAACAAGCACATATATTAGATGGTCTTGCTTTATTACAA
TTTTTCCATTGGTGTGAACAGAAAAGAAAAACAAAAGAATTATTTAATGAAACAGAAATGTC
TTTAAGACATAAAGTAGATTATTTTAGATCAACCAAGAAAAATTTTATCTTCCCATCCTTTT
CAACCATATCAGCAAGTGGTCCTAATGCAGCCGTTATTCATTATGAATGTACAGATAAAACA
AATGCTACCATTAAACCAGCTATTTATCTTTTAGATTCGGGAGGACAATATTTACATGGAAC
TACTGATGTTACTAGAACGACACATTTTGGGGAACCCACGGCTGAAGAAAAGAGAATTTATA
CATTAGTATTAAAAGGACATTTACGTTTAAGAAAAGTTATCTTTGCATCTTATACAAATTCA
TCTGCTTTAGATTTTATTGCACGTGAAAATTTATTCAACAACTTTATGGATTATAATCATGG
TACTGGTCATGGTGTTGGTTTAACTCTCAATGTACATGAAGGTGGCTGTTCTATAGGCCCAG
TAGGTGGAGCACCTCTTAAAAAAAATATGGTCCTTTCTAATGAACCAGGATATTATATGAAA
GATAAATTTGGGGTACGTATAGAAAATATGCAATATGTTATTAGCAAAGAAATTACAGATAC
GACTGAATACCTTTCATTTGATGATTTAACTATGTACCCATATGAAAAGAAATTATTAGATT
TCTCACTTTTAACAAACCAAGAAATTAAAGAACTTAATGAATATCATACAACCATTAGAAAT
ACATTATTACCCTTAGTTAAACAAAGCCCACAAGAATATGGAGAAAGTGTTGAAAAATATTT
AATAGAAATAACAGAACCAATTGCGATTCATAACAATTAA

Sequence length: 2334 bp

<u>APP truncated optimised</u>

ATGCACAACCACAACCACAATCACAATCACAACCACAACGACTATGACATCCCGACCACCGA
GAACCTGTATTTCCAAAGCGATAACAACCCGGCGGCGCGTCTGGAGGAACTGCGTACCATCA
TGAAGAAAAACAAGATTGACGTGTACATCCTGATTAACAGCGATGAACACAACAGCGAGATC
ATCAACGAAAAGGACAAGAAAATCGTTAAGATCACCAACTACAGCGGTGCGGACGGCATCCT
GATTGTGACCAAAGATAAGCCGATCCTGTATGTTAACGCGCTGTACGAGCTGCAGGCGATGA
ACGAACTGGACCAAAACCTGTTCACCCTGCGTATCAGCCGTATTGACAACCGTGATGAGATC
TTTGAAACCATTAGCAGCCTGGAGTTCAACACCATCGCGTTTGATGGCAAGAACACCAGCGT
GGTTTTCTATGAAAAGCTGCGTAAAGCGCTGCTGAACGCGTACCCGAAGAAAAAGATTGTGG
AGAAGATCATCTACAACAACAACTTCGACGATGTTAACAAAAAGGACGATGAAAACGTGCTG

AACTTTCTGGTTCTGGAGAAGAGCCTGGTGGAAATCAAAGACTACCCGGTTAACAACAAGAC
CCTGTATATTCACGATCGTAAATACAACGGTGCGTGCGCGGGCGAGAAGATCGACAAACTGA
AGCAGAGCCTGATGTACGACATTAAAAACGTGGATAACCTGCTGCTGAGCGAGCTGGACGAA
ATCGCGTATCTGCTGAACCTGCGTGGTTACGATTATCAATACAGCCCGCTGTTCTATAGCTA
CCTGCTGTTCCAGTTTGACCGTGAGGAACAAGATTTTAGCAAGATCGTGTTCTTTACCACCG
TTAAGAACCTGCCGGCGGACGTGAAAAACCTGCTGGAGATCAACAAAGTGATTGTTAAAGAA
TATGAGGAAATCGTTCCGTACCTGCGTGATGTGGTTATCCCGAGCATTCCGAAACACAACGA
CGATAACCCGGACTTCAAAAAGTACGATATTAGCCTGAGCCCGTATATCAACCTGATGATTT
ACAAGCTGTTTGACCGTAAAAACGTGCTGCTGCAGAACAGCCCGGTGGTTAAAATGAAGGCG
GTGAAGAACGACGTTGAAATCGATAACATGAAACAAGCGCACATTCTGGATGGTCTGGCGCT
GCTGCAGTTCTTTCACTGGTGCGAGCAAAAACGTAAAACCAAAGAACTGTTCAACGAGACCG
AAATGAGCCTGCGTCACAAGGTGGACTACTTCCGTAGCACCAAAAAGAACTTCATCTTTCCG
AGCTTTAGCACCATCAGCGCGAGCGGTCCGAACGCGGCGGTTATCCACTATGAGTGCACCGA
TAAGACCAACGCGACCATCAAACCGGCGATTTATCTGCTGGACAGCGGTGGCCAGTACCTGC
ACGGTACCACCGATGTTACCCGTACCACCCACTTTGGCGAACCGACCGCGGAGGAAAAACGT
ATCTACACCCTGGTGCTGAAGGGTCACCTGCGTCTGCGTAAAGTTATCTTCGCGAGCTATAC
CAACAGCAGCGCGCTGGACTTTATTGCGCGTGAGAACCTGTTCAACAACTTTATGGATTACA
ACCATGGTACCGGTCATGGTGTGGGTCTGACCCTGAACGTTCATGAAGGTGGCTGCAGCATT
GGTCCGGTGGGTGGCGCGCCGCTGAAAAAGAACATGGTTCTGAGCAACGAGCCGGGTTACTA
TATGAAGGACAAATTCGGCGTGCGTATTGAAAACATGCAATACGTTATCAGCAAAGAGATTA
CCGATACCACCGAATATCTGAGCTTCGACGATCTGACCATGTATCCGTACGAGAAAAAGCTG
CTGGACTTTAGCCTGCTGACCAACCAGGAGATCAAGGAACTGAACGAGTACCACACCACCAT
TCGTAACACCCTGCTGCCGCTGGTTAAACAAAGCCCGCAGGAGTATGGCGAGAGCGTTGAAA
AGTATCTGATTGAAATTACCGAGCCGTAA

Sequence length: 2025 bp

PF3D7_1446800 – Heme Detoxification Protein – introns spliced out

ATGAAAAATAGATTTTATTATAATTTGATAATTAAAAGATTATATACACGAAGTGGCGGTTT
AAGAAAACCTCAAAAGGTAACCAACGACCCAGAAAGTATAAATAGAAAAGTATATTGGTGTT
TTGAACATAAGCCTGTAAAAAGGACAATTATTAATTTAATATATTCACATAACGAACTCAAG
ATATTTTCTAATCTGTTAAATCATCCTACAGTTGGCAGCTCGTTAATACATGAATTATCTCT
CGATGGCCCTTATACTGCATTTTTTCCCTCCAACGAAGCCATGCAATTAATAAATATAGAAA
GTTTCAATAAATTGTATAACGATGAAAATAAATTATCAGAATTTGTTTTAAATCACGTTACG
AAAGAATATTGGCTGTATAGAGATTTATATGGTTCATCTTACCAACCGTGGTTAATGTACAA
TGAAAAAAGGGAAGCTCCAGAAAAATTAAGAAATTTATTGAATAATGATTTAATAGTAAAAA
TTGAGGGGGAATTTAAACATTGCAATCATTCGATATATTTAAATGGCTCAAAAATTATAAGA
CCAAATATGAAGTGCCACAATGGAGTTGTGCATATAGTAGATAAGCCCATCATTTTTTAA

Sequence length: 618 bp

EMBOSS Stretcher Pairwise Alignment of APP

```
                    -101

APP_full          MQLNFLLFVFIFLMVFHLNIFNKGKRQNLVSAYLNHFKKSYFSGVTSGSD   -51

APP_trunc_opt     --------------------------------------------------    0


APP_full       -50 CVNKSEVSSDNNNNNNNNNNKIAHNFFSKKYQRNFENNNLSENQENNKNI   -1

APP_trunc_opt     --------------------------------------------------    0


                        1
APP_full          0 IYSGSNIFKNIYNTEMMSNNNTVDVNMMDNNPAARLEELRTIMKKNKIDV   49
                            ||||||||||||||||||||
APP_trunc_opt     0 -MHNHNHNHNHNHNDYDIPTTENLYFQSDNNPAARLEELRTIMKKNKIDV   49


APP_full         50 YILINSDEHNSEIINEKDKKIVKITNYSGADGILIVTKDKPILYVNALYE    99
                    ||||||||||||||||||||||||||||||||||||||||||||||||||||
APP_trunc_opt    50 YILINSDEHNSEIINEKDKKIVKITNYSGADGILIVTKDKPILYVNALYE    99


APP_full        100 LQAMNELDQNLFTLRISRIDNRDEIFETISSLEFNTIAFDGKNTSVVFYE   149
                    ||||||||||||||||||||||||||||||||||||||||||||||||||||
APP_trunc_opt   100 LQAMNELDQNLFTLRISRIDNRDEIFETISSLEFNTIAFDGKNTSVVFYE   149


APP_full        150 KLRKALLNAYPKKKIVEKIIYNNNFDDVNKKDDENVLNFLVLEKSLVEIK   199
                    ||||||||||||||||||||||||||||||||||||||||||||||||||||
APP_trunc_opt   150 KLRKALLNAYPKKKIVEKIIYNNNFDDVNKKDDENVLNFLVLEKSLVEIK   199


APP_full        200 DYPVNNKTLYIHDRKYNGACAGEKIDKLKQSLMYDIKNVDNLLLSELDEI   249
                    ||||||||||||||||||||||||||||||||||||||||||||||||||||
APP_trunc_opt   200 DYPVNNKTLYIHDRKYNGACAGEKIDKLKQSLMYDIKNVDNLLLSELDEI   249


APP_full        250 AYLLNLRGYDYQYSPLFYSYLLFQFDREEQDFSKIVFFTTVKNLPADVKN   299
                    ||||||||||||||||||||||||||||||||||||||||||||||||||||
APP_trunc_opt   250 AYLLNLRGYDYQYSPLFYSYLLFQFDREEQDFSKIVFFTTVKNLPADVKN   299


APP_full        300 LLEINKVIVKEYEEIVPYLRDVVIPSIPKHNDDNPDFKKYDISLSPYINL   349
                    ||||||||||||||||||||||||||||||||||||||||||||||||||||
APP_trunc_opt   300 LLEINKVIVKEYEEIVPYLRDVVIPSIPKHNDDNPDFKKYDISLSPYINL   349


APP_full        350 MIYKLFDRKNVLLQNSPVVKMKAVKNDVEIDNMKQAHILDGLALLQFFHW   399
                    ||||||||||||||||||||||||||||||||||||||||||||||||||||
APP_trunc_opt   350 MIYKLFDRKNVLLQNSPVVKMKAVKNDVEIDNMKQAHILDGLALLQFFHW   399


APP_full        400 CEQKRKTKELFNETEMSLRHKVDYFRSTKKNFIFPSFSTISASGPNAAVI   449
                    ||||||||||||||||||||||||||||||||||||||||||||||||||||
APP_trunc_opt   400 CEQKRKTKELFNETEMSLRHKVDYFRSTKKNFIFPSFSTISASGPNAAVI   449


APP_full        450 HYECTDKTNATIKPAIYLLDSGGQYLHGTTDVTRTTHFGEPTAEEKRIYT   499
                    ||||||||||||||||||||||||||||||||||||||||||||||||||||
APP_trunc_opt   450 HYECTDKTNATIKPAIYLLDSGGQYLHGTTDVTRTTHFGEPTAEEKRIYT   499


APP_full        500 LVLKGHLRLRKVIFASYTNSSALDFIARENLFNNFMDYNHGTGHGVGLTL   549
                    ||||||||||||||||||||||||||||||||||||||||||||||||||||
APP_trunc_opt   500 LVLKGHLRLRKVIFASYTNSSALDFIARENLFNNFMDYNHGTGHGVGLTL   549
```

```
APP_full        550 NVHEGGCSIGPVGGAPLKKNMVLSNEPGYYMKDKFGVRIENMQYVISKEI    599
                    ||||||||||||||||||||||||||||||||||||||||||||||||||||
APP_trunc_opt   550 NVHEGGCSIGPVGGAPLKKNMVLSNEPGYYMKDKFGVRIENMQYVISKEI    599

APP_full        600 TDTTEYLSFDDLTMYPYEKKLLDFSLLTNQEIKELNEYHTTIRNTLLPLV    649
                    ||||||||||||||||||||||||||||||||||||||||||||||||||||
APP_trunc_opt   600 TDTTEYLSFDDLTMYPYEKKLLDFSLLTNQEIKELNEYHTTIRNTLLPLV    649

APP_full        650 KQSPQEYGESVEKYLIEITEPIAIHNN                          676
                    ||||||||||||||||||
APP_trunc_opt   650 KQSPQEYGESVEKYLIEITEP------                          670
```

Bold: N-terminal His-tag with TEV cleavage site

Deleted N- and C-terminal regions (128 amino acids at N-terminus and 6 amino acids at C-terminus)

Oligonucleotides in pARL1a vector

Name	Sequence
PfPM1_KpnI_fwd	GAGAGGTACCATGGCTTTATCAATTAAAGAAG
PfPM1_strep_AvrII_rev	GAGACCTAGGTTATTTTTCGAACTGCGGGTGGCTCCAAGCGCTCAATTTTTTTTTGGCAAGGGCG
PfPM2_KpnI_fwd	GAGAGGTACCATGGATATTACAGTAAGAGAACATG
PfPM2_myc_AvrII_rev	GAGACCTAGGTTACAGGTCCTCCTCTGAGATCAGCTTCTGCTCGCCTAAATTCTTTTTAGCAAGAGCAATACC
PfPM3_XmaI_fwd	GAGACCCGGGATGGTACCATGAATTTAACCATTAAAGAAGAAG
PfPM3_strep_AvrII_rev	GAGACCTAGGTTATTTTTCGAACTGCGGGTGGCTCCAAGCGCTTAAATTTTTGGCTAAAGCAAATCC
PfPM4_KpnI_fwd	GAGAGGTACCATGGCTCTTACCGTTAAAGAAGAAG
PfPM4_myc_XhoI_rev	GAGACTCGAGTTACAGGTCCTCCTCTGAGATCAGCTTCTGCTCGCCTAAATTTTTAGCTACTGCAAAACC
PfFP2_KpnI_fwd	GAGAGGTACCATGGATTACAACATGGATTATGCTCC
PfFP2_strep_AvrII_rev	GAGACCTAGGTTATTTTTCGAACTGCGGGTGGCTCCAAGCGCTTTCAATTAATGGAATGAATGCATCAG
PfFP3_KpnI_fwd	GAGAGGTACCATGGAATATCATATGGAATATTCACC
PfFP3_myc_AvrII_rev	GAGACCTAGGTTACAGGTCCTCCTCTGAGATCAGCTTCTGCTCGCCTTCAAGTA
PfFl_XmaI_fwd	GAGACCCGGGATGGTACCATGAATTTAACAAAATTAATGAAAG
PfFl_strep_AvrII_rev	GAGACCTAGGTTATTTTTCGAACTGCGGGTGGCTCCAAGCGCTTTCTATTAATACCTTTTAAATTCTCC
PfFl_int_AvrII-rev	CCGATAAATATAATGCACAAGC
PfFl_int_fwd	AAGTATGTCTGCTAATGTTGC
PfDPAP1_KpnI_fwd	GAGAGGTACCATGGCAAAGAGAATTTTTAGTGTAAG
PfDPAP1_myc_AvrII_rev	GAGACCTAGGTTACAGGTCCTCCTCTGAGATCAGCTTCTGCTCGCCATTTCCTAATTCCTTTTGCATTTTTTC
PfDPAP2_XmaI_fwd	GAGACCCGGGATGGTACCATGAATACTTTTTATATTTTCTTTTTATTTGTGC
PfDPAP2_strep_AvrII_rev	GAGACCTAGGTTATTTTTCGAACTGCGGGTGGCTCCAAGCGCTTTCCAAAGAGTCGGATTGAAGTATATTC
PfAap_KpnI_fwd	GAGAGGTACCATGAAAATTAACAAAAGGCTGTGCC
PfAap_myc_AvrII_rev	GAGACCTAGGTTACAGGTCCTCCTCTGAGATCAGCTTCTGCTCGCCTAATTTATTTGTTAATCTTAATAAATATTCC
IBA3_Strep _HindIII_Avr II_rev	GACACCTAGGTCAAGCTTATTATTTTTGGAACTGCGG
PfAPP_KpnI_fwd	GAGAGGTACCATGCAATTGAATTTTCTTTTGTTTG
PfFP2b_KpnI_fwd	GAGAGGTACCATGGATTACCACATGGATTATATTCCG
PfHDP_KpnI_fwd	GAGAGGTACCATGAAAAATAGATTTTATTATAATTTG
PfAAP_GFP_AvrII_rev	GAGACCTAGGTAATTTATTTGTTAATCTTAATAAATATTCC
PfDPAP1_GFP_AvrII_rev	GAGACCTAGGATTTCCTAATTCCTTTTGCATTTTTTC
PfAPP_GFP_AvrII_rev	GAGACCTAGGATTGTTATGAATCGCAATTGGTTC
PfFP2b_GFP_AvrII_rev	GAGACCTAGGTTCAATTAATGGAATGAATGCATCAG
PfDPAP2_GFP_AvrII_rev	GAGACCTAGGTTCCAAAGAGTCGGATTGAAGTATATTC
PfFP2_GFP_AvrII_rev (FV)	GAGACCTAGGATTGTTGTTATTACCTTCGTTG
pARL_Seq_fwd	ATATCCGTTAATAATAAATACACGC
pARL_Seq_rev	CCAGTAGTGCAAATAAATTTAAGGG

Oligonucleotides in pASK IBA3 vector

Name	Sequence
PfFP2b _XbaI_fwd	GAGATCTAGATAACGAGGGCAAAAAATGGATTACCAATGGATTATA TTCCG
PfFP2b_Strep_HindIII_rev	GAGAAAGCTTTATTATTTTCGAACTGCGGGTGGCTCCAAGCGCTTT CAATTAAGGAA
PfAPP_BsaI_fwd	GCGCGCGGTCTCCAATGCAATTGAATTTTCTTTTGTTTG
PfAPP_BsaI_rev	GCGCGCGGTCTCCGCGCTATTGTTATGAATCGCAATTGGTTC
PfHDP_BsaI_fwd	GCGCGCGGTCTCCAATGAAAAATAGATTTTATTATATTTG
PfHDP_BsaI_rev	GCGCGCGGTCTCCAATGAAAAATAGATTTTATTATATTTG
IBA3_Seq_fwd	AGAGTTATTTTACCACTCCCT
IBA3_Seq_rev	GACGCAGTAGCGGTAAACG

Oligonucleotides for RT-PCR

Name	Sequence
PfFP2_qRT_fwd	ATGCCGTTATGCTTGTAGGTTT
PfFP2_qRT_rev	ATTGTTGTCCCCATGAGTTCTT
qRT_GFP_fwd	TCAGTGGAGAGGGTGAAGGT
qRT_GFP_rev	GTTGGCCATGGAACAGGTAG
qRT_ seryl tRNA synthetase _fwd	AAGTAGCAGGTCATCGTGGTT
qRT_seryl tRNA synthetase_rev	TTCGGCAC-ATTCTTCCATAA